City Research Online

City St George's, University of London

Citation: Sugiarto, H. (1980). A study of Trichlorocyanuric acid/carbon cathode. (Unpublished Doctoral thesis, The City University)

This is the accepted version of the paper.

This version of the publication may differ from the final published version. To cite this item please consult the publisher's version.

Permanent repository link: https://openaccess.city.ac.uk/id/eprint/35349/

Copyright and Reuse: Copyright and Moral Rights remain with the author(s) and/or copyright holders. Copies of full items can be used for personal research or study, educational, or not-for-profit purposes without prior permission or charge, unless otherwise indicated, provided that the authors, title and full bibliographic details are credited, a hyperlink and/or URL is given for the original metadata page and the content is not changed in any way. For full details of reuse please refer to City Research Online policy.

City Research Online: http://openaccess.city.ac.uk/ publications@citystgeorges.ac.uk

A STUDY OF TRICHLOROCYANURIC ACID/CARBON CATHODE

A thesis submitted for the degree of

Doctor of Philosophy

by

Herman SUGIARTO

at the

Department of Chemistry
The City University
St. John Street
London, EC1V 4PB

October 1980

These investigations were supported by the Ministry of Defence, Contract No. 7D10030.00, and carried out under the joint supervision of Dr. A.C.C. Tseung, and Professor P.G. Sammes.

ACKNOWLEDGEMENTS

I would like to acknowledge, most gratefully, the help and guidance given to me by my supervisors, Professor P.G. Sammes and Dr. A.C.C. Tseung. I would also like to express my grateful thanks to my student colleagues in the Electrochemical Research Group for many helpful discussion.

My thanks are also due to [redacted]

Finally, I am indebted to my wife for her understanding during my study.

SUMMARY

The use of the trichloroisocyanuric acid (T.C.A.) - aluminium system as a seawater activated primary reserve battery has two advantages. It has a high energy density and in addition the electrode materials are cheap to manufacture.

However, the poor storage stability of the cathode has limited its practical use. Under ambient conditions a 10% loss of chlorine has been detected within a period of one week. This phenomenon is thought to be mainly caused by interfacial contact between the T.C.A. and acetylene black. It involves electrochemical self discharge and free radical and ionic reactions. Several stabilizers such as boric acid (oxide) and zeolites were used in an attempt to reduce the chlorine loss. To date only boric acid improved the stability of the cathode to any extent. Alternative methods to increase stability of the system have been investigated. For example, the cathode design was altered, the T.C.A. powder being sandwiched in between layers of acetylene black. This cathode design has improved storage stability and maintained good discharge performance.

A mathematical model was developed to describe the discharge characteristic of the sandwich type cathode. It suggests that the discharge is mainly an internal diffusion-controlled process.

CONTENTS

Page

CHAPTER 1

1. INTRODUCTION

1.1 The Seawater/Water Activated Reserved Primary Battery 1

1.2 N-Halogenated Compounds as Primary Battery Cathodes 2

1.3 Objectives of Present Studies 4

1.4 Trichloroisocyanuric Acid (T.C.A) 5

1.5 Surface Group on Graphite and Carbon 7

(i) Acid Groups 8

(ii) Basic Groups 9

(iii) Neutral Groups 11

CHAPTER 2

2. THE LOSS OF CHLORINE IN THE T.C.A. CATHODE DURING STORAGE

2.1 Introduction 13

2.2 Experimental 13

2.2.1 Preparation of Samples for Storage Testing 13

2.2.2 Sample Storage 13

(i) Ambient Condition 14

(ii) Nitrogen Atmosphere 14

(iii) Accelerated Conditions 14

2.2.3 Determination of Available Chlorine in the Reaction Mixture 14

2.2.4 Preparation of T.C.A. Aggregates of Controlled Size 15

2.3 Results and Discussion 15

Page

CHAPTER 3

3. MECHANISM OF CHLORINE LOSS FROM THE T.C.A./ ACETYLENE BLACK CATHODE

3.1 Introduction 18

3.2 Electrochemical Behaviour of Graphite and Carbon Surface in Aqueous Solution 18

3.3 Corrosion of Metals in Aqueous Solution 21

3.3.1 Cathodic Reactions 23

3.3.2 Metal Dissolution Reaction 24

3.4 Free Radical Chlorination of Hydrocarbons 27

3.5 Theoretical Approach 32

3.5.1 Electrochemical Self Discharge Reaction 32

3.5.2 The Free Radical Chlorination Reaction 34

3.6 Experimental 37

3.6.1 Half Cell Measurement of the Corrosion Reaction 37

3.6.2 Chlorination of Toluene 37

3.6.3 Reaction of T.C.A. with D.P.P.H. 39

3.7 Results and Discussion 40

3.7.1 Electrochemical Self Discharge Reaction 40

3.7.2 Free Radical Reaction 41

CHAPTER 4

4. STORAGE STABILITY AND ELECTROCHEMICAL DISCHARGE CHARACTERISTIC OF T.C.A. CATHODES

4.1 Introduction 45

4.2 Experimental 47

4.2.1 Sample Preparation for Storage Tests 47

4.2.2 Cathode Preparation 47

Page

4.2.3 Single Cell Assembly 48

4.3 Results and Discussion 49

4.3.1 The Effects of Stabilizer on Cathode Storage Stability 49

4.3.2 Discharge Characteristic of the Sandwich Type Cathode 51

CHAPTER 5

5. THE KINETICS OF CHLORINE REDUCTION ON POROUS GRAPHITE SURFACE

5.1 Introduction 57

5.2 Electrochemical Kinetics of Chlorine 58

5.2.1 The Kinetics of the Cl_2/Cl^- Couple on Platinum Electrodes 58

5.2.2 Kinetics of Cl_2/Cl^- Couple on Metal Oxide Electrode 60

5.2.3 Kinetics of Cl_2/Cl^- Couple on Graphite 63

5.3 Experimental 66

5.4 Kinetic Theory of Chlorine Reduction 67

5.5 Results and Discussion 71

CHAPTER 6

6. MASS TRANSFER BEHAVIOUR IN THE SANDWICH TYPE CATHODE

6.1 Introduction 75

6.2 Macroscopic Description of the Porous Electrode 75

6.3 The Cathode : A Mathematical Description 81

6.4 Experimental 88

6.5 Results and Discussion 89

Page

CHAPTER 7

7. CONCLUSIONS AND SUGGESTIONS FOR FURTHER WORK 90

APPENDIX

TABLES AND DIAGRAMS

REFERENCES

CHAPTER ONE

INTRODUCTION

CHAPTER 1

1. INTRODUCTION

1.1. The Seawater/Water Activated Reserved Primary Battery

As demands for a high energy output battery have increased scientists have begun to look for more active materials than those used previously. There are, in fact, only few systems which are capable of producing a high energy output in aqueous solutions under ambient conditions. Unfortunately, most of these systems do not possess the long-term storage stability required for a practical battery. This is probably due to side reactions between the active materials and the electrolyte which lower the battery capacity.

In some systems, storage stability has been improved by separating these materials from the electrolytes, thus keeping them dry during the storage period. The electrolyte is then introduced when discharge is required. This "Reserved primary battery" has in many cases been successful in preventing deterioration during storage. Although battery systems like the silver chloride-magnesium[1,2,3,4,6] and cuprous chloride - magnesium[5,6] types have achieved some practical success, the high cost of cathode materials has limited their use to emergency and military applications. For wider use therefore it is necessary to find alternative cathode materials which are less expensive.

Attractive substances include combination involving the halogens, as well as with the hypohalous acids and salts. The halogens were a possibility because of their high electrode

potential and high ampere-hour capacity per unit weight. However, cell design difficulties were encountered because of the toxic and corrosive nature of these materials. The hypohalous acids and their salts have low stability which, combined with their high solubility in ambient conditions, have made them unsuitable for a practical battery design.

N-Halogen solid organic compounds have been found to have similar electrochemical properties to those of hypohalous acids and their salts. Most of these compounds normally exist as crystalline powders which are stable in ambient conditions. Moorehouse and Glicksman[7] determined the theoretical capacity and electrochemical characteristics of these compounds. They found that the potential of these electrodes were very stable during discharge. Hence, they may be of great value in battery manufacture.

1.2. N-Halogenated Compounds as Primary Battery Cathodes

Various workers[8,9,10,11] have used N-Halogenated compounds in the design of primary battery cathodes. These substances are easily hydrolysed in aqueous solution and, therefore, the cathodes was mainly designed as a 'reserved primary system'. Arsem[8] used N-Halogenated compounds coupled with a Zn anode for dry cell applications, Gruber[9] developed the 'dry tape battery' using N-Halogenated compounds coupled with magnesium and lithium anodes. With a magnesium anode the cell was reported to be able to deliver an energy density of 100 W-hr/lb at a cell

voltage of 2.0 volts, but, with the lithium anode at a cell voltage of 3.0 volts, it delivered 200 W-hr/lb. It was claimed that these cells have a long shelf life and a stable performance over discharge. Williams et al[10] use dichlorocyanuric acid as a cathode material with lithium as an anode. When the cell was discharged in organic electrolytes, it delivered energy density of 200-400 W-hr/lb. Recently, Pearce et al[11,12] have successfully used trichloroisocyanuric acid (T.C.A.) cathodes coupled with an aluminium alloy anode for the construction of a new type of seawater activated battery. In an acidic environmen (pH2) the cell had an open circuit potential of 2.2-2.3 volts.

In acidified chloride solution the reaction at the cathode and anode are described as follows:-

Cathodic

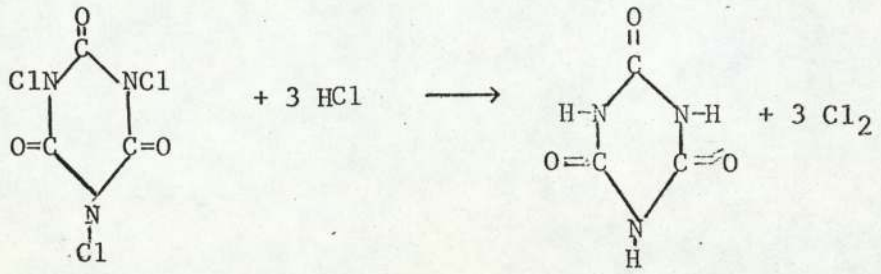

$$Cl_2 + 2\,e \longrightarrow 2\,Cl^-$$

Anodic

$$Al \longrightarrow Al^{+3} + 3\,e$$

$$Al^{+3} + H_2O \longrightarrow Al(OH)^{2+} + H^+$$

The protons produced from the anode reaction maintain the acidity in the cathode.

This cell could be used for both high (100 mA/cm^2) and low (5 mA/cm^2) rate discharge and had a typical energy of 700-800 J/g.

Owing to the incipient chemical reactivity of T.C.A., the storage stability of the compressed T.C.A./acetylene black cathodes presented problems. Preliminary investigations by Hazzard et al[13] showed that an appreciable chlorine loss was detected when the cathode was stored over $CaCl_2$ or P_2O_5 at ambient temperature for a period of one year. The rate of loss was increased considerably at elevated temperatures (40°C). This has therefore precluded the T.C.A. - aluminium battery as a high energy density, low cost system.

Boric acid, sodium tripolyphosphate and trisodium phosphate are useful stabilizers [13] but long term reliability studies on these materials have not yet been carried out.

1.3. Objectives of Present Studies

The present investigation is an extension of work carried out by Pearce et al.[11,12,13] The main topic of the studies are listed below:-

(a) Elucidation of the mechanism of chlorine loss from the T.C.A. cathode.

(b) Elucidation of the mechanism whereby boric acid stabilizesthe T.C.A. cathode.

(c) Investigation of alternative and more efficient stabilizing additives other than boric acid.

(d) Quantitative analysis of the sys tem with a view to predicting the stability of the cathode.

(e) Investigation of the effect of the microstructure of

the cathode mixture on its long-term stability and electrochemical performance.

(f) Investigation of new cathode structures which can maintain long-term stability and good electrochemical performance.

1.4. Trichloroisocyanuric Acid (T.C.A.)

Trichloroisocyanuric acid (T.C.A.) which is also marketed under the trade name Fichlor®, is a white crystalline powder. The dried crystals alone do not lose chlorine when stored for a period of one year.[14] However, in aqueous solution this compound rapidly hydrolyses into hypohalous acid, and therefore has powerful oxidizing activity. It is, at present, a popular new material for detergent applications.

T.C.A. is a cyclic N-Halogenated derivative of isocyanuric acid. Its structure is illustrated below:-

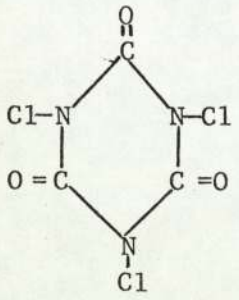

(T.C.A.)

The manner in which the chlorine atoms are introduced into T.C.A. molecules as follows:-

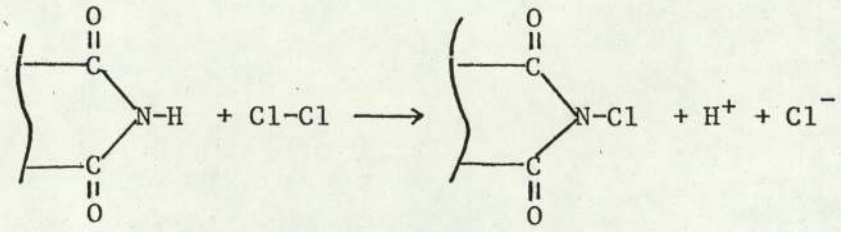

The chlorine atom attached to the nitrogen atom is described as a positive chlorine atom and resembles the chlorine atom that is attached to the oxygen atom in hypochlorous acid.

On dissolution T.C.A. can produce more than ten organic species in water. The equilibrium constants concerned with these species were measured by Brady et al.[15] using titrimetric and spectroscopic techniques. Phillips[16] calculated the concentration profile of T.C.A. in 0.5M sodium chloride solution at pH 2. He claimed that under these conditions three predominant species were present which were chlorine, cyanuric acid and some monochloroisocyanuric acid. These results were confirmed by his cyclic voltametric analysis: Two distinct peaks associated with chlorine and monochloroisocyanuric acid were observed. Phillips suggested that the mechanism of T.C.A. reduction in acid solution was initiated by the formation of chlorine and monochloroisocyanuric acid. The reduction of monochloroisocyanuric acid was a slow process.

In basic solutions T.C.A. was mainly converted into hypohalous acid and sodiumisocyanurate.[7] This was supported by the results obtained by Khan,[17] who studied the reduction of T.C.A. in sodium hydroxide solution. He claimed that only one peak corresponding to OCl^- was observed in the cyclic voltametric

analysis and postulated the T.C.A. reduction mechanism as follows:

$$OCl^- + H_2O + e \xrightarrow{slow} Cl_{ad} + 2\ OH^-$$

$$Cl_{ad} + e \xrightarrow{fast} Cl^-$$

1.5. Surface Groups on Graphite and Carbon

Like many other crystalline solids graphite has many electrolytically unsaturated sites which are normally saturated by the formation of different types of surface oxides. In the crystalline form graphite has a relatively low surface area, with only a small amount of surface oxides. This makes their identification very difficult. Preparation of high surface area graphite, however, facilitates the easy detection of these surface oxides.

The formation of oxygen bonds on high surface area graphite was first identified by Saussure.[18] Smith[19] corroborated these findings. He observed that the chemisorbed oxygen was present on active carbon and could be removed as oxides of carbon on heating. Based on the known structure of several organic compounds, Schillow et al.[20] described the chemical structure of these surface oxides.

A number of workers[21,22,23] found that the catalytic properties of graphite for some specific reactions was accounted for by the nature of its surface groups. These may be acidic, basic or neutral in their chemical character.

(i) Acidic Surface Groups

The formation of acidic groups normally occurs of either at high temperatures in the presence of oxygen or in aqueous solution at low temperatures. Their presence normally gives graphite high surface area and CO_2 will desorb on heating.

Several analytical methods were used to identify the structure of these oxides. These include (a) decarboxylation with Na_2CO_3[24] (b) neutralization with dilute sodium hydroxide[25-28] (c) reaction with diazomethane to give methoxy derivative followed by subsequent hydrolysis with mineral acid[29] (d) infra red spectroscopic analysis.[23,30-38] The infra red spectroscopic analysis has identified the presence of -COOH,[23,38] and lactone[25] groups on the graphite surface.

Puri et al.[40-43] correlated the amount of CO_2 evolved on heating carbon to the amount of the surface oxides which can be neutralized by sodium hydroxide. They noticed that the graphite lost its ability to neutralize sodium hydroxide after it had been heated at 700°C to remove all the CO_2. They, therefore, concluded that a surface group which reacted acidically was the only source of CO_2. Studebaker[44] and Weiss[25] suggested that this acidic group was lactonic in nature but Puri et al.[40-43] considered it had the structure below:-

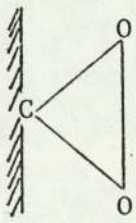

Boehm[45] then postulated two different strengths of acidic groups on the graphite surface which will be attributed to the source of CO_2 evolution on heating. The stronger was a carboxyl (- COOH) group which reacted with sodium bicarbonate, whilst the weaker was a lactone of carboxylic acid which reacted with sodium carbonate. Puri[40-43] criticized these ideas, as even the weak acidic group should be neutralized by alkalis of different strengths.

The structure suggested by Puri was supported by the work of Dollimore et al.[46] and Harkner et al.[47] They found that the rate of CO_2 desorption followed the Elovich equation, which indicated that the release of CO_2 mainly originated from the same type of site on the carbon surface.

However, the exact structure of these oxides are still largely in dispute, as no true account of all the adsorbed oxygen has yet been made.

(ii) Basic Groups

When graphite/carbon is heated above 850°C in the absence of air basic surface groups are formed on its surface.

Early studies by Burstein and Frumkin[39] showed that when carbon was heated to 950°C and cooled in nitrogen, it gained the ability to adsorb mineral acids from a solution containing oxygen. Shilov et al.[48] claimed that this ability was dependent upon the partial pressure of oxygen. They suggested that two basic oxides were present on the carbon surface. One of these was dependent on the partial pressure of oxygen whilst the other

was not. Similar results were obtained by Bretschneider.[49]

Sternberg[50] found that the adsorption of acid on the basic carbon surface was physical in nature and could be removed by shaking in toluene. To account for this he postulated that the adsorption of acid onto the carbon surface involved the adsorption of H^+ which then attracts the main species into the double layer.

The fact that in the hydrochloric acid solution, the presence of basic oxides lead to hydrogen peroxide decomposition was noted by Burstein and Frumkin.[51] Hence, they suggested the following mechanism:

$$C_xO_2 + 2\,H^+Cl^- \longrightarrow C_x^{2+}Cl_2^- + H_2O_2$$

This equation implied that the amount of H_2O_2 evolved was equal to the amount of acid adsorbed. But this was not found to be the case experimentally. This inconsistency could be attributed to the decomposition of peroxides on the carbon surface[52,53] which leads to the reduction of peroxide concentration in the solution.

Garten and Weiss[54] on the other hand suggested that the adsorption of acid on the basic carbon may be caused by both physical and chemical processes. The chemical adsorption was mainly due to the presence of a chromene group. This was oxidized in the presence of acid to the corresponding benzopyran and benzopyrylium systems, together with hydrogen peroxide decomposition. The mechanism of the acid adsorption was therefore proposed to be:-

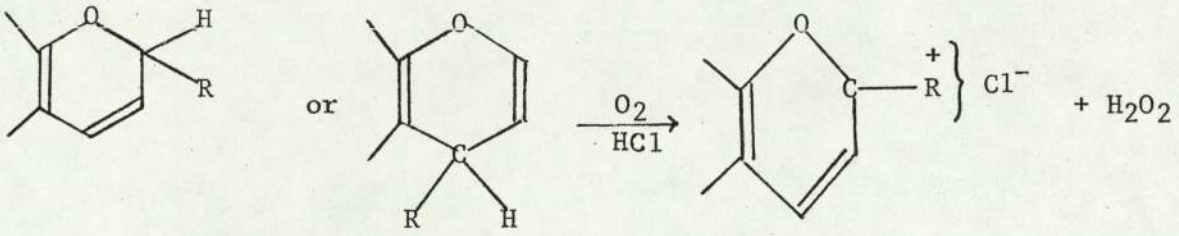

This theory of chromene structure was disputed by Boehm[55] as carbonium bases are normally very weak, and washing would be expected to complete the hydrolysis. Nevertheless, carbon cannot be completely freed from bound acid by washing alone.[56,57]

(iii) Neutral Groups

The neutral surface groups existing on the carbon surface are normally recognized as quinone surface groups which release carbon monoxide on heating. A number of workers have reported the presence of the quinone group on carbon surfaces[29,31,58] The ability of the neutral carbon surface to adsorb acid after electrolytic reduction was therefore attributed to the reduction of quinone into hydroquinone.[59,60,61] In addition, Puri et al.[62-64] suggested a second kind of neutral surface complex. This was formed by the elimination of the adjacent CO_2 molecules from the carbon surface, followed by the fixation of oxygen molecules onto the unsaturated carbon - carbon double bond. The mechanism was described as follows:

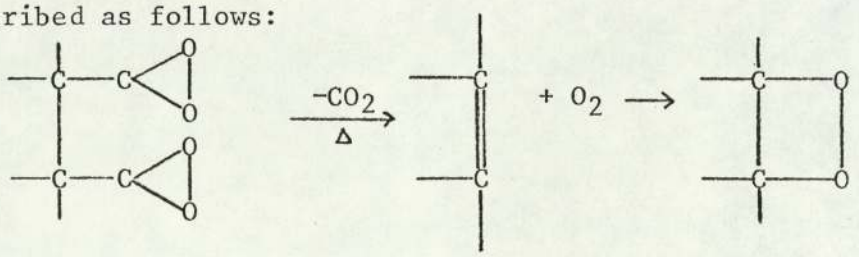

The formation of an unsaturated C=C bonds was later supported by the finding of Stearn et al.[66] They claimed that carbon was capable of fixing bromine in aqueous solution. Of course it is well known that pure graphite contains unsaturated carbon—carbon bonds and it is not too surprising that the surface of graphite crystals can react with bromine in this manner.

CHAPTER TWO

THE LOSS OF CHLORINE IN THE T.C.A. CATHODE DURING STORAGE

CHAPTER 2

2. THE LOSS OF CHLORINE IN THE T.C.A. CATHODE DURING STORAGE

2.1. Introduction

T.C.A. crystals alone are very stable when stored in dry ambient conditions. However, after mixing with acetylene black, chlorine is liberated. This suggests that the presence of acetylene black destabilizes the T.C.A. cathode during storage, and hence diminishes its capacity. Although corresponding reactions have not yet been identified, it is likely that a catalytic reaction is a primary cause of the phenomenon.

A preliminary investigation of the effect of storage environment, the weight ratio of T.C.A to acetylene black and the T.C.A. aggregate size, on the rate of chlorine loss from the cathode was carried out. It was hoped that the results from the experiment would provide useful information from which a concrete understanding of the causes from the system would be achieved.

2.2. Experimental

2.2.1. Preparation of Samples for Storage Testing

0.1g T.C.A. powder was mixed in a glass jar with 0.05g, 0.1g, 0.15g, 0.2g and 0.25g of acetylene black respectively using a chromium plated microspatula.

2.2.2. Sample Storage

The prepared samples were stored under:

(i) Ambient condition:

Where the mixture was exposed to air.

(ii) Nitrogen atmosphere:

The jars holding the mixtures were located inside a silicon tube which was continuously flushed with dry nitrogen at 20°C. The nitrogen was dried by passing it over activated 5A molecular sieve pellets contained in a drying tube.

(iii) Accelerated conditions:

This storage condition was specifically designed to simulate long-term storage. The reaction was accelerated by storing the sample at 40°C under 75% humidity.

2.2.3. Determination of Available Chlorine in the Reaction Mixture

The available chlorine content in pure T.C.A. was determined by using a standard iodotitrimetric method as described below.

T.C.A. powder was transferred into a 250 ml flask containing 10% W/W potassium iodide solution (20 ml) and distilled water (80 ml). The solution was mixed with a magnetic stirrer, until the powder was completely dissolved (1 to 3 minutes) 50% V/V sulphuric acid (10 ml) were added and the mixture was allowed to stand in the dark for 1 minute. The solution was titrated with standard 0.1N sodium thiosulphate until a pale straw colour was achieved. Starch solution was then added as an indicator and the titration continued until the blue colour was discharged, the solution remaining colourless for one minute.

The volume of sodium thiosulphate solution at the end of the titration procedure was recorded. The percentage of chlorine available was calculated by using the formula below:-

$$\% \text{ available chlorine} = \frac{(\text{ml thiosulphate}) \times (\text{normality of thiosulphate}) \times 3.545}{\text{Weight of T.C.A. in solution}}$$

In samples containing acetylene black the use of starch as an indicator was inefficient due to the colour of the solution. An iodopotentiometric titration method was therefore used. The solution was prepared as described previously. A standard calomel and a platinum electrode (5 cm^2) were immersed into it, and connected to a potentiometer. The end of the titration was indicated by a sharp change in potential, and was calibrated using a pure T.C.A. solution.

2.2.4. Preparation of T.C.A. Aggregates of Controlled Size

Coarse grade T.C.A. crystals were crushed in a mortar and pestle. The resultant aggregates were separated by sieving. Thus varied, controlled-size of aggregates were obtained. An Olympus optical microscope was used to assess the mean diameter of the aggregates. These were later mixed with acetylene black powder for storage tests.

2.3. Results and Discussion

The rate of chlorine loss in the T.C.A. - acetylene black mixture during storage was affected by the weight ratio of the T.C.A. - acetylene black as well as the duration of the

storage period.(Figs. 1 & 2) Up to a ratio of 1.5 the rate of chlorine loss was directly proportional to the loading of the acetylene black.(Fig. 1) Thereafter, the rate of loss did not increase. This suggests that the rate is proportional to the interfacial contact area between the two aggregates.

The average diameters of T.C.A. and acetylene black particles were 150 μm and 1.38 μm respectively. Therefore the amount of acetylene black required to form a complete mono-layer over 0.1g T.C.A. is only 4.8×10^{-3}g (see Appendix I). This is clearly much less than the value of 0.15g at which maximum chlorine losses were found. This suggests that factors other than contact area contribute to the rate of chlorine loss.

Acetylene black is capable of adsorbing moisture from its surroundings. An increase in loading will concommitantly raise the total moisture content in the reaction mixture, and this could accelerate the decomposition process. This hypothesis is supported by the result obtained, that the rate of chlorine loss from samples stored in a dry nitrogen stream is 5 times less than that from samples stored under ambient conditions.(Fig. 3)

Thus, as the dry nitrogen was passed over the reaction mixture, moisture was removed from the reaction mixture's surroundings in addition to that which was pre-adsorbed on the acetylene black surface. Hence, the progress of the reaction was inhibited.

It was also found that chlorine losses are reduced as loading was increased from 0.15g to 0.25g, after prolonged storage.

from 7 to 30 days.(Fig. 1) The loss is maximal at 0.15g, any further increase in loading being ineffective in altering the rate of reaction. The excess acetylene black will adsorb some chlorine gas produced from the reaction, thereby preventing its release into the atmosphere.[72,73,74] Further increase in the amount of acetylene black in the mixture, will clearly facilitate an increased adsorption of chlorine.

The relationship between the rate of chlorine loss and the aggregate size of the T.C.A. is illustrated in Fig. 4. The amount of chlorine loss was increased from 33% to 55% as the T.C.A. aggregates diameter were varied from 1.85×10^{-3} cm to 2.287×10^{-2} cm respectively. For an interfacially catalized reaction, the rate of reaction is generally proportional to the amount of interfacial contact i.e. the surface area between T.C.A. and acetylene black aggregates. This is, in turn, dependent upon the specific surface area of both T.C.A. and acetylene black. Assuming these aggregates are spherical the specific surface area can be related to the aggregate diameter as follow :-

$$S = \frac{6}{\rho d}$$

where S = specific surface area (cm^2/g)

ρ = aggregate density (g/cm^3)

d = aggregate diameter (cm)

In this case the rate of reaction is an inverse function of the aggregate diameter of T.C.A. and acetylene black which is in agreement with the results presented in Fig. 4.

CHAPTER THREE

MECHANISM OF CHLORINE LOSS FROM THE T.C.A./ACETYLENE BLACK CATHODE

CHAPTER 3

3. MECHANISM OF CHLORINE LOSS FROM THE T.C.A./ACETYLENE BLACK CATHODE.

3.1. Introduction

The loss of chlorine from T.C.A./acetylene black mixture has been identified as an interfacial reaction where acetylene black acts as a catalyst.

This chapter is concerned with the mechanism of reactions involved in chlorine loss. Several possible reactions mechanisms have been postulated, based on the electrochemical and chemical properties of both the T.C.A. and acetylene black. These include an electrochemical self discharge reaction, free radical reactions and ionic reactions.

The study of these reactions which might occur simultaneously, is extremely difficult. Thus, for simplicity individual reactions were investigated. This was facilitated by careful control of the experimental conditions.

It was hoped that the data obtained would provide useful information by which effective and economic stabilisation of the T.C.A. cathode could be made.

3.2. Electrochemical Behaviour of Graphite and Carbon Surface in Aqueous Solution.

Graphite and carbon anodes have been used in many electrochemical reactions. The surface nature of graphite is of great importance in determining the nature of each individual

reaction. Brennan[75] found that cathodically pretreated pyrolytic graphite inhibited the hydrogen evolution reaction. Janssen et al.[76] reported that the kinetics of chlorine evolution on new and aged graphite electrodes were different.

Pyrolytic graphite is solid in nature and has good conductivity. It is a popular material for electrochemical measurement and surface analysis. This type of graphite has a highly ordered structure, the layers being arranged in almost parallel planes. The planes perpendicular to the C axis are known as basal planes, whilst the planes perpendicular to the basal planes are known as edge planes. These two planes have different electrical characteristics, the basal planes behaving as a semiconductor whilst the edge plane behaves as a metallic conductor.

In acid solution, graphite can be oxidized both chemically[77] and electrochemically.[76,77,78] Mamantov et al[77] reported that oxides were formed when the electrode was anodized at +1.1 volts and +1.5 volt vs SCE or dipped in a $CeSO_4$ solution for several hours. They reported that these oxide films were reduced at a cathodic potential of +0.48 volt vs SCE. This process was highly irreversible.

Kristhalik et al.[80] suggested that a stable oxide was originally formed on the surface of graphite during the manufacturing process. This type of oxide was normally difficult to reduce cathodically but could be removed by anodic oxidation with subsequent release of CO_2 and CO. The fresh surface was

then quickly covered by new types of oxides which were electrochemically less stable. Hine et al.[78] reported that a lower oxide (CO_L) and a higher oxide (CO_H) were formed anodically, and had peak potentials of +0.5 volt and +1.3 volt vs SCE respectively. They also observed that the lower oxide was less stable and was easily reduced cathodically with peak potential of +0.2 volt vs SCE. This view was shared by Laser et al.[81] who obtained similar results and considered the process to be highly reversible. Contradictory results were claimed by Janssen et al.[82] who found that a lower oxide was formed at a potential between +1.2 volt to+1.22 volt vs SCE.

The formation of higher oxide was also found by Janssen et al.[82] The peak of the oxide formation occurred at +1.3 volt vs SCE. Hine et al[78] obtained similar results and claimed that the reduction of the higher oxide had a peak potential at -0.6 volt and was highly irreversible. But Laser[81] and Mamantov et al.[77] suggested that the reaction with peak potential of +1.3 volt vs SCE corresponded to oxygen evolution rather than oxide formation, and the cathodic peak at -0.6 volt was mainly due to oxygen reduction. Whilst these workers obtained similar results, their actual interpretations do not correspond. It is likely that high oxide formation preceeds the oxygen evolution reaction, particularly if oxygen atoms recombination is the rate determining step. Clarification of these hypotheses will only be possible when the mechanisms of oxygen evolution and reduction on graphite is fully understood.

A number of studies have confirmed that the basal and edge planes display different electrochemical characteristics.[75,82,83] For example, Yeager and Marcos[83] found that the edge plane was 5 times more active for oxygen reduction and 17 times more active for peroxide decomposition than the basal plane. They suggested that this difference may be due to the low activity of basal plane to adsorb the reacting species and its intermediate. In addition, Brennan et al.[75] reported that the rate of hydrogen evolution was higher on the edge than the basal planes. A higher rate of chlorine evolution on edge planes was also reported by Janssen et al.[82]

3.3. Corrosion of Metals in Aqueous Solution

Generally, the stability of a metal in the atmosphere or aqueous environment is determined by events occurring at its surface. Metals have good internal strength if the surface is stable in a particular environment.

The atmosphere contains moisture and dissolved carbon dioxide. Since metals corrode when in contact with the atmosphere it has been suggested that this process was mainly due to the charge transfer reaction facilitated by the moisture present on the metal surface. Hence, drying metals would inhibit the charge transfer reaction and significantly reduce the degree of corrosion occurring.

There are basic similarities between the corrosion of metals and electrochemical energy producing cells, such as batteries.

In these systems the current drawn from the cells mainly relies on the spontaneous reaction of metal dissolution and deposition which occurs on separated surfaces. But in the corrosion of metal, the cathodic and anodic reactions normally proceed at the same surface. Occasionally the reaction sites shift along the metal surface during the corrosion process.

Thermodynamically, in a spontaneous reaction, the total free energy change (ΔG^o) of the cathodic and anodic reaction is negative. The relationship between ΔG^o and equilibrium potential of the reactions are:

$$\Delta G^o = - nF \Delta E^o \qquad (3.3.1)$$

where ΔG^o = standard free energy change

n = number of electron transferred

F = Faraday's number

ΔE^o = difference of the standard equilibrium potential

The free energy will therefore be negative only when the difference in the standard equilibrium potential (ΔE^o) is positive. Hence, the standard equilibrium potential of the corroding metal should be more negative than the standard equilibrium potential of the cathodic reactant species.

Although, thermodynamic criteria provides general information concerning the corrosion of metals in specific environments, in practice a more detailed evaluation is required. This includes considerations of mass transfer and the electrochemical kinetics of the reactions involved.

3.3.1. Cathodic Reactions

In most corrosion surfaces, there is no clear boundary between anodic and cathodic reaction sites. Some reaction sites are stationary, whilst others move along the metal surface during the course of the corrosion process. The anodic reaction causes the release of electrons from metal, whilst the cathodic reaction spontaneously accepts electrons.

Generally, two types of cathodic reactions may be involved in the corrosion process. These are illustrated below:-

(a) $O_2 + H_2O + 4\ e \longrightarrow 4\ OH^-$

(b) $2\ H^+ + 2\ e \longrightarrow H_2$

The most common cathodic reaction on metals exposed to air or aqueous solution is oxygen reduction. This reaction is initiated by the dissolution of oxygen molecules into water or moisture covering the metal surface. Thesediffuse into the water - metal interface where reduction takes place. The rate of the reaction may be controlled by either mass transfer or kinetic limitations. Stirring the water increase the rate of reduction when it is mass transfer controlled, but has little effect when it is kinetically controlled.

In acidic solutions, or solutions containing complexing agents, the reduction of protons is the predominant cathodic reaction. This process has received considerable attention and the mechanism is described as follows:-

$$H_3^+O + e \longrightarrow H_{ad} + H_2O \quad (b1)$$

$$H_{ad} + H_{ad} \longrightarrow H_2 \quad (b2)$$

$$H_3O^+ + H_{ad} + e \longrightarrow H_2 + H_2O \quad (b3)$$

In order to evaluate the importance of these processes upon the overall corrosion rate, the metal activity and reaction kinetics must be fully understood. Generally, step b2 is rate limiting, and hence the overall reaction rate will mainly be dependant upon the heat of adsorption of hydrogen atoms on the metals.

3.3.2. Metal Dissolution Reaction

The majority of metals are covered with an oxide layer which is formed during their manufacturing process or storage period. Under atmospheric conditions, the stability of these metal oxides is variable. For corrosion to occur, some of this layer has to be removed, to allow the metal surface to come into contact with atmospheric moisture or water. Some oxides are strongly attacked in both acid and basic environments which leads to the complete exposure of the metal surface. However, in neutral environments, oxide removal is slow and hence only a part of the surface will be exposed to the environment.

For construction and engineering purposes, an accurate preliminary analysis of metal corrosion in specific environments is of paramount importance. Thermodynamics may therefore be of use in this situation. As has been mentioned concerning the spontaneity of the corrosion reaction, however the analysis of

potential versus a pH representation of equilibrium potentials is also useful. The approach is as follows:- suppose reaction $M \longrightarrow M^{+n} + ne$ (metal dissolution) does not involve proton transfer. The equilibrium potential will be independent of pH and can therefore be represented on a potential vs pH diagram as a line parallel to the pH axis, consider that the cathodic reaction is : $2H^+ + 2e \longrightarrow H_2$, and involves proton and electron transfer. Therefore, the equilibrium potential of this reaction is pH dependent and is represented by a line sloping down in the diagram. Once the diagrams of both reactions are constructed, it is possible to predict the corrosion of metal in a specific pH solution.

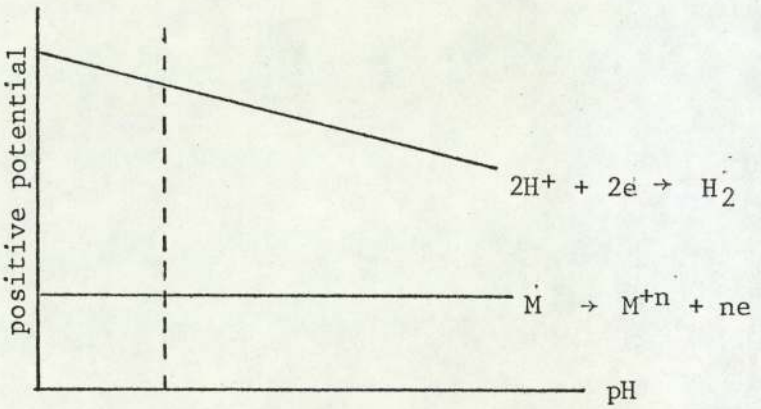

This is accomplished by drawing a line perpendicular to the pH axis at a particular pH value. Corrosion will occur spontaneously if this line intercepts the line representing the $2H^+ + 2e \longrightarrow H_2$ reaction at a more positive potential.

However, both of the methods mentioned above assumed that the ultimate product of the dissolved metal to be an ionic species. This is not necessarily valid, as solid oxides or hydroxides may be produced via a dissolution - precipitation

mechanism. The formation of an oxide/hydroxide film on the metal surface in some cases is thermodynamically stable and hence protects the metal from further dissolution.

Pourbaix[84,85] combined the solubility data of metal oxide/hydroxides with the thermodynamic data of reaction that occur between the metal and water, to construct a detailed potential-pH diagram. This diagram indicates the potential and pH conditions under which a metal and its solid products will be thermodynamically stable.

The potential-pH diagram is based mainly on thermodynamic principles, and therefore does not always indicate a totally accurate picture of the rate of corrosion processes occurring, since the kinetics of various processes need to be considered. However, correlation with electrochemical principles provides a more complete understanding, i.e. Evan's diagram may be used. This is constructed by the graphical superposition of the current-potential relationship for metal dissolution and its corresponding cathodic reactions. The current-potential relationships of each reaction is obtained either experimentally or from electrochemical kinetics combined with mass transfer parameters. These include exchange current density, transfer coefficient and limiting current density, etc. In addition, this diagram demonstrates the effect of the kinetics and mass transfer parameters upon the rate of corrosion.

3.4. Free Radical Chlorination of Hydrocarbons

Direct introduction of chloro-substituents into organic molecules can be achieved by free-radical chlorination. Amongst the most thoroughly studied chlorination reactions is the substitutive chlorination of saturated hydrocarbons. This has long been recognised as being characteristic of a chain reaction with free radicals as chain carriers. An initiation reaction is necessary to generate free radicals and this may be caused in several ways.

(a) Irradiation

Most bonds in organic compounds have energies of the order 50-95 Kcal/mole. To cleave these bonds photolytically, light energy of similar magnitude is required. Hence, ultra violet or visible light is used, provided the substance irradiated can absorb it. This method has two advantages: firstly, it may be used at low temperature. Secondly, the rate of free radical formation may be closely controlled by the adjustment of the light intensity and the concentration of the energy absorbing species. But, there are also disadvantages involved with this technique, particularly if the reaction products are light sensitive. Also, the irradiation reaction may only be carried out in silica glass vessels.

(b) Thermal Homolysis

The production of free radicals for use in the temperature range 50^{o}-150^{o}C in which reaction can most conveniently

be carried out, requires initiators with bond strength in the order of 25-35 Kcal/mole. Several groups of compounds meet this requirement and include some peroxides, peroxy esters and bisazo compounds.

There are several factors which determine the efficiency and usefulness of the initiator. These are:-

(i) the temperature required for a suitable rate of decomposition

(ii) the efficiency of the radical production

(iii) the reactivity of the radicals generated.

To date , azobis isobutyro-nitrile (A.I.B.N.) is the best azo type initiator. This is due to several factors:- firstly, its temperature of decomposition is approximately 65-80^{o}C, which is suitable for most reaction; secondly, its rate of decomposition is little affected by the solvent used. Finally, it is not susceptible to radical attack.

(c) Redox Reactions

The decomposition of peroxides at low temperatures is achieved by the redox reaction between transition metals and peroxides such as ferrous ion and hydrogen peroxide. This method of free radical generation is useful for reactions occurring in aqueous solutions, in particular low temperature emulsion polymerization.

Radical formation by electron transfer is not limited to systems involving metals and their ions. In fact, there is a large group of reactions which proceed by electron transfer

between electron rich (donor) and electron deficient (acceptor) compounds.[86]

The most commonly used agent for free radical chlorination is chlorine gas. The chlorination of some simple saturated hydrocarbons are normally carried out in both the vapour and liquid phase. Steacie[87] summarized several of the kinetic studies of thermal and photolytically induced free radical chlorination reactions. Generally, the mechanisms involved are as follows:-

$$Cl_2 \longrightarrow 2\,Cl\cdot \qquad (3.4.1)$$

$$Cl\cdot + R\text{-}H \longrightarrow HCl + R\cdot \qquad (3.4.2)$$

$$R\cdot + Cl_2 \longrightarrow RCl + Cl\cdot \qquad (3.4.3)$$

$$\left.\begin{array}{l} R\cdot + R\cdot \\ R\cdot + Cl\cdot \\ Cl\cdot + Cl\cdot \end{array}\right\} \quad \text{termination steps.}$$

In the above reaction, the chlorine radical is a chain carrier. However, the detailed kinetics are complex, because the termination steps are not completely understood.

There are several other agents which have been successfully used for chlorination reactions. Sulphuryl chloride was used to chlorinate saturated hydrocarbons with benzoyl peroxide as catalyst.[88] This reaction produced alkyl chloride, hydrogen chloride and sulphur dioxide. In the chlorination of toluene 80-100% yield of the chloride was reported.[88] The reaction was suggested to proceed via the following mechanism:-

$$Cl\cdot + R\text{-}H \longrightarrow R\cdot + HCl \qquad (3.4.4)$$

$$R\cdot + SO_2Cl_2 \longrightarrow RCl + \cdot SO_2Cl \qquad (3.4.5)$$

$$\cdot SO_2Cl \rightleftharpoons SO_2 + Cl\cdot \qquad (3.4.6)$$

$$\cdot SO_2Cl + RH \longrightarrow SO_2 + R\cdot + HCl \qquad (3.4.7)$$

In the chlorination of some hydrocarbons, sulphuryl chloride was found to be more selective than chlorine,[89,90] which suggested step (3.4.6) existed in equilibrium. Hence, the abstraction of hydrogen the atom was performed by both chlorine and chlorosulphuryl radicals.

Russell[90] showed that the use of benzene (8M) as a solvent eliminated the difference in the selectivity of chlorine and sulphuryl chloride. This was thought to be due to complex formation of the radicals with benzene, the reaction proceeding through these complexes rather than chlorine or chlorosulphuryl radicals.

Free radical chlorination of saturated hydrocarbons using t-butylhypochlorite (t-BUOCl) catalysed by AIBN was studied by Walling and Jacksaw.[91] An 84% conversion of toluene into benzyl chloride was achieved from this reaction, which is described below:-

$$t\text{-}BUO\cdot + R\text{-}H \longrightarrow t\text{-}BUOH + R\cdot \qquad (3.4.8)$$

$$R\cdot + t\text{-}BUOCl \longrightarrow RCl + t\text{-}BUO\cdot \qquad (3.4.9)$$

$$2t\text{-}BUO\cdot \qquad (3.4.10)$$

$$2\ R\cdot \qquad (3.4.11)$$

$$t\text{-}BUO\cdot$$

(3.4.10), (3.4.11) and $t\text{-}BUO\cdot$: termination reaction

The reaction was reported to proceed via propagation steps (3.4.8),(3.4.9) and termination steps (3.4.10) to (3.4.11)

This suggested that the t-butoxy radical was a chain carrier, and hence was more selective than chlorine. Since reactions with t-butyl hypochlorite produce non-acidic species, it is useful for the synthesis of acid sensitive substances.

Chlorination of hydrocarbons using N-chlorosuccinimide in carbon tetrachloride in the presence of benzoyl peroxide or ultra-violet light was also reported.[92,93] However, these reactions showed similar selectivity to chlorine, which indicated the involvement of chlorine radical chains rather than succimidyl radicals. Goldfinger[94] suggested that small traces of HCl in the solution could lead to the formation of chlorine via the following reaction:-

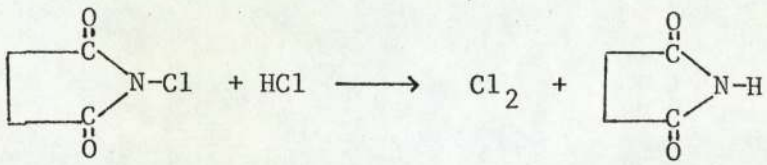

The overall chlorination reaction was described as follows:-

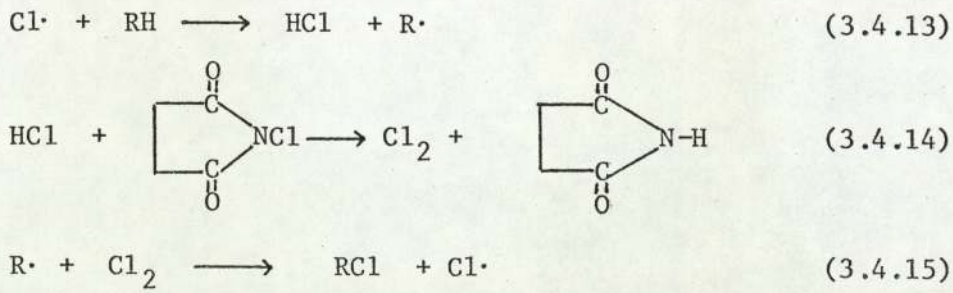

The chlorination of toluene using trichloroisocyanuric acid (T.C.A.) was studied by Jeunge et al.[95] The reaction was found to be sensitive to both the solvent and catalyst used in the reaction. When the reaction was carried out in a non-polar

solvent in the presence of benzoyl peroxide or ultra-violet light, it followed a free radical mechanism proposed by Goldfinger et al.[94] Nascent HCl resulted in the steady state formation of chlorine, with the subsequent formation of chlorine radicals. The reaction mechanism was described as follows:

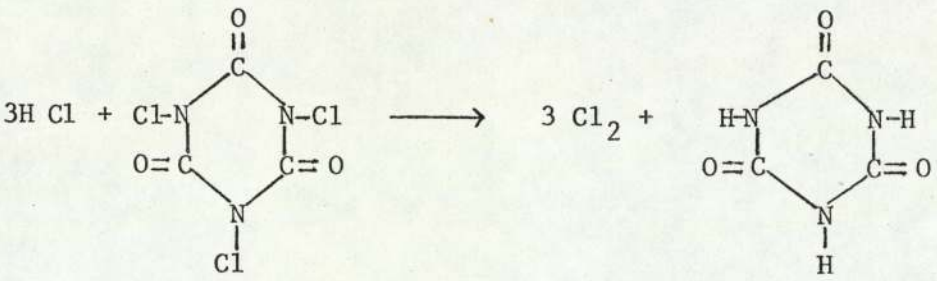

(3.416)

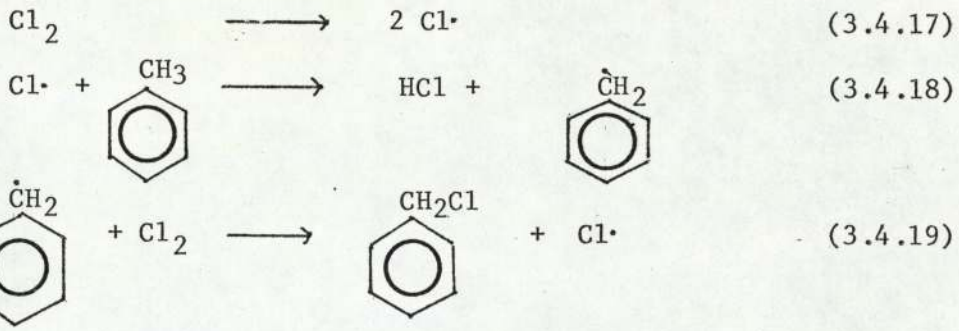

(3.4.17)

(3.4.18)

(3.4.19)

And the presence of sulphuric acid or ferric chloride as catalysts leads to an ionic reaction which results in the formation of chlorotoluene derivatives.[95]

3.5. Theoretical Approach

3.5.1. Electrochemical Self Discharge Reaction

The surface of acetylene black is made more hydrophilic by the presence of adsorbed surface groups, particularly acidic groups. This hydrophilicity leads to the adsorption of moisture on the acetylene black surface. When mixed with T.C.A. powder, this moisture hydrolyze it to form other chlorine carrying species

such as OCl^- or Cl_2. Since these species are highly reactive electrochemically they are easily reduced via the following reactions:-

$$Cl_2 + 2e \longrightarrow 2\,Cl^- \qquad (3.5.1)$$

$$E^o_{Cl_2/Cl^-} = 1.35 \text{ volt}$$

or

$$2\,OCl^- + H_2O + 2\,e \longrightarrow 2\,Cl^- + 2OH^- \qquad (3.5.2)$$

$$E^o_{OCl^-/Cl^-} = 0.86 \text{ volt}$$

Graphite itself is known to be oxidized electrochemically at anodic potentials.[78,81,82] It produces adsorbed oxygen and hydroxides in the form of lower oxides (CO_L) and higher oxides (CO_H) via the reactions described below:-

$$C + H_2O \longrightarrow 2H^+ + CO + 2e \qquad (3.5.3)$$

$$E^o = 0.52 \text{ volt}$$

or

$$C + 2\,H_2O \longrightarrow CO_2 + 4\,H^+ + 4e \qquad (3.5.4)$$

$$E^o = 0.21 \text{ volt}$$

Since these reactions (3.5.1 to 3.5.4.) may occur at the same surface, it is possible that a corrosion cell may be established. This will take place spontaneously only if the ΔG^o value for the reactions is negative, or, if the current-potential curve for both cathodic and anodic reactions intercept, at a point which is negative with respect to the equilibrium potential of the cathodic reaction.

3.5.2. The Free Radical Chlorination Reaction

The use of T.C.A. as a side chain and allylic chlorinating agent was reported by a number of workers.[94-97]

Conventionally, these reactions were initiated in the presence of free radical initiators which included benzoyl peroxide, A.I.B.N. and ultra-violet irradiation. However, it is suspected that free radical reactions may also occur in the presence of acetylene black, which acts as a free radical initiator.

Since free radical species are highly reactive, particularly chlorine radicals, their direct detection is very difficult. There are, however, several methods which are useful. These include:-

(i) Standard free radical chlorination reaction:-

The existence of a side chain and an aromatic ring in the molecule has made toluene a convenient substrate for studying the competition reaction between free radical and nuclear chlorination reactions. It is expected that benzyl chloride will be produced when the chlorination proceeds via a free radical path way, whilst the nuclear reaction will produce chloro-toluene derivatives.

In the presence of acetylene black the chlorination of toluene using T.C.A. may proceed via the mechanism described below:-

Scheme I

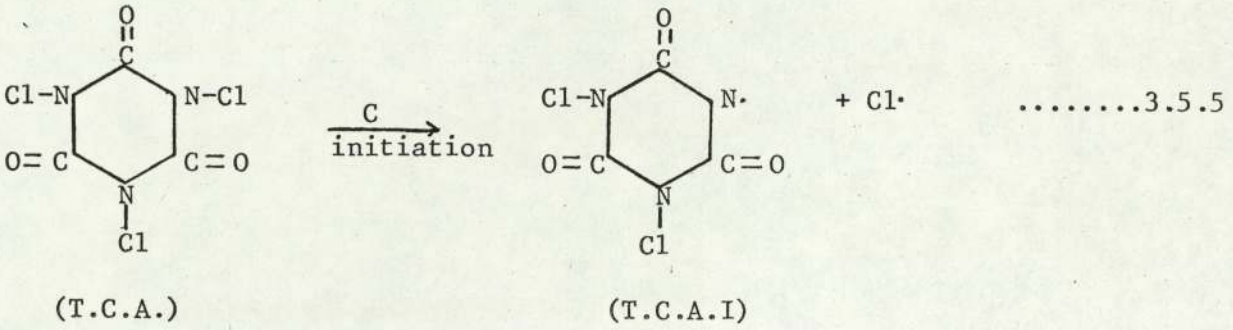

(T.C.A.) (T.C.A.I) 3.5.5

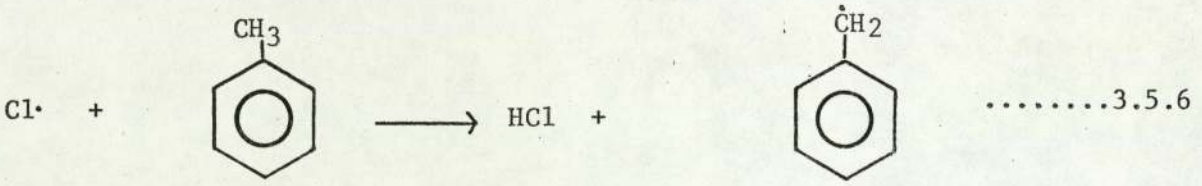

.....3.5.6

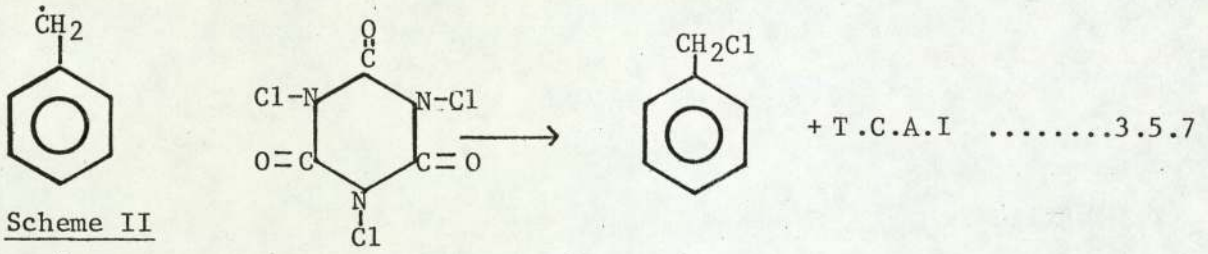

.....3.5.7

Scheme II

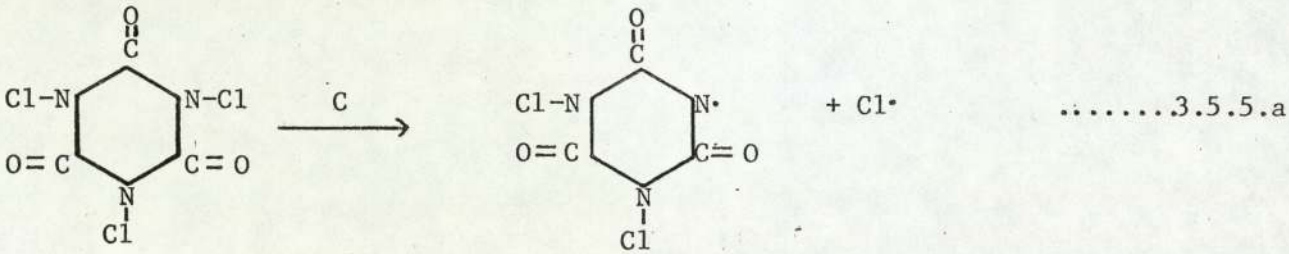

T.C.A. T.C.A.I 3.5.5.a

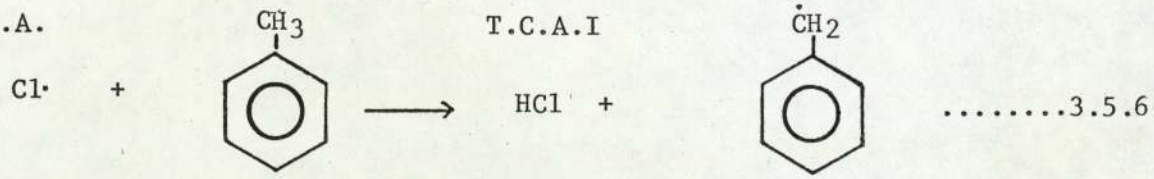

.....3.5.6.a[1]

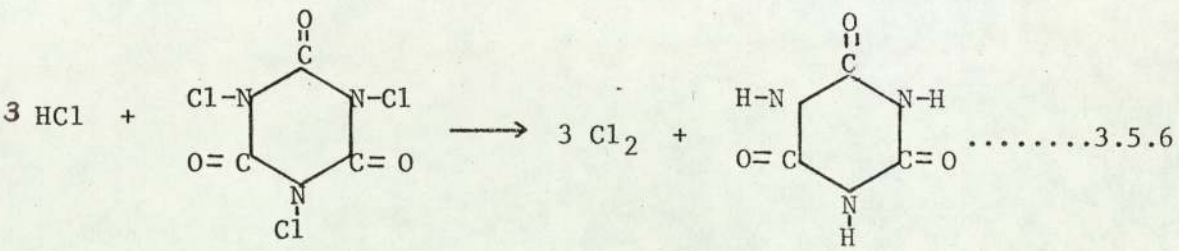

.....3.5.6.a

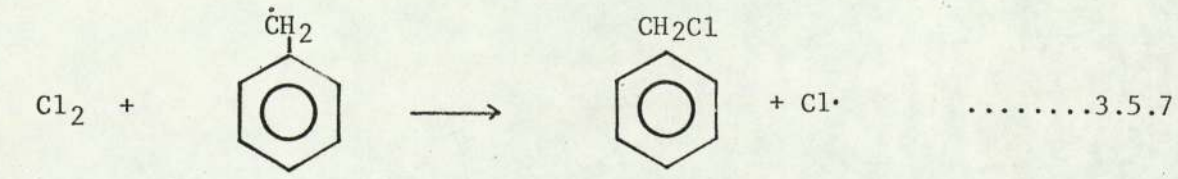

.....3.5.7.a

It is clear that both reaction schemes show the formation of benzyl chloride. The free radical reaction will therefore be confirmed if benzyl chloride was found in the reaction mixture containing toluene, T.C.A. and acetylene black.

(ii) Using α, α-diphenyl -β-picrylhydrazyl (DPPH) as a free radical scavenger

The inhibitory action of the stable free radical (DPPH) on a reaction or polymerization process is generally taken as evidence supporting a free radical mechanism.[98]

DPPH is a stable crystalline solid and easily dissolves in benzene to produce a violet solution. This solution is stable up to 80°C and has an absorption maximum at 520μm and 320μm.[100]

Although DPPH itself is a free radical, it is not sufficiently active to initiate most free radical reactions, but will react rapidly with radical intermediates.[99] As a tool for studying free radical reaction, therefore DPPH is often preferred to more conventional inhibitors such as phenols, quinones and amines for two main reasons Firstly, the reaction of DPPH with radical intermediates can be immediately observed by bleaching of the violet solution. Secondly, the DPPH reaction will proceed in proportion to the concentration of the radical intermediates. The observed bleaching of the solution may be monitored spectroscopically, to give a quantitative analysis of the reaction occurring.

3.6. Experimental

3.6.1. Half Cell Measurement of the Corrosion Reactions

The current-potential relationships of both the cathodic and anodic reactions were obtained using potential dynamic techniques. The experimental set-up is illustrated in Fig. 5 It includes the use of a potentiostat (chemical electronics), a linear sweep generator (chemical electronics) an X-Y recorder (Bryan 2900) and a digital voltmeter (Gould).

The working electrode utilized was $1cm^2$ pyrolytic graphite which was connected to nickel wire using silver araldite. The face in contact with the nickel wire was sealed with silicon rubber solution. A 5 cm^2 platinum screen was used as a counter-electrode, whilst the reference electrode was a standard calomel electrode (SCE), placed inside a luggin capilary compartment. The electrolyte used was 4M NaCl containing 3.3 and 4.3 x 10^{-2} moles/ℓ of T.C.A. respectively. The pH of this solution was adjusted by addition of dilute HCl. The solution was deaerated using nitrogen (white spot, BOC).

Prior to anodic polarization the electrode was cleaned cathodically by holding the potential at -1.0 volt vs SCE for 10 minutes. Both cathodic and anodic polarization were initiated at the open circuit potential of the electrode.

3.6.2. Chlorination of Toluene

(i) The chlorination of toluene was carried out by dissolving 0.3g of T.C.A. in benzene (50 ml) and toluene (20 ml), 0.3g of acetylene black was then added into the solution. The mixture

was mechanically agitated in a closed round bottomed flask for 72 hours.

The acetylene black was then removed by filtration. The unreacted T.C.A. was removed by addition of 10% KI solution, followed by rapid titration with 0.1N sodium - thiosulphate solution until the colour of the solution dissipated. The resulting solution consisted of an aqueous and organic phase. The organic phase was separated, dried over sodium sulphate and filtered. Benzene and toluene were removed by fractional distillation, thereby producing benzyl chloride as a residue. This compound is unstable and deleterious to gas chromatographic columns and inlet parts. Therefore it was converted into benzyl methyl ether, by reaction with sodium methoxide.

(ii) Synthesis of reference compound - benzyl methyl ether.
0.5g of sodium metal were dissolved in methanol (50 ml) and pure benzyl chloride (20 ml) were added. The solution was refluxed at 40°C for one hour. Excess of methanol was removed by distillation. A second distillation was performed in a micro-distillation column to separate the benzyl methyl ether from sodium chloride.

(iii) Analysis of the reaction product.
The reaction product was analysed using a gas liquid chromatograph (Pye series 104) using a 15% carbonwax 20 m on universal support 60 - 80 mesh column. The parameters of the GLC were as follows:- T = 90°C, Carrier gas (N_2) velocity = 60 ml/min recorder speed = 30 inc/hr.

A sample of pure benzyl methyl ether was injected to obtain a reference peak, then a sample of the reaction product was analysed.

3.6.3. Reaction of T.C.A. with DPPH

Approximately 0.005g - 0.1g T.C.A. powder was accurately weighed and dissolved in a benzene solution containing 1.33×10^{-4}M DPPH, and 0.3g acetylene black was added.

The mixture was agitated mechanically in the dark. 5ml aliquots were removed after varying time lapses and filtered. The aliquots were analyzed in a spectrophotometer (Perkin Elmer 402) using benzene as a reference compound.

Simultaneously DPPH solution containing only acetylene black and T.C.A. were analysed separately. This insured there was no interaction between DPPH with T.C.A. or DPPH with acetylene black alone.

3.7. Results and Discussion

3.7.1. Electrochemical Self Discharge Reaction

Based on the standard equilibrium potential shown in equations (3.5.1) to (3.5.4), it was calculated that ΔE^{o} was a positive value. This indicated that ΔG^{o} was negative, and suggested that thermodynamically the corrosion reaction would take place spontaneously.

Additionally, the current-potential curve of both the graphite oxidation and chlorine reduction intercepted at a potential negative with respect to the equilibrium potential of the chlorine.(Fig. 6) These results further confirmed the spontaneity of the corrosion reaction.

Figures 6 and 7 also showed that the anodic polarization curve was not affected when pH of the solution varied from pH = 1 to pH = 7. These results were similar to those obtained by Hine[78] and Laser.[81] A low oxide (CO_L) peak was found at V=+0.5 volt vs SCE. At potentials greater than +0.9 volt a sharp increase in anodic current was observed, which was due to the formation of a higher oxide (CO_H).[78,82]

However, the pH of the solution profoundly affected both the open circuit potential as well as the magnitude of current at a specific potential of chlorine reduction reaction. Both of these values were higher in acidic environments (pH=1) than in neutral solution (pH=7). This could be due to the fact that at low pH T.C.A. was predominantly converted into chlorine,[16] whilst at pH = 7 the solution may contain a mixture of chlorine, hypochlorite and

other chloro-cyanuricacid derivatives. These species not only affect the open circuit potential of the electrode but also the polarization behaviour of the system. At present the behaviour of T.C.A. in neutral solutions is not yet clear, and hence concrete conclusions cannot be drawn from these results.

It is important to note that protons were produced during the graphite oxidization reaction.(see equations 5.3.3. and 5.3.4) The presence of these ions will consequently increase the acidity of the T.C.A./acetylene black mixture. Thus the reaction between T.C.A. and HCl will be favoured and will increase the rate of chlorine liberation.

3.7.2. Free Radical Reaction

The gas liquid chromatographic analysis illustrated that benzyl chloride was found in the reaction mixture containing T.C.A., toluene and acetylene black.(Fig. 8c) However, no trace of benzyl chloride was found in the mixture containing no acetylene black.(Fig. 8b) This indicated that the acetylene black was of paramount importance in promoting the formation of the benzyl chloride via a free radical mechanism. The formation of chlorine radicals possibly being caused by interaction between T.C.A. and acetylene black. The overall reaction mechanism may proceed via reactions (3.5.5) to (3.5.7). Since HCl was produced during the reaction (3.5.6) it is possible that it will react with T.C.A. and generate chlorine molecules. If this reaction is fast, the chlorination will proceed via reactions

(3.5.5.a) to (3.5.7.a) as suggested by Goldfinger et al.[94] Hence, after a period of time reaction (3.5.5.a) becomes unimportant and the chlorine radical will mainly be generated from a reaction between chlorine and acetylene black. The T.C.A acts only as a chlorine source providing chlorine molecules by reacting with HCl.

Further evidence of the presence of chlorine radicals in the reaction mixture containing T.C.A. and acetylene black was obtained from DPPH analysis. This showed that a depletion of DPPH occurred when both T.C.A. and acetylene black were present. But no sign of DPPH depletion was apparent when only DPPH - T.C.A. and DPPH - acetylene black were present.(Fig.10) This strongly suggests that formation of the free radicals was mainly due to the T.C.A./acetylene black interaction. Additionally, the results illustrated that the initials rate of DPPH depletion was directly dependant upon T.C.A. concentration.(Fig.9) The rate was accelerated when T.C.A. was replaced by chlorine gas.(Fig. 10) This may be caused by the presence of the Cl-Cl bond which is weaker in comparison to the N-Cl bond ($D^{298^oC}_{Cl-Cl}$ = 57.93 KCal/mole, $D^{298^oC}_{N-Cl}$ =93 KCal/mole)

Solomon et al.[101] studied the reaction of DPPH with aqueous HCl as well as chlorine. They suggested the bleaching of DPPH was mainly due to the formation of DPPH-H and its chloroderivatives. They also found that when chlorine gas was introduced into the solution containing DPPH-H the violet

colour of the solution was gradually restored which was an indication of traces of free radicals. They showed that the new radicals was 2(p-chloro)phenyl-2-phenyl picryl hydrazyl.

According to their results it was clear that DPPH did not react directly with chlorine. Similarly, in this investigation no depletion of DPPH was observed in solutions containing only chlorine and T.C.A.(Fig. 10), but depletion did occur when this solution was irradiated with ultra violet light (Fig. 10), which suggested a free radical reaction was occurring.

The depletion increased when acetylene black was introduced into the chlorine containing solution, indicating its catalytic action. Hence, chlorine became reactive to DPPH only when radical initiators were present. In this system chlorine radicals may abstract hydrogen atoms from the acetylene black surface and subsequently form HCl which will react with DPPH in the manner suggested by Solomon.[101] However, this is not the only reaction causing DPPH depletion, as it also occurs in the absence of acetylene black, under U.V. irradiation. Eventually, in such systems no hydrogen atoms will be available for abstraction and consequently HCl will no longer be formed. It is possible therefore, that depletion of DPPH may be caused by a direct reaction with chlorine radicals, thus forming DPPH-Cl. Since the analysis of this compound has not yet been carried out, no definite conclusions may yet be made.

The results in this chapter indicate that chlorine losses from T.C.A./acetylene black mixture may be attributed to

either free radical formation or electrochemical self-discharge reactions, or a combination of both. There is little information concerning the kinetics of these reactions and therefore identification of the dominant reaction is difficult. But analysis has shown that both reactions tend to produce hydrochloric acid which reacts quickly with T.C.A. to liberate chlorine gas.(Fig. 11)

The production of hydrochloric acid will eventually saturate the limited moisture adsorbed on the acetylene black surface. Once this is supersaturated, HCl will exist as gaseous HCl. This excess gas may penetrate deeply into every individual T.C.A. aggregate and extend the reaction zone from the interface to the inside of the aggregate and hence accelerate chlorine liberation.

CHAPTER FOUR

STORAGE STABILITY AND ELECTROCHEMICAL DISCHARGE CHARACTERISTIC OF T.C.A. CATHODES

CHAPTER 4

4. STORAGE STABILITY AND ELECTROCHEMICAL DISCHARGE CHARACTERISTIC OF T.C.A. CATHODES

4.1. Introduction

The addition of boric acid powder in the T.C.A./acetylene black cathode to suppress the rate of chlorine liberation during storage has achieved some success,[12] although only temporary since, after prolonged storage, a considerable amount of chlorine loss still occurs. Further improvements on the storage stability of these systems are required.

In order to achieve such an improvements on the long term storage stability, it is important to have a good understanding of the reasons why chlorine losses occur. The data provided in Chapter 3 indicated several factors which may be related to this problem. The reaction was found to be initiated by the interfacial contact of the T.C.A. and acetylene black aggregates, which was followed by electrochemical self discharge and free radical reactions. Subsequently, HCl was produced during these processes, which tended to react quickly with T.C.A., thereby resulting in the evolution of free chlorine in the cathode mixture.

Based on this information, the following preventative measures were undertaken:-

(i) Removal of HCl generated in the cathode

Several zeolites such as zeolite A, zeolite X, mordenite and cliptonoliolite are known to be effective HCl quenching agent in aqueous solution. The zeolites consist of interlinked metal oxides which remove HCl by an ionic exchange reaction. If removal

is efficient, then the reaction between HCl and T.C.A. will be significantly reduced, thereby diminishing chlorine liberation.

(ii) Segregation of T.C.A. and acetylene black aggregates

Perhaps the most efficient method for preventing chlorine loss is to minimize the surface contact between the T.C.A. and acetylene black aggregates. Ideally, these aggregates would be stored separately and mixed only when discharge is required, but, in practice, many difficulties will be encountered unless an appropriate arrangement for the segregation of these two components is made in the design of the cathode.

One possibility is the bulk separation of T.C.A. and acetylene black aggregates. In this system, the cathode consists of a few layers of T.C.A. sandwiched in between layers of acetylene black, as shown below:-

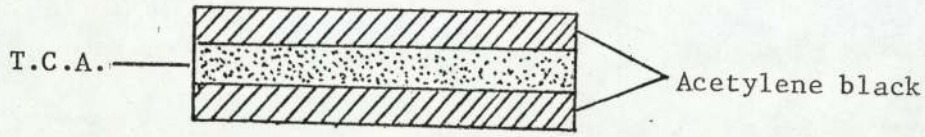

Hence, contact is limited to the interface of each layer. This contact may be completely eliminated by the addition of boric acid (or boric oxide) powder at the interface. In such an arrangement, however, the cathode performance will be adversely affected by mass transfer limitations. These may be reduced by careful design of layer thickness and porosity. In practice, a compromise has to be made between the storage stability and the electrochemical performance of sandwich type cathodes.

4.2. Experimental

4.2.1. Sample Preparation for Storage Tests

The mixed type cathodes were prepared by mixing acetylene black and T.C.A. powders, followed by addition of boric acid and zeolites. The composition of these samples is illustrated in Table 3.

The sandwich type cathodes were prepared by layering T.C.A. powder between two layers of acetylene black powder. This was pressed in a mould. In some cases, boric acid (or boric oxide) was added at the T.C.A. acetylene black interface.

4.2.2. Cathode Preparation

The mixed type cathode discs were prepared by mixing T.C.A, viscous fibre and acetylene black. This was compressed in a steel mould. The cathode specification is shown in Table 1.

The sandwich type cathode plaques were manufactured as follows:-

Known amounts of T.C.A. powders (Table 2) were equally divided either into 4 (low rate) or 6 (high rate) portions. Each portion of the T.C.A. powder was sandwiched between two layers of acetylene black powder in a mould. In some instances boric acid (or boric oxide) was added at the interfaces. This process was repeated until all the T.C.A. powder was utilized. The mould was then pressed and the resulting cathode plaques were transferred into a desiccator for storage. The cathode specification is shown in Table 2.

4.2.3. Single Cell Assembly

A single cell was designed to examine the discharge characteristics of the various types of cathodes:-

(a) High rate discharge

The cell assembly is illustrated in Fig. 12. A cathode disc (5 cm^2) was located on a platinum current collector, and a gasket of appropriate thickness encircled it to control its compression and bulk density during discharge. Whatman filter paper was used to separate the cathode and anode. The anode was manufactured from quarternary aluminium alloy (British Non-Ferrous Metal Research Association) whose surface was dimpled and perforated to allow the uniform distribution of electrolyte. The anode was also encircled by a gasket. The cell was then compressed between two parallel steel sheets, which possessed inlet and outlet parts for the electrolyte passage. At the beginning of the discharge the cell was primed by the circulation of electrolytes (1.5M $AlCl_3$/0.5M NaCl) at 60°C, for two minutes, this was then replaced by 0.5M NaCl solution at 60°C. The temperature of the electrolyte was gradually increased to 95°C at a rate of 10°C/minute, in order to maintain the voltage plateau. A 5 ohm resistor was connected across the cell and the cell voltage was monitored by a pen recorder (J.J. Instruments, model 520).

(b) Low rate discharge

The cell assembly was basically similar to that described above. The electrolyte was a mixture of 1.5M $AlCl_3$ and 0.5M NaCl.

The cell was discharged under static electrolyte conditions at 25°C. The cell components were compressed between two perspex sheets. The sheet adjacent to the anode was perforated in order to allow electrolyte penetration into the cathode plaque. Additionally, a P.V.C. mesh was placed between the anode and separator to release bubbles which would otherwise be trapped during discharge.(Fig. 13)

The cell was discharged at a current density of 5 mA/cm^2, and the cell voltage was monitored using a pen recorder (J.J. Instrument, model 520).

4.3. Results and Discussions

4.3.1. The Effects of Stabilizer on Cathode Storage Stability

The addition of zeolites into the T.C.A.-acetylene black mixture does not inhibit loss of chlorine, in fact they tend to accelerate it (Table 3). Since these compounds consist of interlinked oxides, this structure may contribute to their catalytic action. The quenching action of these zeolites is mainly dependant upon an exchange reaction between H^+ with the metal ions in the zeolite and this reaction requires the presence of water. As only a limited amount of moisture is available in the reaction mixture, it is possible that this will inhibit the quenching reaction.

The sandwich type cathodes generally exhibit better storage stability in comparison to the mixed type cathodes (Table 4). The addition of boric acid at the T.C.A.-acetylene black interface further improved the cathode stability.

Theoretically the presence of this substance should completely prevent the interfacial contact between the T.C.A. and acetylene black layers, hence eliminating chlorine losses during storage. However, the data indicate a considerable loss of chlorine still occurs. It is possible that this is due to the fact that as only a small amount of boric acid was used, it was insufficient to cover the interface of the plaque. The aggregate size of acetylene black powder is generally much smaller than those of boric acid. Hence, it is very likely that these aggregates will inevitably go through the boric acid layer and come into contact with the T.C.A. layer and these species will react together. Any HCl produced at the interface will penetrate into and react with the T.C.A. layer, thereby evolving chlorine.

Two possible methods may be used to prevent the contact between acetylene black and T.C.A. layer. Firstly, the amount of boric acid added at the interface may be increased. Alternatively, the size of the boric acid aggregates may be reduced. However, both methods tend to prevent the diffusion of chlorine from the T.C.A. layer into the acetylene black layer during discharge and thus lead to an increase in the mass transfer polarization. Further work is necessary therefore to optimize the cathode design so that good storage stability and good performance can be achieved.

4.3.2. Discharge Characteristics of the Sandwich Type Cathode

(a) High rate discharge

The single cell discharge characteristics of both sandwich and mixed type cathode before storage are illustrated in Figures 14 and 15. The mixed type cathode has an average voltage plateau of 2.1 volts when the cathode had consumed 34% of its capacity. However, the sandwich cathode only has an average voltage plateau of 2.0 volts. This indicated that at high rate discharge the mixed type cathode generally give the best performance of the two types of cathodes. It may be that the sandwich type cathode tends to suffer more significant polarization effects, probably because of the slow diffusion of chlorine from T.C.A. layer into the acetylene black layer. This becomes crucial when the cathode is discharged at high rate.

The cathode with boric acid or filter paper at the T.C.A.-acetylene black interface generally illustrated low cell voltage and discharge efficiency (Fig. 14), the cathode with boric acid at the interface had an average voltage plateau of 1.9 volts this diminishing very rapidly after a period of time. More significant polarization was encountered when filter paper was present at the interface, as the cell produced an average plateau of only 1.6 volts. Both systems seem to indicate severe mass transfer polarization when an extra diffusion layer was introduced into the T.C.A. acetylene black interface.

The sandwich type cathode exhibited more stable storage characteristics and hence it would be expected to retain greater

amounts of chlorine in comparison to the mixed type cathode. Therefore, it should illustrate better performance after a period of storage. After 24 hours storage at 40°C and 75% humidity, the cell voltage of both types of cathode was slightly reduced, particularly in the initial stages of discharge. The mixed type cathode discharged only 28% of its capacity at a voltage plateau of 2.05 volts (in comparison to 40% before storage), and its voltage was quickly diminished.(Figs. 15 & 16) At 1.5 volts it was able to deliver only 43% of its capacity (in comparison to 53% before storage). However, the sandwich type cathode generally exhibited a performance similar to that observed before storage.(Fig.15) This cathode only suffered a voltage drop at the beginning of discharge (Figs. 15 and 16). This was mainly due to the fact that reaction still occuredat the T.C.A.-acetylene black interface during storage, and this produces a sparingly soluble cyanuric acid, which therefore inhibits the diffusion of chlorine from the T.C.A. layer into the acetylene black layer. But the cell voltage recovered to the value similar so that observed before storage after 20% of its capacity.

After 120 hours storage under similar condition, both types of cathode suffered a significant drop in cell voltage during discharge. The average voltage plateau of the mixed and sandwich type cathodes are 1.85 volts and 1.75 volts respectively. (Figs. 15 and 16) The sandwich type cathode consistently illustrated superior storage stability, as it possesses a higher capacity in comparison to the mixed type cathode. Unfortunately,

however, the sandwich type cathode has a low cell voltage and an unexpectedly low discharge efficiency after storage. In theory, the sandwich type cathode should maintain a good performance in comparison to the mixed type cathode, particularly after storage, even though the interfacial reaction between T.C.A.-acetylene black cannot be avoided. This reaction should cease when the T.C.A. in contact with acetylene black has been consumed. This should not affect the T.C.A. in the bulk T.C.A. layer, which should remain stable. Therefore, the performance is expected to be similar to that after 24 hours storage. The fact that this was not the case may be due to the following reasons:-

(i) The formation of sparingly soluble reaction products e.g. cyanuric acid at the interface, which will inhibit the diffusion of chlorine into the acetylene black layer and decrease the cathode performance. This effect was shown when pure cyanuric acid was deliberately added at the acetylene black - T.C.A. interface.(Fig. 21) The diffusion is increasingly restricted after prolonged storage under humid and high temperature (40°C) conditions, when crystallization of cyanuric acid occurs.

(ii) Crystal growth of T.C.A. after prolonged storage at high humidity and temperature (75% humidity, 40°C), particularly after compression. The crystallization effect tends to enlarge the T.C.A. crystals hence reducing its surface area and the rate of chlorine liberation during discharge.

(iii) Apart from cyanuric acid, one of the main products was HCl.

It is likely that this substance may diffuse into the T.C.A. layer where it can react and liberates chlorine during storage, ultimately reducing the cathode capacity.

(b) Low rate discharge

The single cell discharge characteristics of both mixed and sandwich type cathode are illustrated in Figs. 17 and 18.

Without boric oxide at the T.C.A.-acetylene black interface the sandwich type cathode has an average cell voltage plateau of 2.25 volts when discharged at 5 mA/cm^2.(Fig. 18) Similar results were obtained with the mixed type cathode. Thus at low rate discharge, the sandwich type cathode does not seem to suffer from mass transfer limitation. At V = 1.5 volts the cathodes have a discharge efficiency of 50%.(Fig.22)

As was mentioned earlier, an interfacial reaction caused a deterioration in the capacity of the cathode. The addition of boric oxide (or boric acid) inhibits this reaction and consequently may diminish the performance of the cell due to mass transfer polarization. But on long-term storage this may be beneficial as a high amount of chlorine is retained in the sandwich type cathode, in comparison to that in the mixed type cathode.

The voltage-time profile of the sandwich cathode with boric oxide at the interface is illustrated in Fig. 17. The average voltage plateau was 2.05 volts which is lower than that observed in the mixed type cathode. Both types of cathode have a discharge efficiency of 50% at 1.5 volts.

After 24 hours storage, both cathodes showed a slight decline in cell voltage.(Figs.19 and 22) But this diagram clearly shows that the sandwich cathode has the higher capacity of the two. The mixed type cathode reached 1.0 volt after 3 hours discharge, whilst the sandwich cathode reached the same cell voltage after 4 hours. This indicates that the sandwich type cathode contained 25% more capacity than the mixed type cathode after storage.

The fact that the sandwich cathode appeared to possess better storage stability than the mixed type cathode gained further support when these systems were stored under similar condition for 48 hours.(Figs. 20 & 22) A further decline in the cell voltage was observed in both cathodes. The mixed type cathode took only 30 minutes to reach a cell voltage of 1.0 volt, whilst the sandwich type cathode took $2\frac{1}{4}$ hours to reach a similar voltage. Therefore, it had a capacity of approximately $4\frac{1}{2}$ times that of the mixed type cathode.

Generally, this data suggests that the sandwich type cathodes possess better storage stability in comparison to the conventional mixed type cathode. However, chlorine liberation still occurs to some extent, even in the presence of boric oxide at the T.C.A.-acetylene black interface. In addition, the cell voltage was consistently low, particularly after storage. These phenomena may be caused by the incomplete separation of the T.C.A. and acetylene black and the crystallization of T.C.A. as well as as the formation of interfacial reaction products, e.g. cyanuric acid, after storage at high temperature and humidity condition

(40°C, 75% humidity). However, it is possible that this type of cathode may be useful for low rate applications. Further work is required to further improve the cathode stability and electrochemical performance.

CHAPTER FIVE

THE KINETICS OF CHLORINE REDUCTION ON POROUS GRAPHITE SURFACE

CHAPTER 5

5. THE KINETICS OF CHLORINE REDUCTION ON POROUS GRAPHITE SURFACE

5.1. Introduction

In Chapter 4 it was claimed that sandwich type cathodes exhibit better storage stability and maintained good electrochemical performance at low current densities (5 mA/cm^2).

However, at low temperatures and with a static electrolyte, the performance of this system was controlled by the transportation of chlorine within the system. This could be due to the diffusion of chlorine in the T.C.A. or acetylene black layer. When the cathode was discharged,chlorine was immediately available at the acetylene black - T.C.A. interface, therefore its diffusion inside the T.C.A. layer was thought to be less important. Initially, the diffusion problem may be limited within the acetylene black layer, and a mathematical model was developed to describe this phenomena.

Prior to the evaluation of this model, it was important to completely understand the kinetics of the chlorine reduction from which the related rate equation and kinetic parameters such as real exchange current density and Tafel slope could be determined. In which the reliability of this model depended upon.

At present, this investigation is concerned mainly with the kinetics of chlorine reduction on graphite. However, the study of this process is difficult because of the instability of the graphite surfaces, due to oxide formation. According to Hine et al[78] and Littauer et al[69], oxides are formed electrochemi-

cally at anodic potentials. In some cases reaction occurred simultaneously with the reaction under study. Major changes in the composition of surface oxides tend to alter the state of the electrode surfaces which would then lead to a complication of the reaction. In order to prevent this, it is necessary that only a small amount of oxides is allowed to be formed or removed during the reaction. Hence, a stable surface state is maintained.

5.2. Electrochemical Kinetics of Chlorine

In the last decade, the electrochemical kinetics of the Cl_2/Cl^- couple have been widely studied. The importance of the chlor-alkali industry, however, meant that most of the studies have been concentrated on the kinetics of the chlorine evolution and very few kinetics studies of chlorine reduction have been reported.

Most of the kinetic work has been carried out on noble metals, graphite and metal oxides.

5.2.1. The Kinetics of the Cl_2/Cl^- Couple on Platinum Electrodes

The reaction of the Cl_2/Cl^- couple could proceed via the following schemes:-

$$Cl^-(aq) \rightleftarrows Cl_{ad} + e \quad \text{.....(5.1.a)}$$

$$2\,Cl_{ad} \rightleftarrows Cl_2(aq) \quad \text{.....(5.1.b)}$$

and

$$Cl^-(aq) \rightleftarrows Cl_{ad} + e \quad \text{.....(5.2.a)}$$

$$Cl_{ad} + Cl_{ad} \rightleftarrows Cl_2(aq) \quad \text{.....(5.2.a.1)}$$

$$Cl^-(aq) + Cl_{ad} \rightleftarrows Cl_2(aq) + e \quad \text{.....(5.2.b)}$$

The first theoretically important kinetic study of Cl^- oxidation was contributed by Wick and Chang[71], they carried out steady state polarization studies of Cl^- oxidation on platinum and iridium electrodes. From the current-voltage curves obtained, they suggested a slow electrochemical discharge step (5 .2.a).

Later Frumkin and Tadoradse[70] investigated chlorine reduction on a rotating disc platinum electrode in detail. Based on the results obtained, i.e. γ(stoichiometric number) = 2, $n^1_{Cl^-} = 0$, they proposed mechanism 5.2 in which 5.2.b was the rate determining step. It is important to note that the reaction order was obtained at an overpotential less than 40 mV, under which conditions the reverse rate of reaction (5.2.b) was completely neglected. There results have created some doubts amongst other researchers. Dickinson et al[134] studied the reduction of chlorine on rotating disc platinum electrode and found that the reaction order of chlorine ($n^1_{Cl_2}$) was a function of chlorine concentration. At low chlorine concentration $n^1_{Cl_2} = 1$ and at high concentration $n^1_{Cl_2} = 2/3$. The dependence of the reaction rate on Cl^- concentration and the non linearity of $(\frac{i_L i}{i_L - i})$ vs E suggests that the reduction goes through mechanism (5.2), with reaction (5.2.a) as the rate determining step. The galvanostatic pulse technique (10 m sec) was used recently by Yokohama and Enyo[135] to study cathodic and anodic reactions of the Cl_2/Cl^- couple on platinum electrodes. They found that a change in mechanism occurred over a relatively narrow range of potential, and the γ and $n^1_{Cl_2}$ values were potential dependent. At E < 1.3 V vs SHE, the reaction

proceeded according to mechanism (5.1), reaction (5.1.b) being the rate limiting step. The value of γ , $n^1_{Cl_2}$, $n^1_{Cl^-}$ were 1, 0.9 and 0 respectively. At E > 1.42 V vs SHE, the same mechanism applied, but the rate determining step was (5.1.a).

It is generally agreed that oxide coverage of platinum electrodes inhibited the oxidation of Cl^-[136]. Littauer and Shreir[69] found that the presence of an oxide layer inhibited the Cl^- oxidation, at high voltage the current-voltage curve showed two distinct linear relationships (e.g. E < 1.6 V, E > 2.0 V). A Tafel slope of 40 mV - 70 mV/decade and 120 mV/decade was reported at low and high surface coverage of oxide respectively.[138]

To date it is thought that the oxidation of Cl^- follows the mechanism (5.1) and the reduction of chlorine on platinum followed the mechanism (5.2), but there is disagreement upon which is the rate determining step. Indeed, experiments have shown that it is very much dependent on surface pretreatment of the electrode and the method of collecting experimental data.

5.2.2. Kinetics of Cl_2/Cl^- Couple on Metal Oxide Electrode

Since the introduction of the Dimensionally Stable Anode (D.S.A.) into the chlor-alkali industry, considerable efforts have been expanded to develop less expensive anodes.

Fiori and Fiata[137] studied the mechanism of Cl^- oxidation on thermally decomposed Ti, Ir and Ru mixed oxides. They obtained a Tafel slope of 40 mV/decade over a wide range of current densities, and concluded that Cl^- oxidation proceeded via

mechanism (5.1), with (5.1.b) being rate determining. Bianchi[139] suggested that the oxidation of Cl^- on RuO_2/TiO_2 followed the discharge - recombination pattern (5.1) but gave no proof for this mechanism. A Tafel slope of 33 mV/decade was obtained on the Ru/Ti mixed oxides[140] in the oxidation of Cl^-, but no limiting current was observed on the cathodic reduction of chlorine on the same electrode. Therefore, the recombination step (5.1.b) was discounted as a possible rate limiting step, as the γ value of the anodic region was less than one. Instead, they suggested that two parallel reactions were taking place, e.g. a retarded recombination (5.2.a1) and an electrochemical desorption (5.2.b) which preceeded the equilibrium discharge step (5.2.a).

Possible use of mixed $Cl^-/SO_4^=$ electrolyte for Cl^- oxidation on the Ru/Ti oxide has been studied by Bondar et al[141]. They found that at low current densities, (i.e. 500 A/m^2) $SO_4^=$ ion does not affect the potential at room temperature. But as current densities increased (e.g. 1000 A/m^2), a small amount of $SO_4^=$ significantly altered the anode potential, mainly the double layer effect. Recently, Erenberg et al[142] carried out a detailed study on the Ti/Ru oxide. They obtained a Tafel slope of 30 mV/decade, $\alpha = 1$ and $n^1_{Cl^-} = 1$, and postulated that the mechanism of Cl^- oxidation proceeded via the following routes:-

$$Cl^- (aq) \rightleftarrows Cl(ad) + e \quad \ldots\ldots\ldots\ldots\ldots\ldots (1)$$

$$Cl(ad) \rightleftarrows Cl^+ + e \quad \ldots\ldots\ldots\ldots\ldots\ldots (2)$$

$$Cl^+ + Cl^- \rightleftarrows Cl_2(aq) \quad \ldots\ldots\ldots\ldots\ldots\ldots (3)$$

Reaction (2) was the rate determining step. Further experiments

on chlorine reduction revealed a Tafel slope of $\geq$ 60 mV/decade with $n^1_{Cl_2} = 1$, $n^1_{Cl^-} = -1$.[143,144] Hence, they concluded that the reaction in the cathodic branch and anodic branches proceeded via the same route, and additionally, step (2) controlled the overall rate of reaction. A non-activation limiting current was also found during the cathodic polarization which was equal to the anodic exchange current. When this 'limiting' current was exceeded, the linear relationships between η and log i was re-established, but had a higher Tafel slope (e.g. 120 mV), and $n^1_{Cl_2} = 1$, $n^1_{Cl^-} = -1$. They therefore suggested that the chlorine reduction on the Ru/Ti mixed oxide proceeded via route (1) to (3), α changing from 1 to 0.5. This data also indicated that on the Ti/Ru mixed oxide, two active sites were contributing to the reduction of chlorine. This argument gained further support by experiments on the RuO_2 electrode. No break in the Tafel plot was observed it being maintained at 120 mV/decade over a wide range of potential.

Janssen et al[154] more recently used a potential decay method to study the oxidation of Cl^- on the Ru/Ti mixed oxide. A potential - decay time relationship for the Tafel and Heyrovsky type reactions was investigated. When mass transfer limitations were considered, the results showed that $\alpha = 0.5$ and Tafel slope = 40 mV/decade. After analysis they suggested that chlorine was evolved at both the anodic and open circuit potential. The chlorine evolution proceeded via the Tafel - Heyrovsky mechanism, and the Heyrovsky step controlled the reaction rate.

There is as yet no common agreement on the kinetics of the Cl_2/Cl^- couple on metal oxide electrodes, as the only data available are contradictory. This is probably due to the methods used in preparing the metal oxide electrode such as curing temperature.[137]

5.2.3. Kinetics of Cl_2/Cl^- Couple on Graphite

(a) Aqueous Solutions

The kinetics of Cl^- oxidation on graphite has been extensively studied. However, little work has been done on the reduction of chlorine on graphite.

Cl^- oxidation has been carried out both on porous and pyrolytic graphite. It was found that the kinetics of the reaction was dependent upon the history of the graphite, such as its method of manufacture and the period of time the electrode has been used for electrolysis.

The kinetics of Cl^- oxidation on a rotating disc porous graphite electrode was studied by Krishtalik et al.[145] They obtained a Tafel slope of 120 mV/decade and 240 mV/decade from the polarization curve which was double the value obtained on the planar electrode. Ksenzhek[146] claimed that this was due to the porous structure of the electrode.

By sealing the electrode with polyethylene, AgCl and $PbCl_2$ respectively, Krishtalik et al obtained a Tafel slope of 60 mV/decade, and 120 mV/decade whilst the γ value was 1 to 1.7. Additionally, pretreatment of the anode increased the activity

of the electrode, but had no effect on the shape of the polarization curve. This observed change of the Tafel slope from 60 mV/decade to 120 mV/decade in polarization curve is due to a change in the value of α from 1 to 0.5. This indicated a shift of reaction from a barrier - less discharge to a normal discharge. They therefore concluded that the oxidation of Cl^- proceeded via mechanism (5.2) and that reaction (5.2.a) was the rate determining step. The insensitivity of potential at low potential regions toward Fe^{3+} and $SO_4^=$ ions provided further support for this discharge mechanism, which is independent of the double layer structure.

More recently Hoogland and Janssen[76] carried out the oxidation of Cl^- on both aged and new porous graphite electrodes. In the new electrode the Tafel slope was 120 mV/decade over the whole range of potential, whilst on the aged electrode two different slopes were observed (i.e. 40 mv/decade, 120 mV/decade). However, $\alpha = 0.5$ for both types. They therefore suggested that the Cl^- oxidation proceeded via mechanism (5.2). Reactions (5.2.b)(5.2.a) occurred at the same rate on the aged electrodes, whilst step (5.2.b) was rate determining on new electrodes.

(b) Molten salt

The kinetics of Cl_2/Cl^- in molten salt has gained some attention recently, due to the development of a high energy density chlorine battery and production of sodium metal. Polarographic,[147] steady state[148] and transient[151] techniques have been used to study the kinetics of the Cl_2/Cl^- couple in molten salt.

Shain El Din[148] claimed that the kinetics of chlorine evolution in molten salt differed completely from that of aqueous solution. He suggested that the Cl^- oxidation reaction in molten salt was an activationless reaction. The overpotential-current relationships followed Ohm's law e.g. IR = η and the polarization was mainly originated from the ohmic resistance produced by the gas film trapped on the anode. Murgulescu[149] similarly showed that the oxidation of Cl^- in AgCl melt was a non-activated reaction at T = 400°C - 600°C, but intense depolarization occurred at higher temperatures (e.g.> 600°C). This was due to the difficulties in the desorption of Cl_2(ad) and its diffusion into the melt.

Bockris et al[151] obtained a Tafel slope of $\frac{RT}{2F}$ and $\gamma = 1$ for Cl^- oxidation and chlorine reduction on the graphite electrode. They suggested that the oxidation proceeded via mechanism (5.1), with (5.1.b) as the rate determining step. However, in the reduction of chlorine the same mechanism (i.e. 5.1) was followed, but the dissociation of chlorine was the slow step at low current densities. At high current density the reduction was controlled by the diffusion of the chlorine molecules to the electrode surface. A similar investigation was carried out by Tunold et al[150] using steady state and transient techniques. They revealed a similar Tafel slope (e.g. $\frac{RT}{2F}$) at low current density, but at high current density they suggested that the reaction mechanism was via route (5.2).

5.3. Experimental

(a) Electrodes

Porous graphite and pyrolytic graphite were used to manufacture electrodes.

(a.i) Porous graphite

The graphite (Morganite Ltd., CY 111) used had 30% porosity and a density of 1.6-1.7 g/cm^3, it was made into a 5 mm diameter disc, 1 to 1.5 mm thick. This was mounted on a teflon tube and polished. Platinum wire was used for electric connections.

(a.ii) Pyrolytic graphite

1 cm^2 pyrolytic graphite was sealed onto a nickel wire using silver araldite. The nickel wire was screened from the electrolyte using silicon rubber solution.

(a.iii) Electrode pretreatment

The prepared electrode was washed thoroughly with deionized distilled water, and cleaned electrolytically at a cathodic potential of -1.6 V vs SCE (Standard Colomel Electrode). It was dipped in 1N HCl for 24 hours.

(b) Electrolyte

1N HCl and saturated NaCl solution were prepared by dissolving analar grade chemicals in deionized distilled water. The electrolytes were purged with oxygen free nitrogen, before chlorine gas was introduced.

(c) Potentiostatic pulse technique

The circuit included a potentiostat (Wenking, 10A,30V) wave form generator (Chemical Electronic, Type 01), a transient recorder (Data lab, DL 901), and an XY/t recorder (Bryans, 29000).

The electrode was allowed to equilibrate with chlorine for 30 minutes until a steady open circuit potential was reached (1045 mV vs SCE). The cathode voltage was set at this value potentiostatically, and a small voltage pulse (10 mV, 5 ms duration) was applied to the electrode. The response of the pulse was recorded for later analysis.

Experiments were carried out both in the presence and the absence of chlorine. Net current was obtained by sub traction of the two readings.

5.4. Kinetic Theory of Chlorine Reduction

The reduction of chlorine on graphite in the aqueous solution may be shown schematically as follows:-

(5.1) $Cl_2(aq) + 2C \underset{k_{-1}}{\overset{k_1}{\rightleftarrows}} 2Cl - C$ .....(5.1.b)

$Cl - C + e \underset{k_{-2}}{\overset{k_2}{\rightleftarrows}} Cl^- + C$ .....(5.1.a)

(5.2) $Cl_2(aq) + C + e \underset{k_{-3}}{\overset{k_3}{\rightleftarrows}} Cl - C + Cl^-$ .....(5.2.b)

$Cl - C + e \underset{k_{-4}}{\overset{k_4}{\rightleftarrows}} Cl^- + C$ .....(5.2.a)

The evaluation of the rate equation for the above mechanism is based on the following assumptions:-

(a) Adsorption obeys Langmuir's isotherm

(b) The transfer coefficient is potential independent

(c) The concentration of chlorine on the electrode surface before polarization is equal to the concentration in the bulk of the solution

(d) The foward and reverse rate of the reaction other than the rate determining step is in equilibrium.

Mechanism (5.1)

When (5.1.a) is the slow step and (5.1.b) is in equilibrium : $K_1 C_{Cl_2} (1-\Theta)^2 = K_{-1} \Theta^2$ (Θ = surface coverage)

$$\frac{\Theta^2}{(1-\Theta)^2} = \frac{K_1}{K_{-1}} C_{Cl_2} \qquad (C_{Cl_2} = \text{concentration of } Cl_2)$$

when $\Theta \to 0$ $\qquad \Theta^2 = \frac{K_1}{K_{-1}} C_{Cl_2}$

and $$\Theta = \left(\frac{K_1}{K_{-1}}\right)^{\frac{1}{2}} C^{\frac{1}{2}}_{Cl_2} \qquad \ldots\ldots\ldots\ldots\ldots\ldots\ldots\ldots(1)$$

when $\Theta \to 1$ $\qquad \frac{\Theta^2}{(1-\Theta)^2}$ has no physical meaning

hence $$i_{cathodic} = F K_2 \Theta \exp \frac{-\beta F}{RT} \eta \qquad \ldots\ldots\ldots\ldots\ldots\ldots(2)$$

(η = overpotential)

substituting (1) into (2)

$$i_{cathodic} = F K_2 \left(\frac{K_1}{K_{-1}}\right)^{\frac{1}{2}} C^{\frac{1}{2}}_{Cl_2} \exp \frac{-\beta F}{RT} \eta \qquad \ldots\ldots\ldots(3)$$

$n^1_{Cl_2} = \frac{1}{2}$ $\qquad (n^1_{Cl_2}$ = the reaction order with respect to $Cl_2)$

and $b = 120$ mV/decade (assuming $\beta = 0.5$, $\Theta \to 0$)

(b is the Tafel slope which is equal to $\frac{\beta F}{RT}$)

When (5.1.b) is slow and (5.1.a) is in equilibrium

$$K_2\ \theta \exp\frac{-\beta F}{RT}\eta = K_{-2}\ C_{Cl^-}\ (1-\theta)\exp\frac{(1-\beta)F}{RT}\eta$$

(C_{Cl^-} = concentration with respect to Cl^- ion)

$$\theta = \frac{K_{-2}C_{Cl^-}\exp\frac{F}{RT}\eta}{K_2 + K_{-2}\,C_{Cl^-}\exp\frac{F}{RT}\eta} \qquad \ldots\ldots(4)$$

$$(1-\theta) = \frac{K_2}{K_2 + K_{-2}\,C_{Cl^-}\exp\frac{F}{RT}\eta} \qquad \ldots\ldots(5)$$

Hence $i_{cathodic} = F\,K_1\,C_{Cl_2}(1-\theta)^2$ .....(6)

substituting (5) into (6)

$$i_{cathodic} = F\,K_1\,C_{Cl_2}\left(\frac{K_2}{K_2 + K_{-2}C_{Cl^-}\exp\frac{F}{RT}\eta}\right)^2 \ldots(7)$$

when $\theta \to 0$ $\qquad K_2 >> K_{-2}\,C_{Cl_2}\exp\frac{F}{RT}\eta$

$$i_{cathodic} = F\,K_1\,C_{Cl_2} \qquad \ldots\ldots(8)$$

$n^1_{Cl_2} = 1$ and $i_{cathodic}$ is independent of η

when $\theta \to 1$ $\qquad K_2 << K_{-2}\,C_{Cl^-}\exp\frac{F}{RT}\eta$

$$i_{cathodic} = F\,K_1\,C_{Cl_2}\left(\frac{K_2}{K_{-2}\,C_{Cl^-}\exp\frac{F}{RT}\eta}\right)^2$$

$$i_{cathodic} = F\,K_1\,C_{Cl_2}\left(\frac{K_2}{K_{-2}\,C_{Cl^-}}\right)^2\exp\frac{-2F}{RT}\eta \qquad \ldots..(9)$$

Hence $n^1_{Cl_2} = 1$ $\qquad$ b = 30 mV/decade

Mechanism (5.2)

When (5.2.a) is slow, and (5.2.b) is in equilibrium

$$K_3(1-\Theta)C_{Cl_2} \exp\frac{-\beta F}{RT}\eta = K_{-3}\,\Theta\,C_{Cl^-}\exp\frac{(1-\beta)F}{RT}\eta$$

$$\Theta = \frac{K_3\,C_{Cl_2}}{K_3C_{Cl_2} + K_{-3}C_{Cl^-}\exp\frac{F}{RT}\eta} \qquad \text{.....(13)}$$

$$i_{cathodic} = K_4F\,\Theta\exp\frac{-\beta F}{RT}\eta \qquad \text{.....(14)}$$

When $\Theta \to 0$ $\qquad K_3C_{Cl_2} << K_{-3}C_{Cl^-}\exp\frac{F}{RT}\eta$

After substituting (13) into (14)

$$i_{cathodic} = F\frac{K_3K_4}{K_{-3}}\frac{C_{Cl_2}}{C_{Cl^-}}\exp\frac{(1+\beta)F}{RT}\eta \qquad \text{.....(15)}$$

hence $n^1_{Cl_2} = 1$ $\qquad$ b = 40 mV/decade

when $\Theta \to 1$ $\qquad K_3C_{Cl_2} >> K_{-3}C_{Cl^-}\exp\frac{F}{RT}\eta$

Hence, $i_{cathodic} = F\,K_4\exp\frac{-\beta F}{RT}\eta$ $\qquad$ .....(16)

and $n^1_{Cl_2} = 0$ $\qquad$ b = 120 mV/decade

When (5.2.b) is slow, and (5.2.a) is in equilibrium

$$K_4\,\Theta\exp\frac{-\beta F}{RT}\eta = K_{-4}\,C_{Cl^-}\,(1-\Theta)\exp\frac{(1-\beta)F}{RT}\eta$$

$$\Theta = \frac{K_{-4}\,C_{Cl^-}\exp\frac{F}{RT}\eta}{K_4 + K_{-4}\,C_{Cl^-}\exp\frac{F}{RT}\eta} \qquad \text{.....(17)}$$

$$(1-\Theta) = \frac{K_4}{K_4 + K_{-4}\,C_{Cl^-}\exp\frac{F}{RT}\eta} \qquad \text{.....(18)}$$

since $i_{cathodic} = F\,K_3C_{Cl_2}(1-\Theta)\exp\frac{-\beta F}{RT}\eta$ $\qquad$ .....(19)

and substituting (18) into (19)

$$i_{cathodic} = F\,K_3C_{Cl_2}\left(\exp\frac{-\beta F}{RT}\eta\right)\left(\frac{K_4}{K_4 + K_{-4}\,C_{Cl^-}\exp\frac{F}{RT}\eta}\right)$$ is obtained

When $\theta \rightarrow 0$ $\quad K_4 \gg K_{-4}\, C_{Cl^-} \exp \frac{F}{RT}\eta$

$$i_{cathodic} = F\, K_3\, C_{Cl_2} \exp \frac{-\beta F}{RT}\eta \qquad \text{.....(20)}$$

$n^1_{Cl_2} = 1$ $\qquad$ b = 120 mV/decade

When $\theta \rightarrow 1$ $\qquad K_4 << K_{-4}\, C_{Cl^-} \exp \frac{F}{RT}\eta$

$$i_{cathodic} = F\frac{K_3K_4}{K_{-4}}\frac{C_{Cl_2}}{C_{Cl^-}} \exp \frac{-(1+\beta)F}{RT}\eta \qquad \text{.....(21)}$$

$n^1_{Cl_2} = 1$ $\qquad$ b = 40 mV/decade.

5.5. Results and Discussions

(a) Potentiostatic pulse

Since the voltage is applied on the electrode for a very short time interval (e.g. 5 msec.), the consumption of reactant is very little, and therefore mass transfer polarization is negligible.

Furthermore, ∂s the current obtained is very small (e.g. maximum 16 mA see Fig. 24) ohmic polarization is also negligible. Therefore, current-overpotential relationships will be governed solely by a charge transfer process. Mass transfer effects will become significant only as reaction time increases and steady state values will be obtained.

In order to avoid the mass transfer effect, it was important to determine the time interval at which current readings were taken. Ideally, the current should be measured immediately after the double layer charging. Unfortunately, in the case of

chlorine reduction on graphite, the double layer charging time could not be measured, as the non Faradaic region is absent (on the graphite surfaces, oxide is formed and reduced at a wide range of potentials).[76,78] Jasem[152] measured the double layer charging time on the nickel cobalt oxide porous electrode and found it was approximately 200 μsec. Hence, the current in this study was measured at 600 μsec.

Since oxide was formed and reduced in the range of potential in which the experiment was carried out, the current response from the potential applied was a mixed type. To obtain a value of current for chlorine reduction alone, the current of oxide reduction is substracted from the total current response.

(b) Porous electrodes

A modification of the Tafel equation is required when studying the kinetics of the chlorine reduction on porous electrodes, due to the possibility of severe ohmic and mass transfer polarizations inside the pores. In some cases this may lead to the doubling of the Tafel slope, as compared with a planar electrode.[146,153]

Polarization curves obtained from porous electrodes illustrated two different Tafel slopes e.g. 40 mV - 60 mV/decade at low η and 120 mV - 140 mV/decade at high η (Fig. 23). The reaction order with respect to chlorine concentration ($n^1_{Cl_2}$) is approximately 1 (Fig. 25), measured at η = 100, 80 and 60 mV. Based on these findings, it is therefore possible to describe the reaction mechanisms occurring.

(b.1) Mechanism of chlorine reduction

(b.1.1) Scheme 5.1

It has been mentioned that (section 5.4) when 5.1.b is the rate determining step, current density is independent of potential at low surface coverage (Θ). However at high surface coverage, the Tafel slope is 30 mV/decade and $n^1_{Cl_2} = 1$.(Table 5)

If reaction (5.1.a) is rate determining step, then the current density is independent of the over-voltage at high surface coverage and at low surface coverage, the Tafel slope is 120 mV/decade and $n^1_{Cl_2} = \frac{1}{2}$. These are not consistent with the results obtained experimentally and thus the possibility of the reaction proceeding through scheme 5.1. is unlikely.

(b.1.2) Scheme 5.2

In scheme 5.2. if 5.2.a is the rate determining step, it was predicted that b = 40 mV/decade, $n^1_{Cl_2} = 1$ and b = 120 mV/decade, $n^1_{Cl_2} = 0$ at low and high surface coverage respectively. These predictions disagree with the observed results.

If (5.2.b) is rate determining, b = 120 mV/decade and 40 mV/decade at low and high surface coverage respectively, with $n^1_{Cl_2} = 1$. This is in agreement with the data obtained. Therefore, it seems that scheme (5.2) offers the most likely mechanism for chlorine reduction reaction in which route(5.2.b) is thought to be the rate determining step.

(c) Pyrolytic Graphite

A similar pattern of current density - overvoltage

relationships were found with the pyrolytic graphite electrode.(Fig. 24) Generally, the current density was higher in comparison to the porous graphite electrode; this was mainly due to its more active surface.

There were no significant differences in the Tafel slope in the polarization curve between porous and pyrolytic graphite electrodes. Thus under the operating conditions of $\eta < 100$ mV and short pulsing times (5msec.), the porous structure does not seem to interfere with the polarization behaviour.

(d) Reaction order

The reaction order was measured based on the slope obtained from the variation of current density with chlorine concentration at a fixed overvoltage (η). The reaction order was represented by the slope of the log C (mol/ℓ) vs log i (mA/cm^2) plot.

Transient and rotating disc techniques were used respectively on pyrolytic and porous graphite. For porous graphite, a linear relationship between log C (mol/ℓ) and log i (mA/cm^2) was observed with a slope of approximately one.(Fig. 25) A similar result was obtained on pyrolytic graphite at η = 80 and 60 mV. (Fig. 26)

CHAPTER 6

6. MASS TRANSFER BEHAVIOUR IN THE SANDWICH TYPE CATHODE

6.1. Introduction

The development of the sandwich type cathode has so far been limited to an experimental study. However, there is no clear understanding of the relationships between some important parameters, such as porosity, bulk density and T.C.A./acetylene black layer thickness, on the discharge characteristics of the cathode.

A mathematical description of the cathode based on electrochemical kinetics and transportation theories is required. It was hoped that this model will facilitate better understanding of the relationship between the discharge characteristics and the parameters mentioned above, from which better design criteria can be drawn.

For the present cathode system, a mathematical model was evaluated using the theory, developed by Austin et al.[121,122] which considered the mass transfer in a flooded porous electrode where ohmic polarization along the porous structure was neglected.

6.2. Macroscopic Description of the Porous Electrode

The applications of planar electrodes in practical energy-converter electrochemical cells are restricted, due to their low surface areas, which give very low apparent exchange current densities and limiting current densities.

Generally, after roughening the planar electrode surface the

area is increased thereby enhancing the apparent exchange current densities. However, the apparent limiting current density is relatively unaffected by this treatment and hence the planar electrode has limited practical value.

In order to achieve a higher apparent exchange current density combined with a high limiting current density, the electrode structure must be modified. Amongst the most successful electrode designsis the porous electrode. This electrode usually has a much higher real surface areas in comparison to the conventional planar electrode. For example, a porous electrode of 1 mm thickness 50% porosity and 1 μm pore diameter may provide a surface area of 1000 cm^2/cm^3. Consequently, the current output at a particular potential is greatly increased. In addition, the diffusion layer thickness of the porous electrode is normally lower than that of the planar electrode, which increases the limiting current density.

The porous electrode consists of catalysts particles either distributed on to a conducting substrate, or sintered together. There are two types of pores, i.e. macro and micro. Macro pores are distributed between the catalyst particles. These are variable in size as the distribution of these particles is usually non-uniform. The micro pores lie only on the particle surface and therefore cover less area than the macro pores. The total surface area inside the porous electrode is defined as the specific volumetric area S (cm^2/cm^3), and is given by the BET surface area.

Owing to the "tortuousity" inside the porous electrode, the diffusion pathways taken by the reactants toward the reacting sites are somewhat longer than those found on the planar electrode. Therefore the diffusion coefficient of reactants inside the porous electrode require some correction as below:-

$$\overline{D}eff = D_b \times \varepsilon/q$$

where $\overline{D}eff$ = effective diffusion coefficient (cm^2/sec)

D_b = diffusion coefficient in bulk electrolyte (cm^2/sec)

ε = porosity

q = "tortuousity" (for normal solids q ranged from $\sqrt{2}$ to 2)[102]

The validity of ε/q for the correction of mass transfer was also found to be valid for the correction of resistivity.[103,104] Hence:

$$\overline{\rho}_{eff} = \rho_b \times \varepsilon/q$$

$\overline{\rho}_{eff}$ = effective resistivity of electrolyte (ohm-cm)

ρ_b = resistivity in bulk electrolyte (ohm-cm)

Although porous electrodes have a high exchange current density, and thus a lower activation polarization, generally not all their available surface area is fully utilized. This degree of utilization is dependent upon local electrochemical kinetics, the resistance of the electrode matrix and pore electrolyte, the electrode thickness, plus the mass transfer of the reactants as well as products within the matrix.

At present there are three types of porous electrodes

which are widely used; these include:-

(a) Gas diffusion electrode

In this electrode the reaction sites are located at the three phase interface, which is the boundary between a liquid and a solid. The gaseous reactant dissolves in the liquid phase and diffuses toward the reaction sites. The mode of operation in this system depends on the electrode properties and therefore on its method of preparation. For example, electrodes with Teflon binder have poorer 'wetability' than those without Teflon binder. Research has provided several hypothetical models describing the behaviour of the gas diffusion electrode.[105-109] These include the thin film model, the finite contact angle minicus model, the double porous model, the cone model and the intersecting pore model. A detailed review is beyond the scope of this investigation, but has been provided by Srinivasan.[110]

(b) Flow-through porous electrode

This type of electrode possesses advantages over the planar electrode with flowing solution and porous electrode without flow. Kalnoki-Kis and Brodd[118] demonstrated that an increase in the current by a factor of 10^2 to 10^4 at a given potential is feasible with this type of electrode. The high interfacial area allows the attainment of a high volumetric reaction rate, whilst the flowing solution improves the mass-transport of the reacting species, thereby increasing the limiting current of the system. The flow-through electrode has attracted great interest in the

pollution control industry. It has been used in several systems e.g. the removal of heavy metal ions such as Cu^{2+} [111,112,113], Sb^{4+} [114], the conversion of ferric cyanide into ferrous cyanide[115], the electro-organic synthesis and the oxidation of the waste organic pollutants.[116] A review by Newman and Tiedemann[117] provides a more comprehensive analysis of these processes.

(c) Flooded non-flow porous electrodes

The majority of flooded porous electrodes are immersed into an electrolyte containing the reactant species, for example, the methanol fuel-cell system. Occasionally, the reactant itself is deposited inside the porous structure of the electrode which is filled with electrolyte. This is mainly used in some primary and secondary battery systems.

A number of workers have investigated the flooded porous electrode system.[119-135] Euler and Nonenmacher[119] analysed the one-dimensional porous electrode system with a metal backing current collector. Their analysis was based on the assumption of constant concentration throughout the porous structure and a linear polarization equation was used. Newman and Tobias[120] examined a similar system using a Tafel type polarization equation and, in addition, considered the variation of concentration along the porous structure. They concluded that the current distribution within the porous structure was affected by pore electrolyte and porous matrix conductivity together with the mass transfer of the reacting species. The combination mass transfer/activation and ohmic/activation effects on the porous electrode

system were studied by Austin and Lerner.[120,121] Both studies illustrated that the Tafel slope was doubled.

However, some of these theories are considered to be over-simplistic and have only limited applications to some porous electrodes systems. For example, the Ag/AgCl and $Cd/Cd(OH)_2$ electrode systems are more complicated. During discharge, the pore size as well as the conductivity of both electrolyte and porous matrix were varied. Hence a more elaborate mathematical model had to be considered. Alkire et al.[123] evaluated a mathematical model for copper dissolution, under pseudo-steadystate conditions. This analysis included the consideration of structural changes occurring during the reaction. The current distribution of electrodes containing sparingly soluble reactants such as $Cd/Cd(OH)_2$ or Ag/AgCl were investigated by Dunning et al.[124,125] In this system the effects of variation in pore size, conductivity as well as electrolyte concentration during discharge were taken into account. Similar analyses were reported by several workers[126-129] concerning the lead acid electrode. The transient behaviour of current distribution, pore size and electrolyte concentration in Ag/AgCl was recently analysed by Gu et al.[130]

Experimental evaluation of the current distribution of flooded porous electrodes was carried out by measuring the distribution of discharge material, particularly in battery systems. Bro and Kang[132] analysed the current distribution in the $Cd/Cd(OH)_2$ electrode. However, this involved washing and drying, followed by sectioning of the electrode. Consequently, this will introduce

new errors in the data obtained. The use of an internal reference electrode to measure potential distribution in the MnO_2 electrode was carried out by Brodd.[132] It was possible that the presence of the internal reference electrode would also interfere with the structure of the electrode and therefore could lead to errors in the interpretation of the results. However, Brodd found his results were in agreement with the theoretical equations developed by Newman and Tobias.[120]

So far mathematical descriptions of the behaviour of many porous electrodes have been made, but they do not always correspond accurately with experimental results. However, the reliability of these theoretical predictions is greatly affected by the physical and electrochemical parameters selected for the analytical solution of the mathematical model. The porosity of an electrode has an important effect on the value of electrolyte conductivity as well as the diffusion coefficient of reactant species inside the porous structure. These parameters have, in turn, paramount effects upon the behaviour of the predicted polarization curve of the system. Therefore, it is important that these parameters are carefully selected and controlled.

6.3. The Cathode: A Mathematical Description

The cathode consists of four layers of T.C.A. powder; each layer was sandwiched between two layers of acetylene black powder, and considered to be identical and therefore may be used as a model for the mathematical description of the discharge

behaviour of the whole cathode. The cathode is illustrated below:-

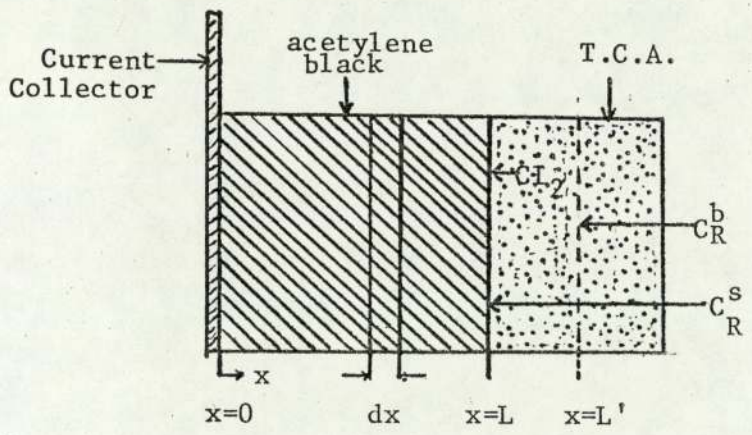

During discharge the cathode was flooded with a mixture of 1.5 M $AlCl_3$ and 0.5 M NaCl. Several factors are thought to be important in affecting the cathode discharge characteristics. These are:-

(i) The rate of reaction between T.C.A. and $AlCl_3$/NaCl solution.

(ii) The diffusion of chlorine from the bulk of the T.C.A. layer to the T.C.A./acetylene black interface.

(iii) The diffusion of chlorine from the T.C.A./acetylene black interface into the acetylene black layer.

Assuming the reaction between T.C.A. and $AlCl_3$/NaCl solution is fast, after the initiation of discharge, chlorine is available at the T.C.A./acetylene black interface, and its diffusion through the bulk of the T.C.A. is negligible. Then the process is mainly limited to the diffusion of the chlorine into the acetylene black layer.

For a redox couple of Cl_2/Cl^-, the rate equation is represented by:-

$$i_1 = i_o \left[\frac{C_R}{C_R^b} \exp \frac{\alpha nF}{RT} \eta - \frac{C_p}{C_p^b} \exp \frac{-(1-\alpha)nF}{RT} \eta \right] \quad \text{.....(6.3.1)}$$

Where i_1 = the current density per cm^2 of graphite-electrolyte interface.

i_o = the exchange current density on the same basis

C_R, C_p = the reactant and product concentration at an arbitary point inside the acetylene black layer.

C_R^b, C_p^b = bulk concentration of reactant and product in the T.C.A. layer.

η = the overpotential.

n = the number of electron transfer in the rate limiting step.

α = transfer coefficient.

F = Faraday number

R = gas constant

T = temperature

If S is the volumetric reacting surface area at an element dx, then the reacting area available will be S dx and the current at dx is di ($di = i_i S\,dx$), di is the current density per unit exposed surface area.

$$di = io\ S \left[\frac{C_R}{C_R^b} \exp \frac{\alpha nF}{RT} \eta - \frac{C_p}{C_p^b} \exp \frac{-(1-\alpha)nF}{RT} \eta \right] dx \quad \text{...(6.3.2)}$$

Let $\frac{RT}{nF} = b$, then

$$di = io\ S \left[\frac{C_R}{C_R^b} \exp \frac{\alpha}{b} \eta - \frac{C_p}{C_p^b} \exp \frac{-(1-\alpha)}{b} \eta \right] dx \quad \text{.....(6.3.3)}$$

Since the flux of reactant diffusing out of dx at the plane x is

$$\bar{D}\frac{dC_R}{dx} \qquad (\bar{D} = D_{free}\frac{\varepsilon}{q})$$

at steady state : $$\frac{di}{dx} = n'F\bar{D}\frac{d^2C_R}{dx^2} \qquad \text{.....(6.3.4)}$$

n' = total number of electrons transferred in the reduction of one mole of chlorine.

From 6.3.3. and 6.3.4. it may be deduced that

$$\frac{d^2C_R}{dx^2} = \frac{i_o\ S}{n'F\bar{D}}\left[\frac{C_R}{C_R^b}\exp\frac{\alpha}{b}\eta - \frac{C_p}{C_p^b}\exp\frac{-(1-\alpha)}{b}\eta\right] \qquad \text{..(6.3.5)}$$

when the ohmic drop through out the porous matrix is negligible, and η is constant.

If the diffusion coefficients of both reactants and products are equal, then for equi-molar counter-current diffusion:-

$$C_R + C_p = C_R^b + C_p^b$$

or $$C_p = C_R^b + C_p^b - C_R$$

Substituting C_p into 6.3.5.:

$$\frac{d^2C_R}{dx^2} = \frac{i_o\ S}{n'F\bar{D}}\left[\frac{1}{C_R^b}\exp\frac{\alpha}{b}\eta + \frac{1}{C_p^b}\exp\frac{-(1-\alpha)}{b}\eta\right]C_R$$

$$- \frac{i_o\ S}{n'F\bar{D}}(C_R^b + C_p^b)\left(\frac{1}{C_p^b}\right)\exp\frac{-(1-\alpha)}{b}\eta \qquad \text{.....(6.3.6)}$$

Let : $$A = \frac{i_o\ S}{n'F\bar{D}}\left[\frac{1}{C_R^b}\exp\frac{\alpha}{b}\eta + \frac{1}{C_p^b}\exp\frac{-(1-\alpha)}{b}\eta\right]$$

$$B = \frac{i_o\ S}{n'F\bar{D}}\left[\frac{C_R^b + C_p^b}{C_p^b}\right]\exp\frac{-(1-\alpha)}{b}\eta$$

Hence:

$$\frac{d^2C_R}{dx^2} = AC_R - B \qquad \text{.....(6.3.7)}$$

Boundary conditions:

$$x = 0 \qquad \frac{dC_R}{dx} = 0$$

$$x = L \qquad C_R^s = C_R$$

$$C_p^s = C_p$$

Since the total steady-state current density in the interior of the electrode is

$$i = n' F \bar{D} \left(\frac{dC_R}{dx}\right)_{x=L} \qquad \text{.....(6.3.8)}$$

Let: $\bar{C}_R = AC_R - B$

$$x = 0 \qquad \frac{d\bar{C}_R}{dx} = 0$$

(6.3.7) becomes

$$\frac{d^2\bar{C}_R}{dx^2} = A\bar{C}_R \qquad \text{.....(6.3.9)}$$

and

$$\bar{C}_R = k_1 \text{ Sinh } (\sqrt{A}\, x) + k_2 \text{ Cosh } (\sqrt{A}\, x) \qquad \text{.....(6.3.10)}$$

$$\frac{d\bar{C}_R}{dx} = k_1 \sqrt{A} \text{ Cosh } (\sqrt{A}\, x) + k_2 \sqrt{A} \text{ Sinh } (\sqrt{A}\, x) \qquad \text{..(6.3.11)}$$

$$\text{at } x = 0 \qquad \frac{d\bar{C}_R}{dx} = 0$$

therefore $k_1 = 0$

$$\bar{C}_R = k_2 \text{ Cosh } (\sqrt{A}\, x) = AC_R - B \qquad \text{.....(6.3.12)}$$

$$\text{at } x = L \qquad C_R = C_R^s$$

and $k_2 = (AC_R^s - B) / \text{Cosh}\ (\sqrt{A}\ L)$

Substituting k_2 into (6.3.12)

$$AC_R - B = (AC_R^s - B)\ \frac{\text{Cosh}\ (\sqrt{A}\ x)}{\text{Cosh}\ (\sqrt{A}\ L)}$$

$$\frac{AC_R - B}{AC_R^s - B} = \frac{\text{Cosh}\ (\sqrt{A}\ x)}{\text{Cosh}\ (\sqrt{A}\ L)}$$

Hence:

$$i = n' F \overline{D}\ \left(\frac{dC_R}{dx}\right)_{x=L} = \frac{n' F \overline{D}}{\sqrt{A}}\ (AC_R^s - B) \tanh(\sqrt{A}\ L) \quad \ldots\ldots(6.3.13)$$

by substitution of A and B into (6.3.13)

$$i = i_o SL \left[\frac{C_R^s}{C_R^b} \exp \frac{\alpha}{b}\eta - \frac{C_p^s}{C_p^b} \exp \frac{-(1-\alpha)}{b}\eta\right] \left[\frac{1}{L\sqrt{A}} \tanh\ (L\sqrt{A})\right] \ldots(6.3.14)$$

the η in equation 6.3.14 represents the combined effects of activation and mass transfer polarization inside the electrode short time after the discharge is started. The variation of chlorine concentration between the bulk T.C.A. and the interface is expected to be small.

where $\frac{C_R^s}{C_R^b} = 1$ and $\frac{C_p^s}{C_p^b} = 1$

Hence 6.3.14 may be simplified to:

$$i = i_o\ SL \left[\exp \frac{\alpha}{b}\eta - \exp \frac{-(1-\alpha)}{b}\eta\right] \left[\frac{1}{L\sqrt{A}} \tanh\ (L\sqrt{A})\right] \quad \ldots.(6.3.15)$$

However, this equation assumes that only the concentration variation along the electrode is important. However, in many cases, ohmic effects outweigh the mass transfer effects where η varied along the pore electrolyte, particularly in a system involving non ionic reactants having no supporting electrolyte.

Austin[122], reported that the relative importance of internal mass transfer or ohmic effects upon the polarization of a porous electrode can be examined by using a factor ϕ.

$$\phi = \rho\ n\ F\ D\ C_R^b\ \alpha/b$$

For $\phi < 0.5$ the system is controlled by mass transfer, and $\phi > 5$ the system is controlled by ohmic resistance. The present system, ρ (1N HCl) = 3.3 ohm-cm. $n = 2$, $F = 96500$, $D = 1.74 \times 10^{-5}$ cm^2/sec, $C_R^b = 2.15 \times 10^{-5}$ mole/cm^3, $\alpha = 0.5$, $b = 0.0265$. Thus, $\phi = 4.5 \times 10^{-3}$, it is therefore reasonable to assume that the system is mass transfer controlled.

Errors involved in neglecting ohmic drop

According to Austin and Lerner[121], the error can be obtained by comparing the current obtained in the presence and absence of ohmic gradient along the pore. The ohmic gradient is assumed to be in the same direction as the concentration gradient in the electrode. When $C_R = 0$, and the irreversible reaction

$$\xi = (\text{predicted current})/(\text{instantaneous current})$$

$$\xi = \phi(1 - e^{-\phi})$$

when $\phi < 1$

$$\xi = 1/(1 - \frac{\phi}{2})$$

for $\phi = 4.5 \times 10^{-3}$

$\xi = 1$

which in turn suggests that the predicted irreversible current, with ohmic drop neglected, will only result in a very small error ($\doteq 0\%$).

6.4. Experimental

The steady-state current-potential relationship was measured by using a rotating disc electrode.(Fig. 28)

The electrode was prepared by mounting a disc on a Teflon tube. The disc was manufactured from porous graphite (Morganite Ltd) and was 1.1 mm thick (approximately), 0.7 cm in diameter and 30% porosity. It was backed by a platinum wire acting as a current collector which was welded onto a nickel rod. The electrode resistance was measured between the disc and the nickel rod to check that good electrical contact has been established. (Fig. 27)

The polarization was carried out in saturated sodium chloride solution containing 1M HCl. It was purged with nitrogen gas (white spot B.O.C) and then bubbled with chlorine gas until saturated (approximately 30 minutes). The chlorine concentration in the solution was analysed before and after experimentation, using iodometric titration.

The polarization measurements were taken only after the equilibrium potential was established (e.g. 1045 mV vs SCE). This process was repeated at several rotation speeds between 2000 and 3000 rpm.

6.5. Results and Discussion

The current density dependence upon overpotential including the effects of activation and mass transfer in a flooded porous electrode is given by equation (6.3.15). It showed that, at a given overpotential, the current density is directly proportional to the exchange current density and to the characteristic diffusion current.

For many porous electrode systems, because of the lack of availability of some of the parameters such as real exchange current density, effective diffusion coefficient, etc, an accurate theoretical prediction of the system has been made difficult. In many cases, the theoretical parameters can only be determined by fitting the theory to the experimental results. In this work the value of real exchange current density has been measured experimentally using transient techniques.

The mathematical solution of equation (6.3.15) based on the data in Table 5, was computed (mini computer, PET 2001, see appendix 2).

The polarization curves predicted by equation (6.3.15) for several electrode thickness are illustrated in Fig. 29. These predict that for electrode thicknesses greater than 0.7 mm, no further increase in current density will be observed. Also, as the overpotential is increased, utilization of available electrode thicknesses concomitantly decreased, ultimately being limited to the outermost electrode surface. Figure 30 shows the theoretical solution plotted as current density against thickness used for several values of overpotential.

The above argument assumes that the electrode process is an activation or an diffusion controlled; this must be verified by comparison with the experimental results. Half-cell measurements on the original sandwich cathodes were practically difficult to obtain for the following reasons:

(i) The presence of T.C.A. layer on the acetylene black cathode may create a high IR drop and hence mask the activation and mass transfer overpotential determinations.

(ii) The cathode has poor mechanical strength and prolonged immersion in the electrolyte during measurement disturbs its structure. Hence, the porosity and conductivity of the electrode would be altered. To overcome some of these difficulties, a rotating disc electrode was used. This consisted of a sintered porous graphite disc, having greater mechanical strength than that used in the sandwich battery and therefore capable of maintaining constant porosity and conductivity.

It is important to note that, in the initial stage of the discharge in the original sandwich type cathode, chlorine originated from T.C.A. - acetylene black interface; under this condition it was reasonable to assume that $C_R^b = C_R^s$. This condition can be obtained in the rotating disc electrode by careful control of its rotating speed.

The effect of the speed of rotation upon the current density - overpotential relationship of chlorine reduction on porous graphite is illustrated in Fig. 31. At $\eta \leqslant 200$ mV no significant change in current density was observed as rotating

speed was varied from 2500 to 3000 rpm. This suggested that the surface concentration approximated that of the bulk. Levich correlated the relationship between current density and concentration of reactant species as follows:-

$$i = B\,(C_R^b - C_R^s)\,\omega^{\frac{1}{2}}$$

where i = current density (mA/cm^2)

B = constant

C_R^b = bulk concentration of reactant species mol/ℓ

C_R^s = surface concentration of reactant species mol/ℓ

ω = rotating speed (Hz)

When $C_R^s = 0$ $\quad i = i_L$ (limiting current density)

Hence $i/i_L = 1 - C_R^s/C_R^b$

or $C_R^s/C_R^b = 1 - i/i_L$

From Fig. 31, it was found that at $\eta < 200$

$i/i_L = 0.15 \quad C_R^s/C_R^b = 0.850 \quad$ at $\quad \omega = 2500$ rpm

$i/i_L = 0.11 \quad C_R^s/C_R^b = 0.89 \quad$ at $\quad \omega = 3000$ rpm

indicating that the possibility of bulk diffusion limitation was a minimum.

However, the theoretically predicted curves calculated from data in Table 5 did not correlate well with the experimental curve. (Fig. 32) The major discrepancy lies in the difference between the slope of the theoretical and the experimental curves. This is largely a function of the diffusion coefficient. The discrepancy could be attributed to the mechanism of the diffusion

of chlorine inside the graphite matrix, being that of surface diffusion rather than bulk diffusion. However, the surface diffusion coefficient (D_s) is less than that of the bulk (D_b) (see Table 5). This emphasis on the former diffusion coefficient would in fact aggravate the discrepancy. However, the mechanism of chlorine diffusion inside the matrix is the combination of both mechanisms mentioned above. Thus, the effective diffusion coefficient will be, in practice, the summation of the two, which is illustrated by the following equation:-

$$\overline{D}_{eff} = D_b \times \frac{\varepsilon}{q} + D_s \lambda \qquad (0 < \lambda \leq 1)$$

and λ is a function of particle size and pore structure, the maximum value of $\overline{D}_{eff}$ if obtained when $\lambda = 1$, this gives $\overline{D}_{eff} = 4.9 \times 10^{-6}$ cm^2/sec. But the curve obtained using this value still did not correlate with the experimental curve.(Fig.32) Instead, the curve was fitted by parameterizing $\overline{D}_{eff}$ to 3×10^{-4} cm^2/sec. (Fig. 33) a value, which is larger than the D value in Table 6 by a factor of 10^2. This suggests that diffusion through a static electrolyte and surface diffusion is inadequate. This large value of $\overline{D}_{eff}$ could arise from the fact that a rotating disc electrode was used to obtain experimental data. The high rotating speed may have created turbulence at the electrode surface and this may have affected the flow of electrolyte within the pore, hence giving a greater diffusion coefficient. Despite this limitation these results have suggested that the process is subject to internal diffusion control, this is demonstrated by the curve

in Figure 33. At present, positive conclusions concerned with the mechanism of this process are difficult to draw. This situation can only be clarified when a proper measurement of $\overline{D}_{eff}$ has been achieved.

CHAPTER SEVEN

CONCLUSIONS AND SUGGESTIONS FOR FURTHER WORK

CHAPTER 7

7. CONCLUSIONS AND SUGGESTIONS FOR FURTHER WORK

(a) Conclusions

The T.C.A. - aluminium primary reserve battery is a promising high energy density and low cost system. However, the cathode has poor storage stability, and hence its practical application has been limited. After one week storage under ambient conditions, a maximum of 10% of the chlorine content of the cathode may be lost. T.C.A. itself is a very stable compound; no loss of chlorine being detected after one years storage under similar conditions. It destabilises only after mixing with acetylene black powder, which acts as the electrical conductor in the cathode. It was thought that this phenomenon was occurring at the interface of the two substances, the acetylene black acting as a catalyst.

The data illustrated in (Figs. 1 & 2) indicated that during storage, the rate of chlorine loss accelerated when the amount of acetylene black in the mixture was increased. This was thought to be caused by an increase in the moisture content of the mixture, thereby enhancing the hydrolysis of T.C.A. Samples stored under a constant flow of dry nitrogen, exhibited a greatly reduced loss of chlorine (Fig. 3). The dry nitrogen not only reduced the moisture in the surroundings, but also the moisture preadsorbed on the acetylene black surface, and hence prevented the hydrolysis of T.C.A.

Since this reaction is an interfacial process, the rate

will be dependent upon the amount of contact surface area between the T.C.A. and acetylene black aggregates. This area is a function of the aggregate diameter of these components and an increase in the rate of chlorine loss from 33% to 55% was detected when the aggregate size of T.C.A. was varied between 1.85×10^{-3} cm to 22.87×10^{-3} cm.(Fig. 4)

A detailed knowledge of the reaction mechanism involved in the chlorine liberation in this system is necessary to facilitate further improvements in cathode stability. This study revealed that several reactions were involved in the destabilization process. These include:

(i) An electrochemical self discharge reaction. This reaction was mainly governed by the anodic oxidation of graphite/acetylene black, and chlorine reduction. It followed the mechanism shown below:

Anodic $\quad C + H_2O \rightarrow CO + 2H^+ + 2e$

Cathodic $\quad Cl_2 + 2e \rightarrow 2Cl^-$

Measurements taken from the half cell showed that these reactions occurred spontaneously, as the cathodic and the anodic polarization curves were intercepted at the potential more anodic to the equilibrium potential of the first reaction.

(ii) A free radical process. This was mainly catalysed by the acetylene black and produced chlorine radicals. These radicals may subsequently abstract a hydrogen atom from the acetylene black surface, thus producing HCl. Two methods were used to detect the presence of these radicals: (a) Toluene was added to

the reaction mixture containing T.C.A. and acetylene black, thereby forming benzyl chloride, when the reaction involved chlorine radicals. (b) DPPH solution was added to a similar reaction mixture, the presence of chlorine radical leads to the depletion of DPPH concentration in the solution. Both analysis confirmed the presence of the chlorine radicals. However, the exact mechanisms involved in this process is not yet fully understood.

(iii) Direct reaction between HCl and T.C.A. Since both reactions mentioned above produce HCl, a direct reaction between HCL and T.C.A. is very likely, particularly at low pH. (Fig.11)

It is therefore hoped that the destabilization of the cathode may be resolved either by one of the combination of the following methods:

(i) the addition of stabilizers such as boric acid, boric oxide or zeolites into the reaction mixture. It was thought that zeolites would assist in the removal of H^+ via an ionic exchange reaction, thus reducing the acidity of the system, consequently chlorine losses. In fact, the results obtained illustrated that the reaction was accelerated (Table 3). It was possible that a lack of water in the mixture inhibited the ionic exchange mechanism. Boric acid, however, was thought to act as a buffer tending to reduce the acidity of the mixture, and, as the results indicated (Table 3), suppressed the chlorine losses.

(ii) The prevention of interfacial contact between the T.C.A. - acetylene black aggregates. This involved an alteration of cathode design. The T.C.A. aggregates were sandwiched between two layers of acetylene black powder. Boric acid (oxide) was added at the interface, to complete the separation of the two aggregates. It was thought that this design would introduce severe mass transfer limitations during discharge, particularly when boric oxide layer was present at the interface, in which the diffusion of chlorine molecules from T.C.A. layer into the acetylene black layer. In practice, however, this effect becomes only serious at high discharge rates, whilst at low-rate discharges, such an effect was minimal, and the system attained a cell voltage of 2.05 volts. An improvement in storage stability was also obtained. In comparison with the mixed type cathode, the sandwich type cathode retained 25% and 400% more capacity after 24 hours and 48 hours storage respectively at 40°C and 75% humidity. (Figs. 19 & 20)

To date, the results obtained from the sandwich type cathode are therefore very promising. Further improvements upon cathode design are necessary. Previous studies have relied on empirical tests, which are both tedious and time consuming. It is therefore important to establish a mathematical model to describe the discharge characteristics of the cathode. Based on existing flooded porous electrode theories, the current densities overpotential relationship of this cathode was evaluated. At a given overpotential the current density was dependent upon

exchange current density and the characteristic diffusion current. This relationship was then compared with the results obtained from half-cell measurements, obtained using the rotating disc electrode. It was found that the correlation between theoretical and experimental results was largely dependent upon the effective diffusion coefficient. The best fit curve was obtained when the effective diffusion coefficient was 100 times the bulk and surface diffusion coefficient. This may be due to an inherent effect of the rotating disc electrode, which may involve turbulence at the electrode surface. Hence, creating an electrolyte flow inside the pores and thereby producing a large value for the effective diffusion coefficient. Despite this, the two results suggest that the process is mainly an internal diffusion controlled process.

(b) Suggestions for Further Work

Theoretical and practical data show that the sandwich type cathode may be of use as a stable high energy density and low cost cathode in the future. However, there are several areas which need to be further investigated to improve the overall performance of this electrode. These are:

(i) Cathode fabrication

(ii) Separation of T.C.A.-acetylene black layers

(iii) Understanding the mechanism of the stabilization by boric acid

(iv) Long term stability tests

(v) Mathematical modelling of the cathode discharge characteristics.

(i) Cathode fabrication

The cathode used in this study was fairly small, i.e. 5 cm^2, and was manufactured by pressing the powder in a steel mould. For commercial applications however an electrode of larger dimensions is required. Hence, the mechanical strength of the electrode, and its method of manufacture have to be modified to be commercially viable. This may be resolved by the use of T.C.A. and acetylene black painted tapes, which are stacked together to form cathode plaques.

(ii) Separation of T.C.A. - acetylene black layers

A search for efficient methods for separating the T.C.A. and acetylene black layer is essential. The previous method of spreading boric acid powder at this interface was insufficient to prevent all contact between the T.C.A. and acetylene black layers. Thus chlorine losses still occurred. An alternative method may include the coating of T.C.A. and acetylene black tape with boric acid by either spraying or the use of thin membranes at the interface. Preliminary studies using tissue paper were encouraging. Despite severe mass transfer polarization, a cell voltage of 1.7 volts was obtained. Further investigations of the effect of the membrane porosity and thickness upon cathode performance are necessary.

(iii) Mechanism of the stabilisation by boric acid

A study of the mechanism of the reaction of boric acid with the cathode mixture would be useful to find alternative organic

or inorganic compounds which may lead to further improvements in cathode stability.

(iv) Long term stability test of the cathode

The long term stability tests of the cathode were originally carried out at high temperature ($40^{o}C$) and humidity (75%). Such an environment may alter the mode of the decay mechanism. Hence, further tests should be conducted in milder condition, thereby reducing any interference with the decay mechanism.

(v) Mathematical models of the cathode discharge characteristics

The mathematical model describing the initial stage of the cathode discharge characteristics was inconclusive. The predicted value of effective diffusion coefficient was found to be too high. This was thought to be caused by the use of the rotating disc electrode. This discrepancy, consequently affected the reliability of the model, which was used to predict the effect of some parameters such as porosity, electrode thickness etc. on the discharge characteristic of the cathode. In order to obtain more reliable correlations between theoretical and experimental results, it is necessary to use a floating cell thereby eliminating effects of turbulence on the polarization curve.

APPENDIX I

Calculation of the weight of acetylene black required for complete coverage of 0.1g T.C.A.

$d_{T.C.A.}$ = mean aggregate diameter of T.C.A. = 1.5×10^{-4} m

$d_{A.B.}$ = mean aggregate diameter of acetylene black = 1.38×10^{-6} m

$\rho_{T.C.A.}$ = density of T.C.A. = $1.21 g/cm^3$

$\rho_{A.B.}$ = density of acetylene black = $1.6 g/cm^3$

Total volume of 0.1g T.C.A. (V^T)

$$V^T = \frac{Wt}{\rho} = \frac{0.1}{1.21} = 8.26 \times 10^{-2} \text{ cm}^3$$

The volume of a single T.C.A. aggregate (V^s)

$$V^s = \frac{4}{3} \pi r^3$$

$$= \frac{4}{3} \pi (0.75 \times 10^{-2})^3 \text{ cm}^3$$

$$V^s = 1.767 \times 10^{-6} \text{ cm}^3$$

Number of T.C.A. aggregate in 0.1g T.C.A. ($^nT.C.A.$)

$$^nT.C.A. = \frac{V^T}{V^s} = \frac{8.26 \times 10^{-2}}{1.767 \times 10^{-6}} = 4.67 \times 10^4 \text{ aggregates}$$

The external surface area of a single T.C.A. aggregate.

$$A_{T.C.A.} = \pi d^2$$

$$= 3.14.6 \times (1.5 \times 10^{-2})^2 \text{ cm}^2$$

$$A_{T.C.A.} = 7.07 \times 10^{-4} \text{ cm}^2$$

Assuming the total surface area of acetylene black required to cover completely one T.C.A. aggregate is equal to the total cross section area of the acetylene black aggregate.

Thus, the total cross section area will be:

$$A^{T}_{A.C.} = n_{A.C.} \times A^{s}_{A.C.} \qquad \left(A^{s}_{A.C.} = \frac{\pi}{4} d^{2}_{A.C.} \right)$$

$A^{T}_{A.B.}$ = Total cross section area of acetylene black aggregate, covering one T.C.A. aggregate.

$A^{s}_{A.B.}$ = Cross section area of a single acetylene black aggregate.

Since $A^{T}_{A.B.} = A_{T.C.A.} = 7.07 \times 10^{-4}$ cm^2.

The number of acetylene black aggregate required for complete coverage of one T.C.A. aggregate will be :

$$n_{A.B.} = \frac{A_{T.C.A.}}{A^{s}_{A.B.}} = \frac{7.07 \times 10^{-4} \times 4}{3.1416 \times (1.38 \times 10^{-4})^2}$$

$$n_{A.B.} = 4.73 \times 10^{4} \text{ aggregates.}$$

Total number of acetylene black aggregates required (N)

$$N = n_{A.B.} \times n_{T.C.A.} = 4.67 \times 10^{4} \times 473 \times 10^{4}$$

$$N = 2.2 \times 10^{9} \text{ aggregate}$$

Total volume of acetylene black ($V^{T}_{A.C.}$)

$$V^{T}_{A.C.} = 2.2 \times 10^{9} \times \frac{4}{3} \pi r^{3}$$

$$V^{T}_{A.C.} = 2.2 \times 10^{9} \times \frac{4}{3} \times 3.1416 \times (0.69 \times 10^{-4})^{3}$$

$$V^{T}_{A.C.} = 3.02 \times 10^{-3}$$

Total weight of acetylene black required

$$W_{A.C} = V^{T}_{A.C.} \times \rho_{A.C.}$$

$$= 3.02 \times 10^{-3} \times 1.6$$

$$W_{A.C.} = 4.8 \times 10^{-3} \text{ g.}$$

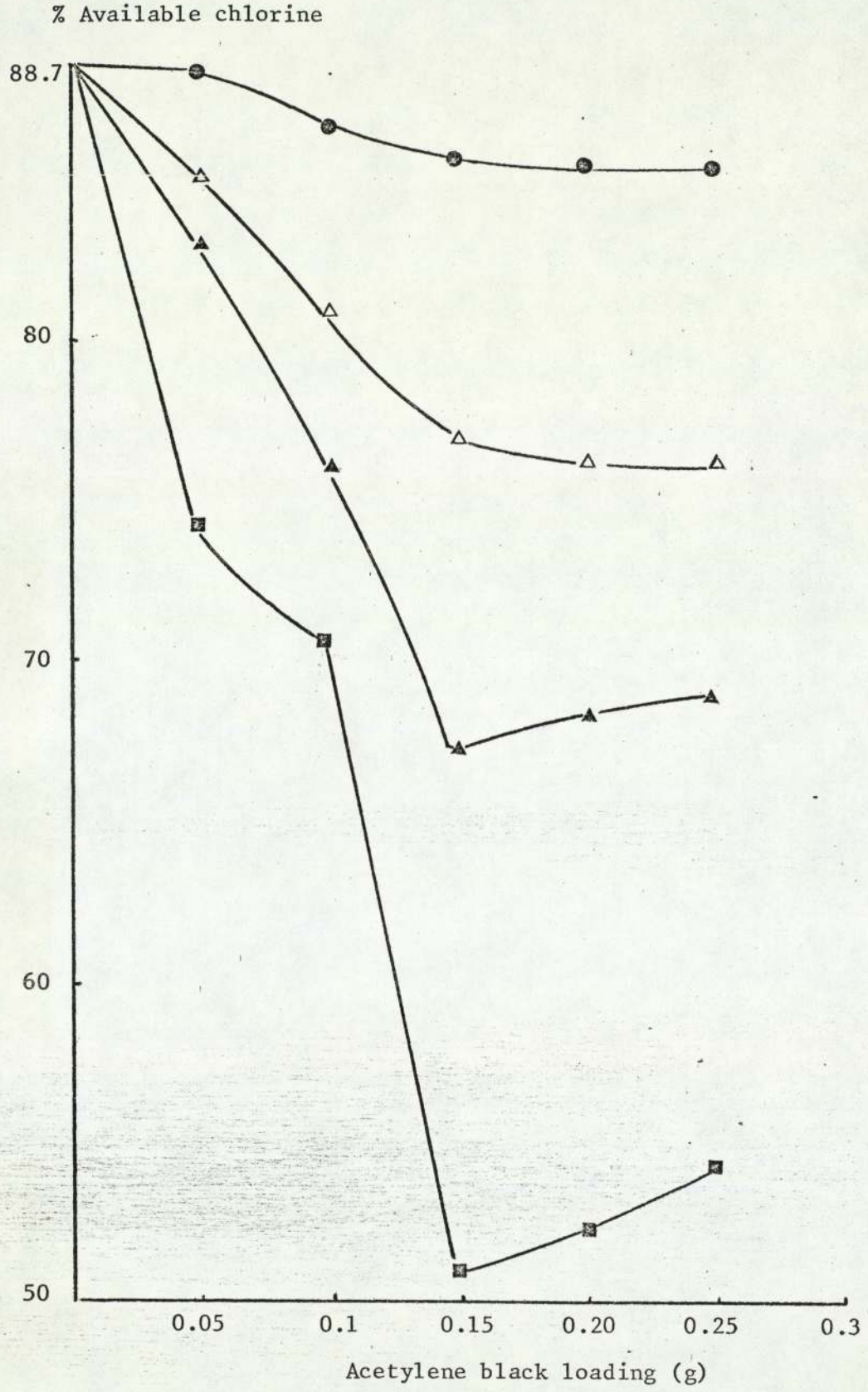

Figure 1 Percentage available chlorine vs acetylene black loading diagram for samples stored for 4,7,14 and 30 days in ambient condition.

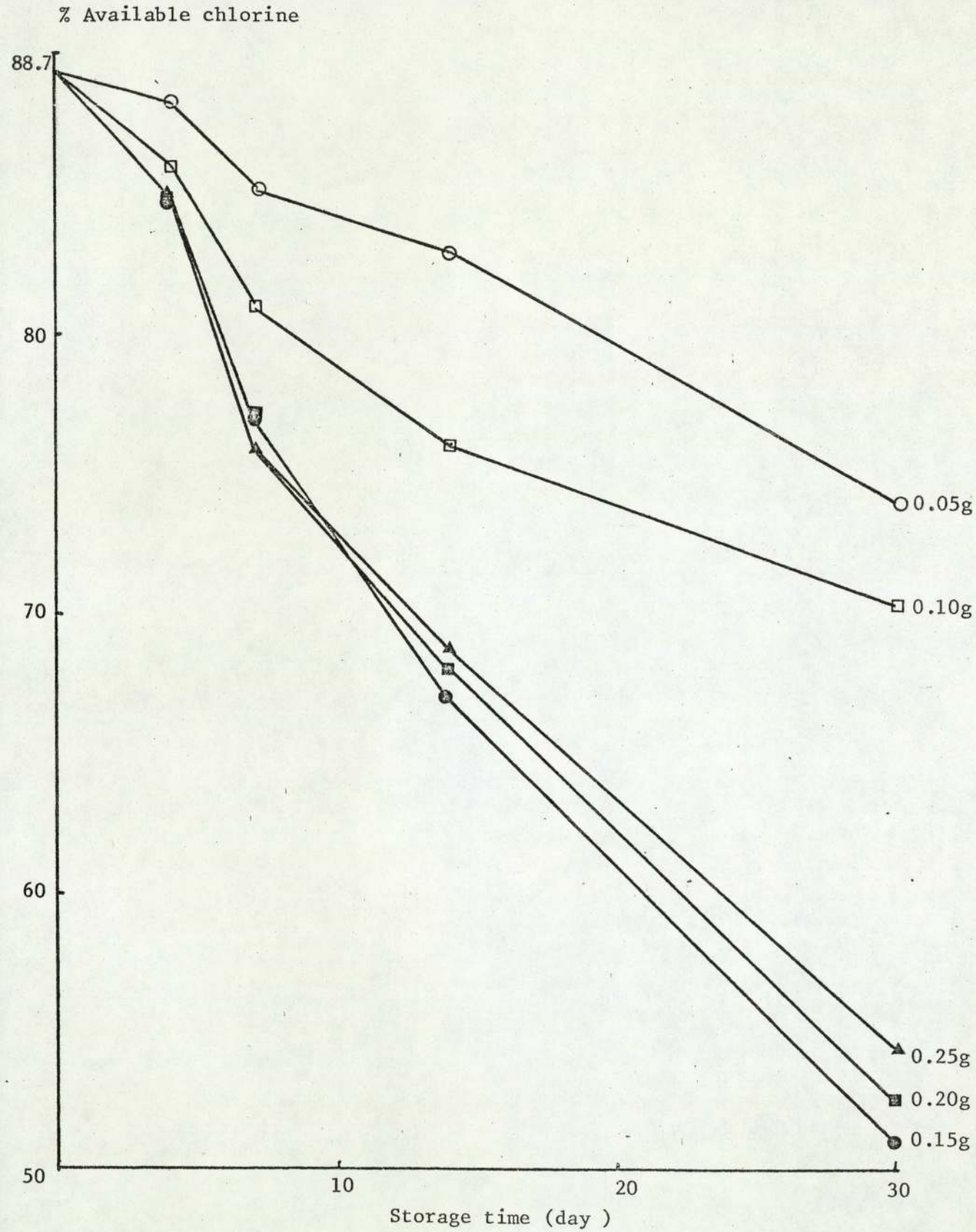

Figure 2 Percentage available chlorine vs storage time relationships for sample with different acetylene black loading.

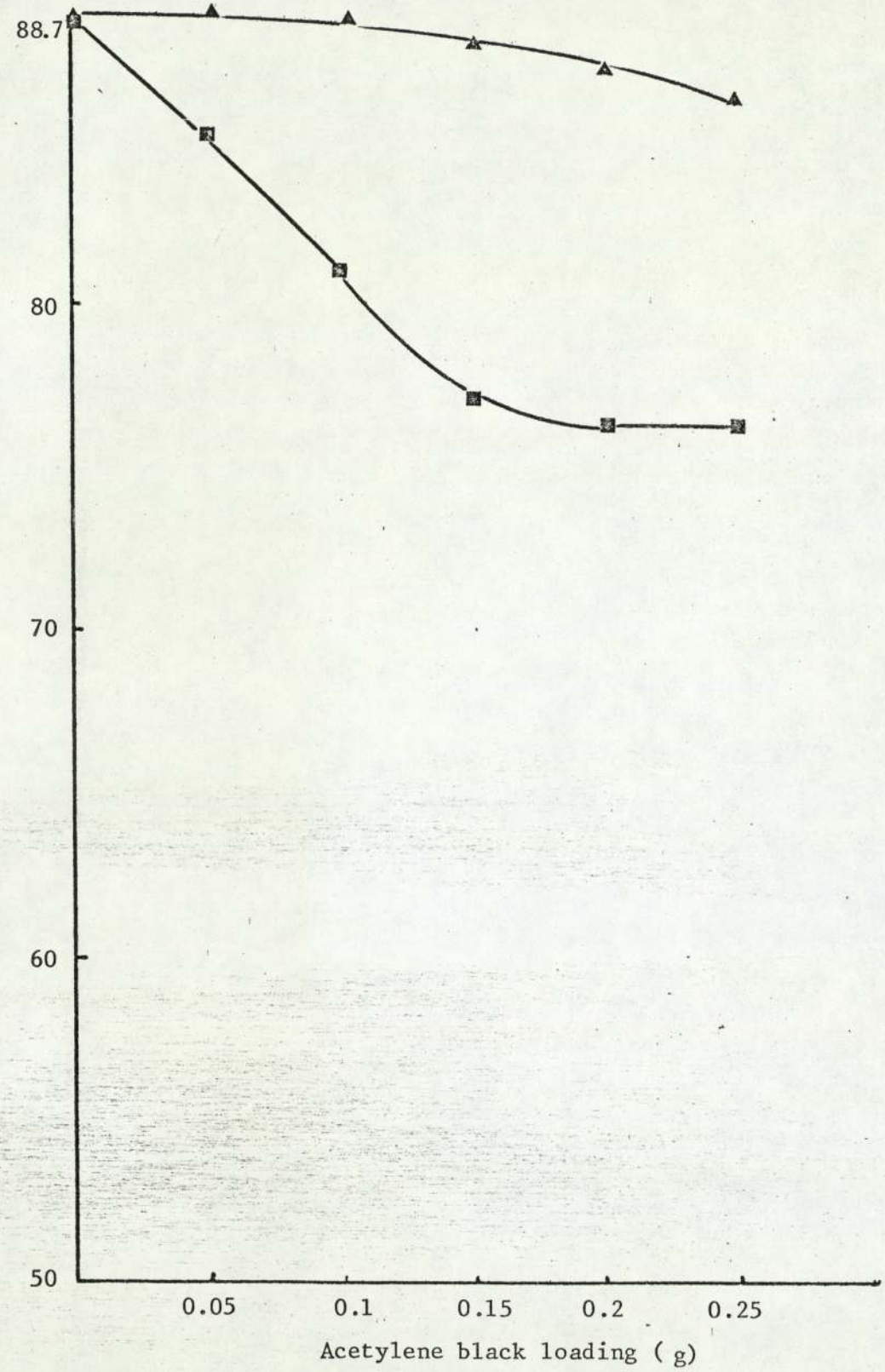

Figure 3 Percentage available chlorine vs acetylene black loading diagram for sample stored under —▲— nitrogen atmosphere and —■— ambient condition.

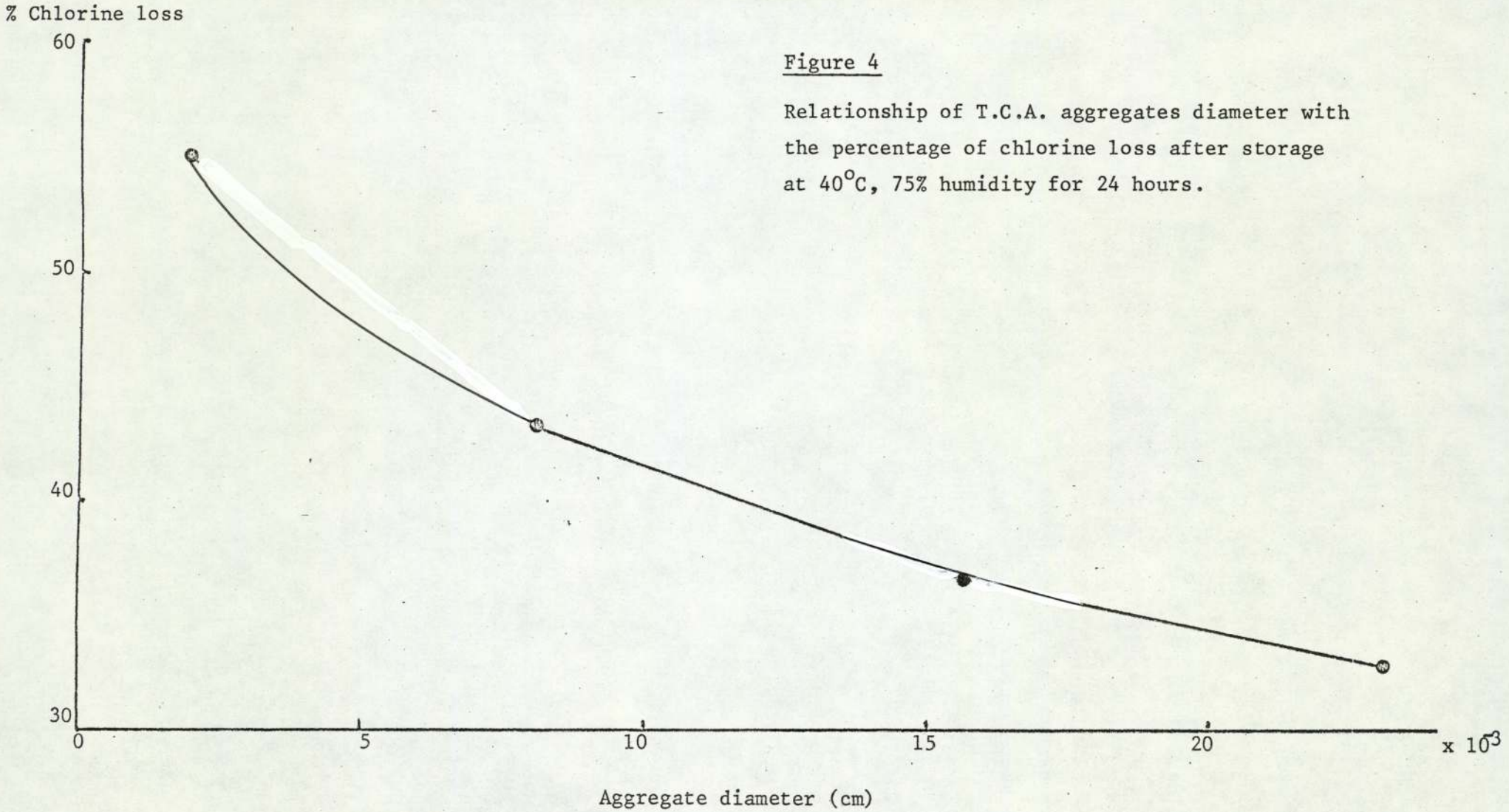

Figure 4

Relationship of T.C.A. aggregates diameter with the percentage of chlorine loss after storage at 40°C, 75% humidity for 24 hours.

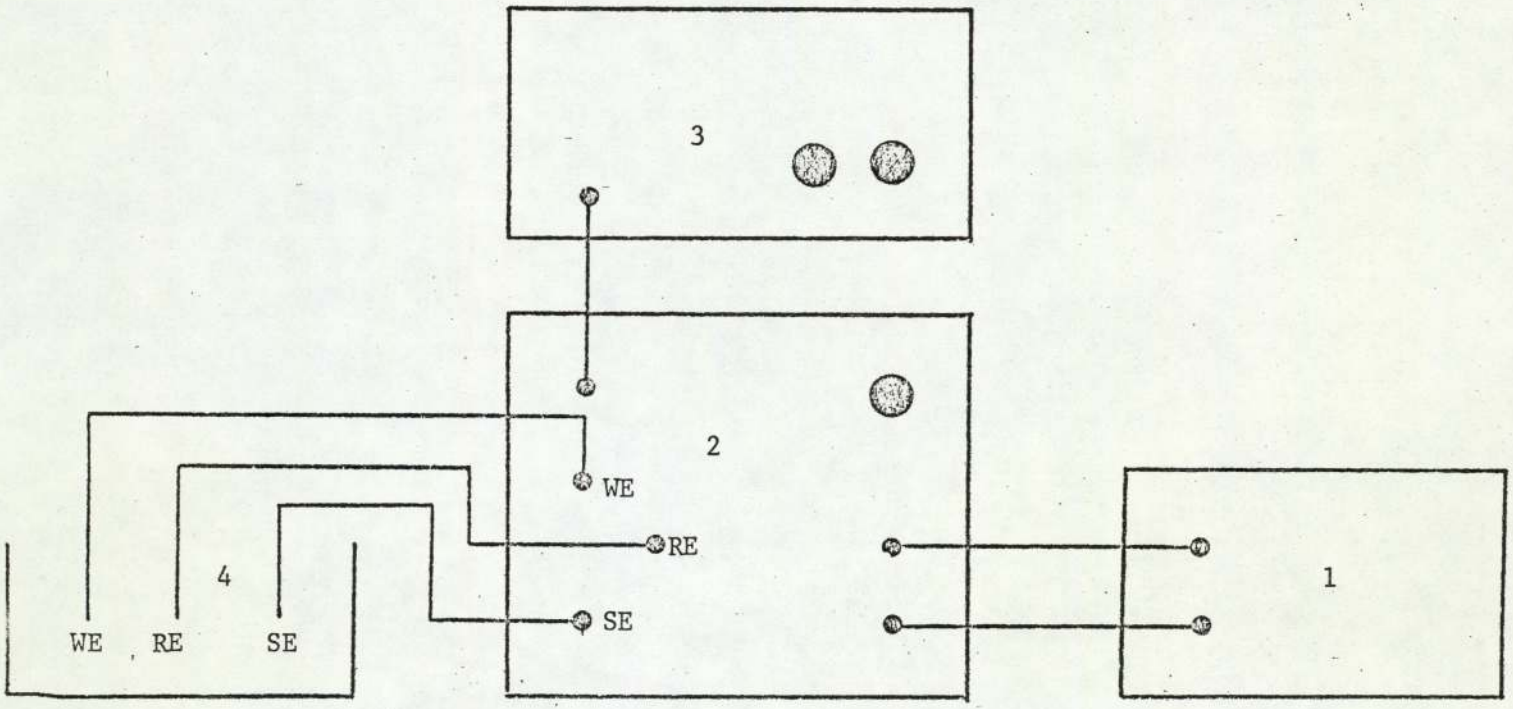

Figure 5 Circuit diagram of the potential dynamic measurement.

1. Chart recorder. 2. Potentiostat. 3. Linear sweep generator. 4. Cell.

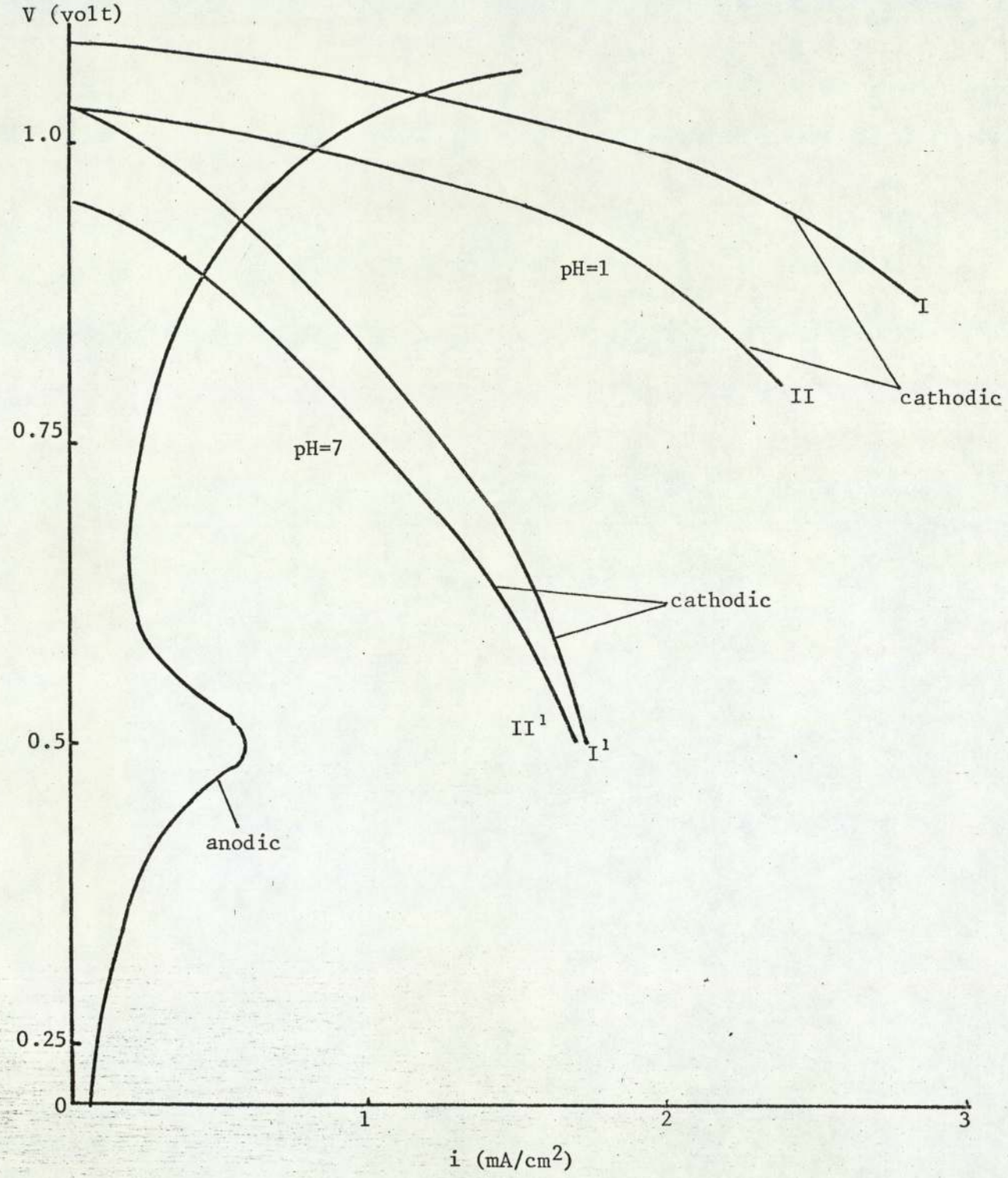

Figure 6 Cathodic and anodic polarization curve for T.C.A. reduction and graphite oxidation at T = 20°C, pH = 1 and pH = 7.

Curve I & II : $C_{T.C.A.} = 4.30 \times 10^{-2}$ mole/liter

Curve I^1 & II^1: $C_{T.C.A.} = 3.23 \times 10^{-2}$ mole/liter

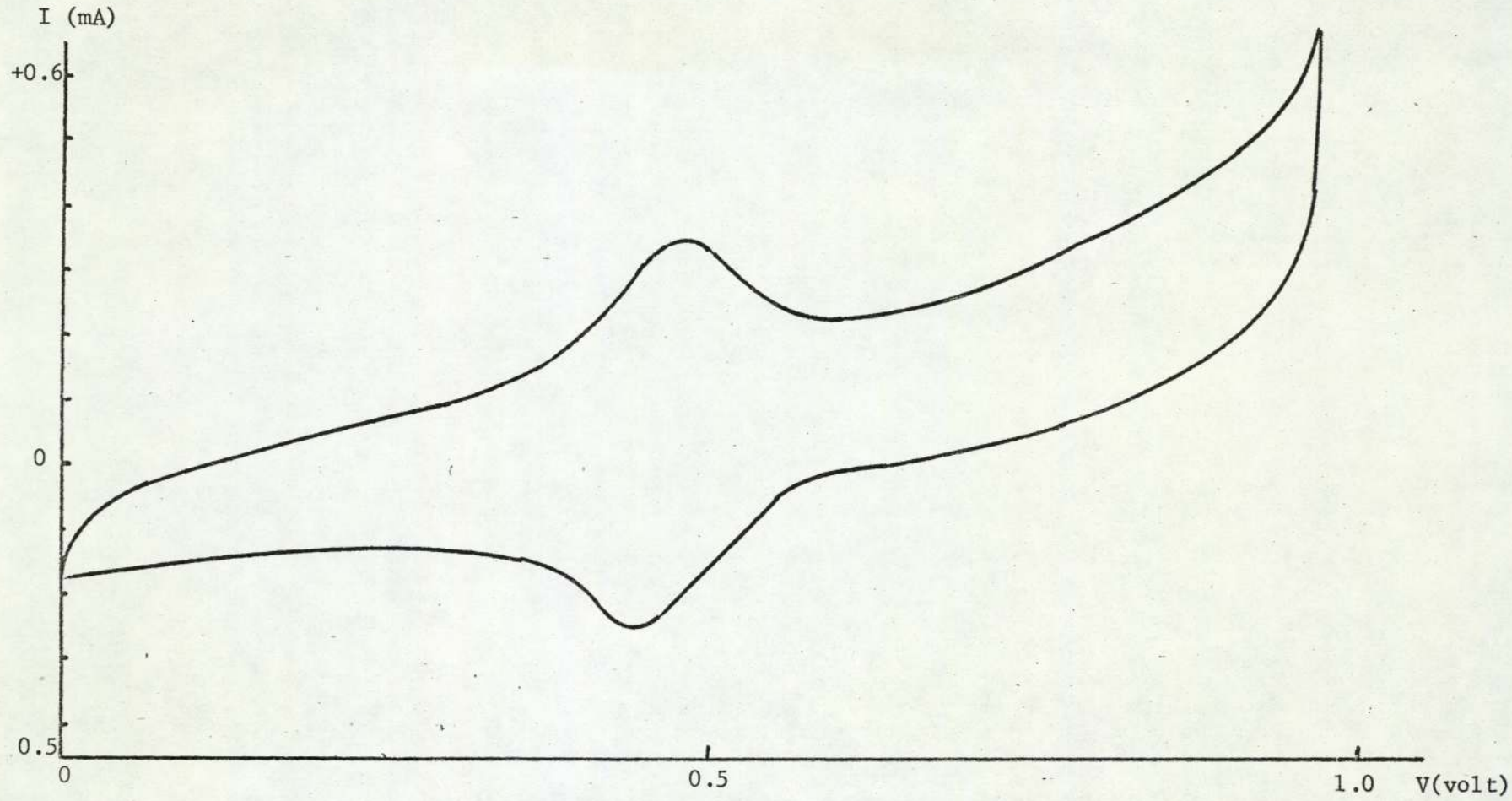

Figure 7 Cyclic voltammogram of graphite electrode in 4M NaCl solution pH = 1 and 7.

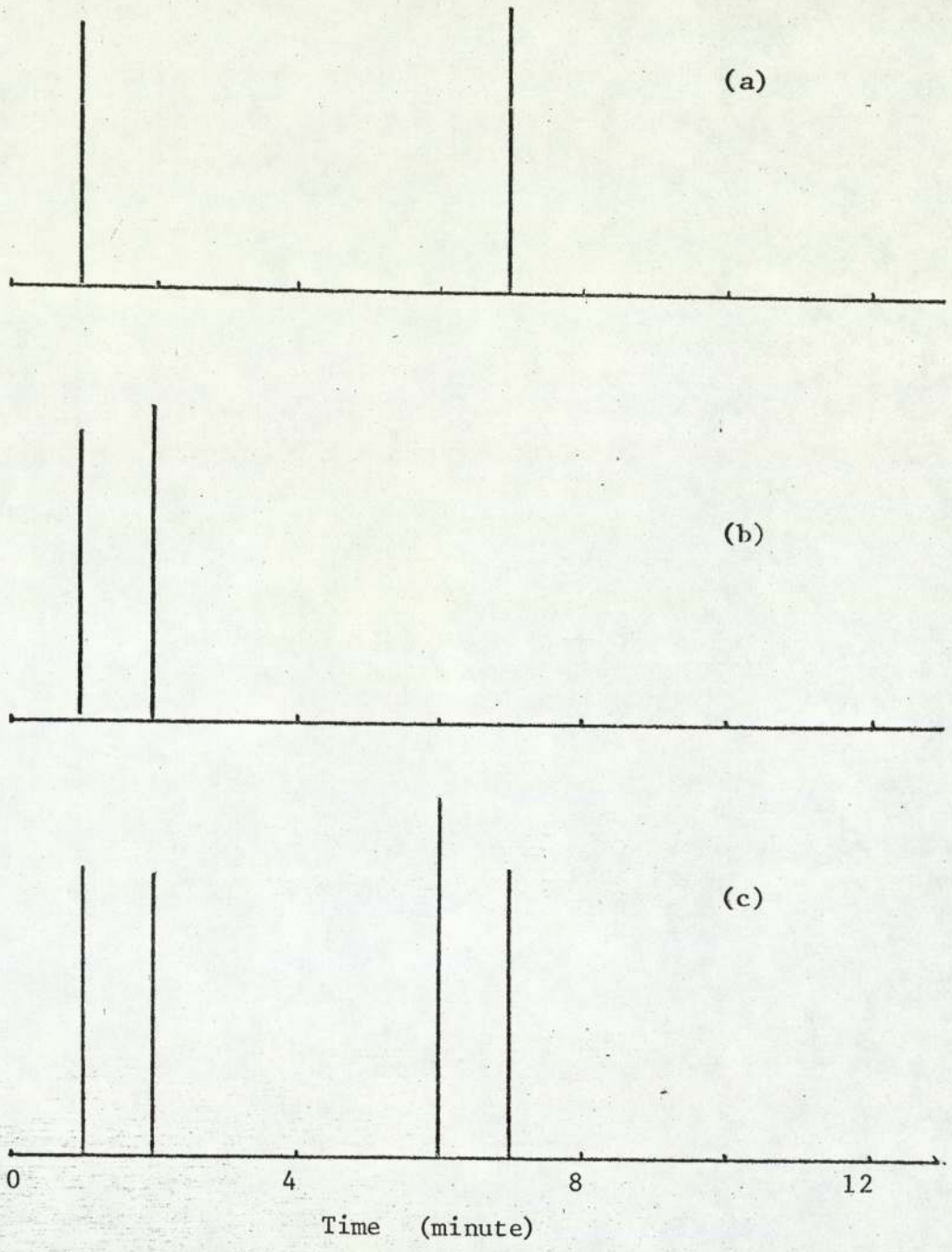

Figure 8 Liquid gas chromatograph of benzyl methyl ether.

(a) Reference compound (pure benzyl methyl ether)

(b) Product from mixture containing benzene, toluene, and T.C.A.

(c) Product from mixture containing benzene, toluene, T.C.A. and acetylene black.

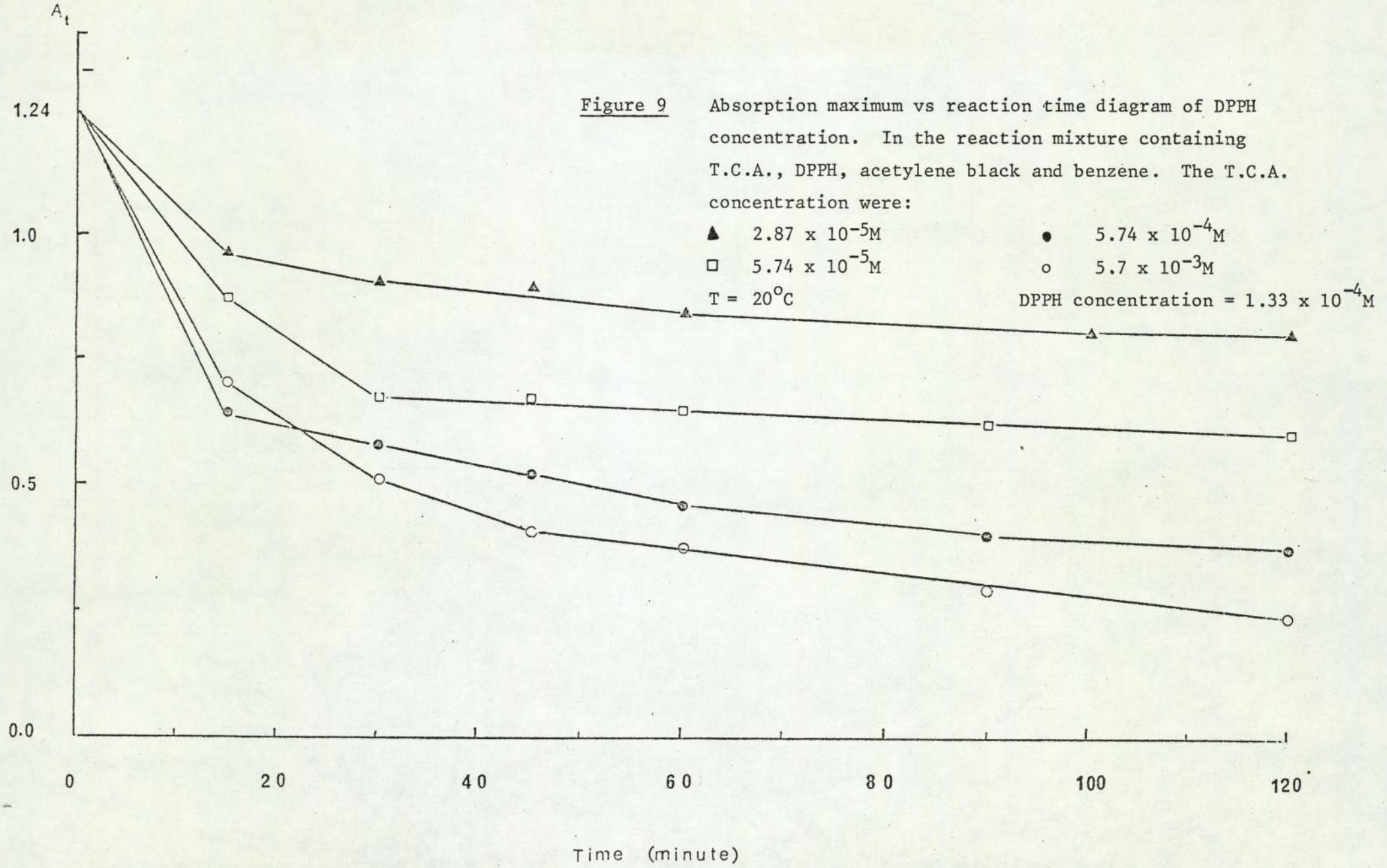

Figure 9 Absorption maximum vs reaction time diagram of DPPH concentration. In the reaction mixture containing T.C.A., DPPH, acetylene black and benzene. The T.C.A. concentration were:

▲ 2.87×10^{-5}M ● 5.74×10^{-4}M

□ 5.74×10^{-5}M o 5.7×10^{-3}M

T = 20°C DPPH concentration = 1.33×10^{-4}M

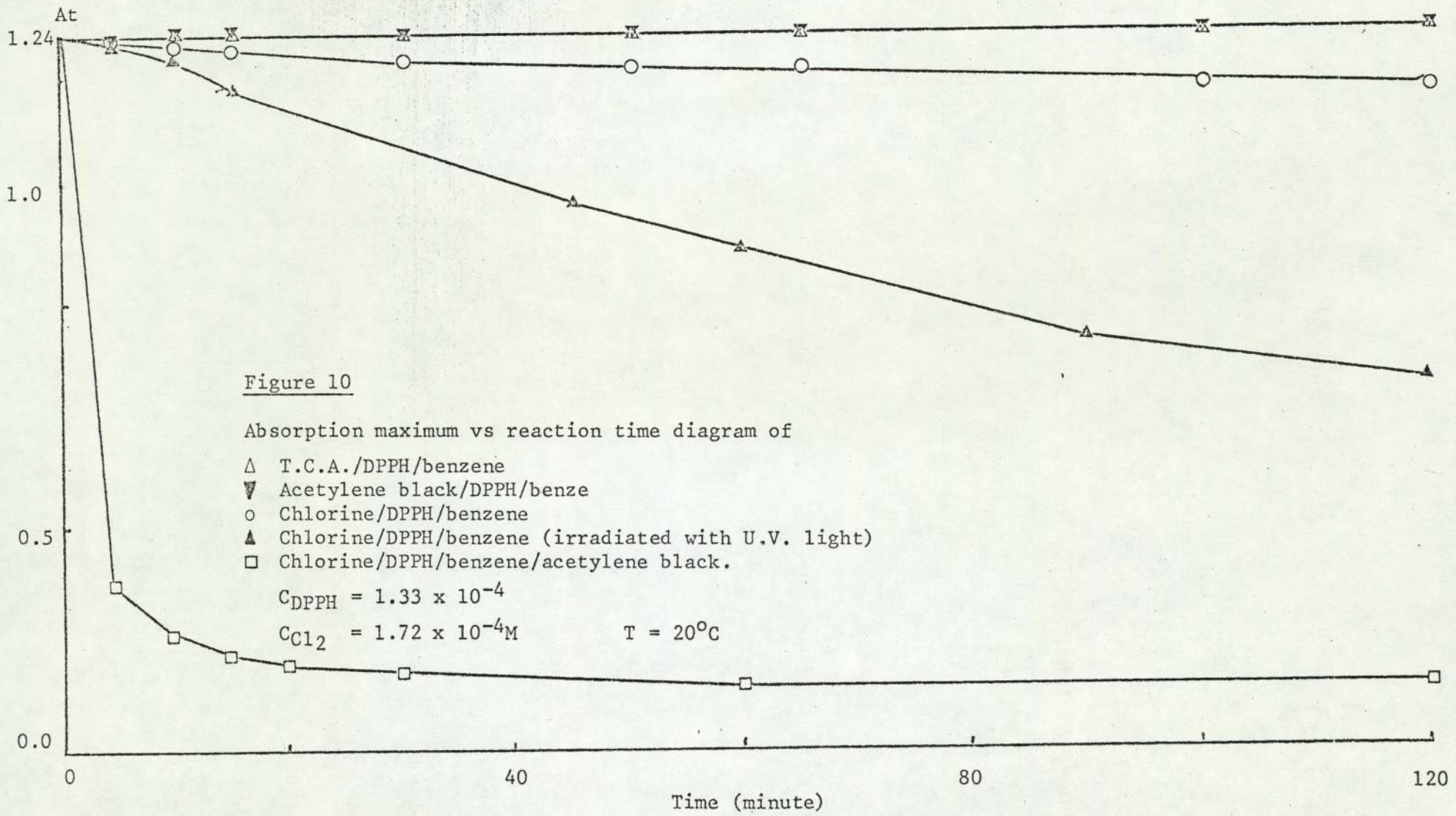

Figure 10

Absorption maximum vs reaction time diagram of

Δ T.C.A./DPPH/benzene
▼ Acetylene black/DPPH/benze
o Chlorine/DPPH/benzene
▲ Chlorine/DPPH/benzene (irradiated with U.V. light)
□ Chlorine/DPPH/benzene/acetylene black.

$C_{DPPH} = 1.33 \times 10^{-4}$

$C_{Cl_2} = 1.72 \times 10^{-4}M$ T = 20°C

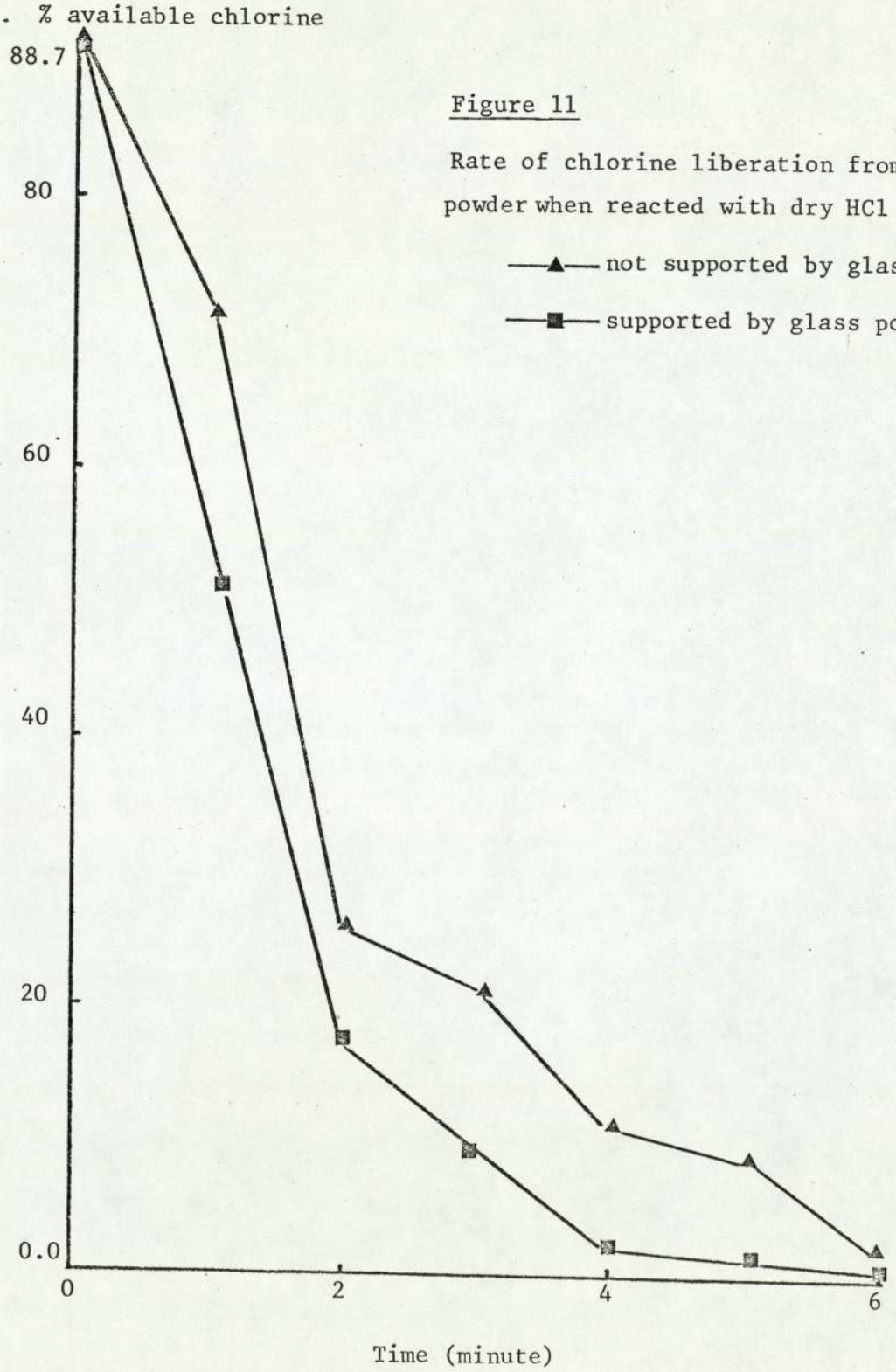

Figure 11

Rate of chlorine liberation from T.C.A. powder when reacted with dry HCl gas at 20°C.

—▲— not supported by glass powder

—■— supported by glass powder

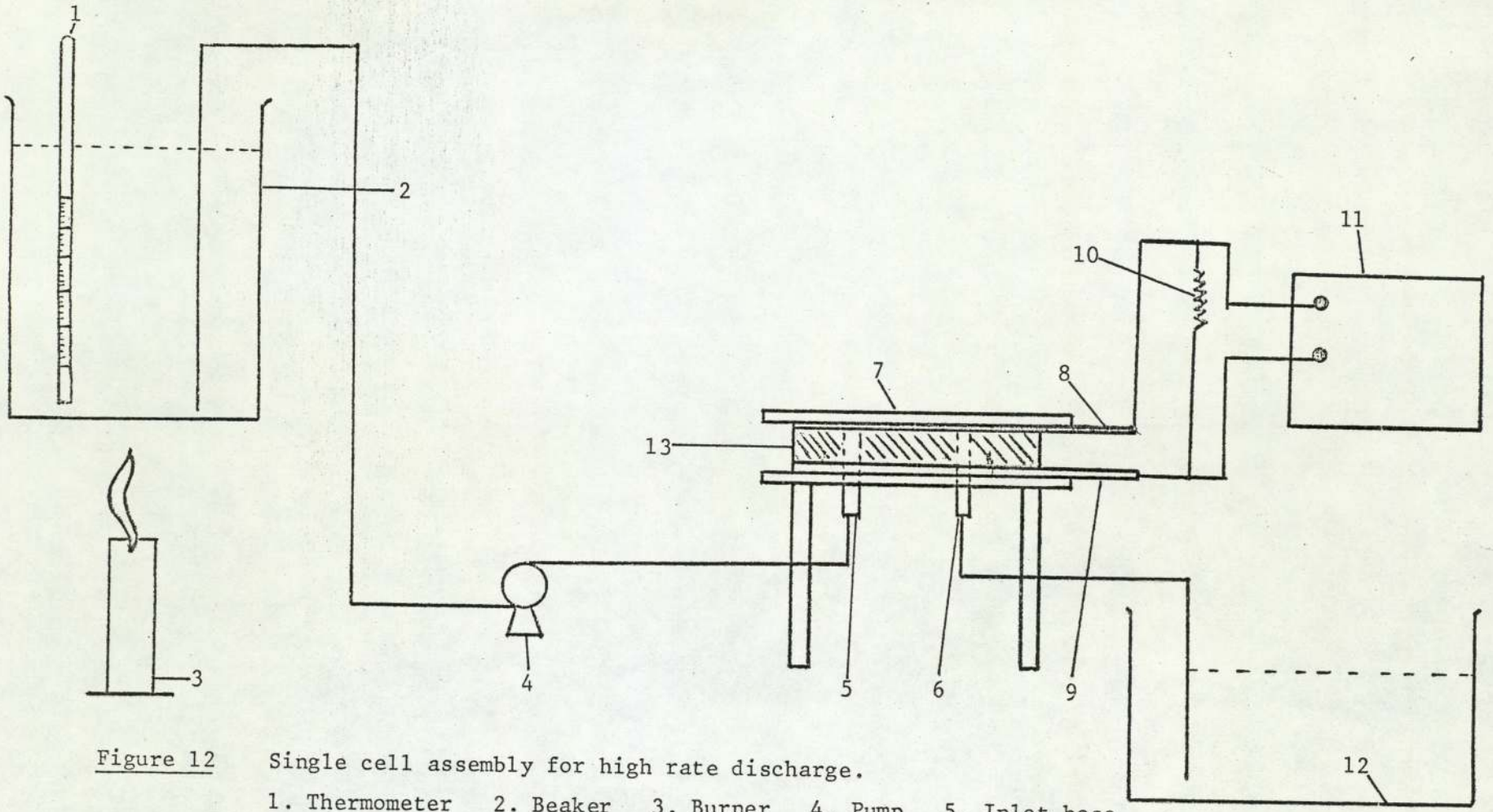

Figure 12 Single cell assembly for high rate discharge.

1. Thermometer 2. Beaker 3. Burner 4. Pump 5. Inlet hose
6. Outlet hose 7. Cell 8. Anode 9. Cathode current collector
10. Resistor 11. Pen recorder 12. Electrolyte reservior 13. Cathode plaque.

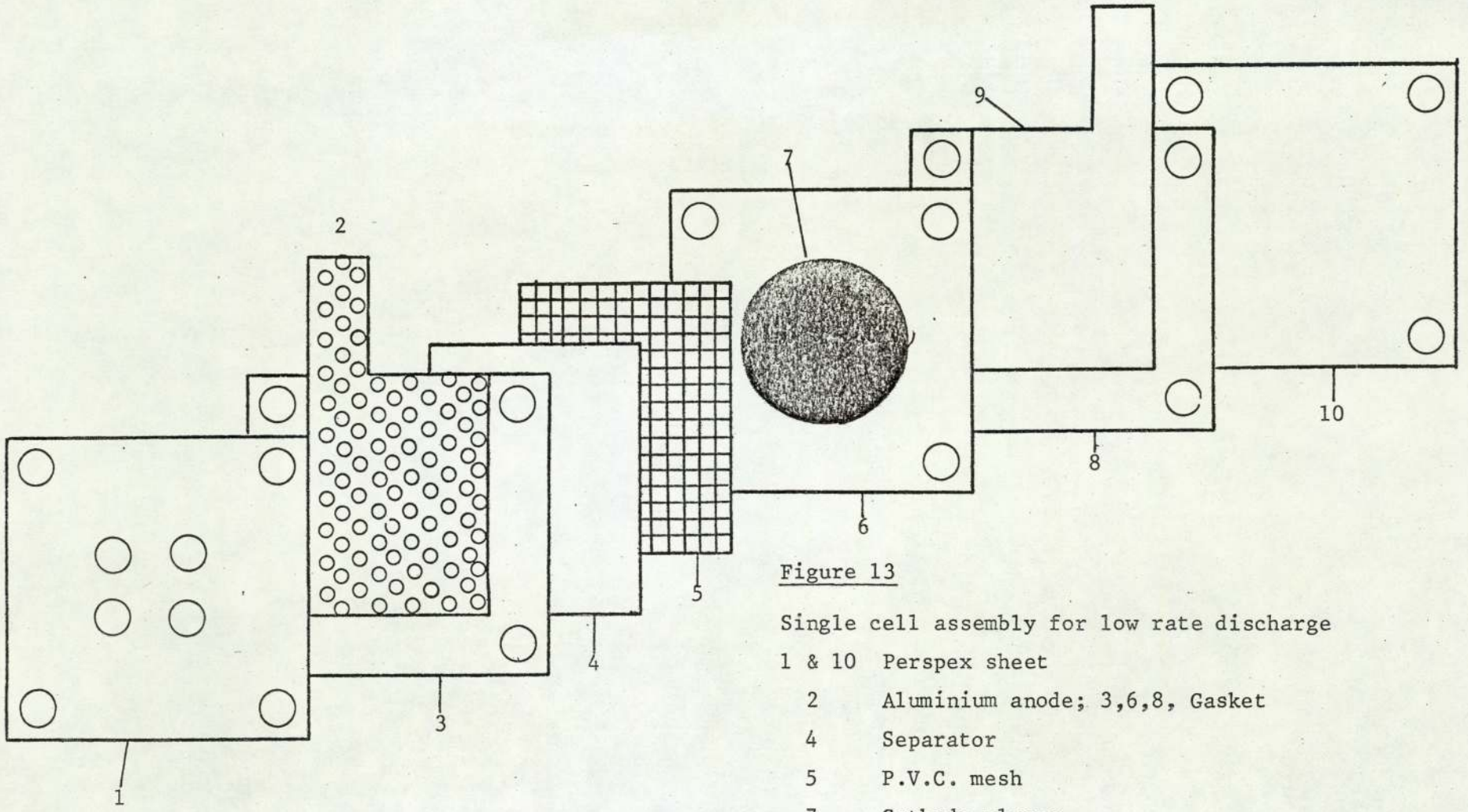

Figure 13

Single cell assembly for low rate discharge

1 & 10 Perspex sheet

2 Aluminium anode; 3,6,8, Gasket

4 Separator

5 P.V.C. mesh

7 Cathode plaque

9 Cathode current collector

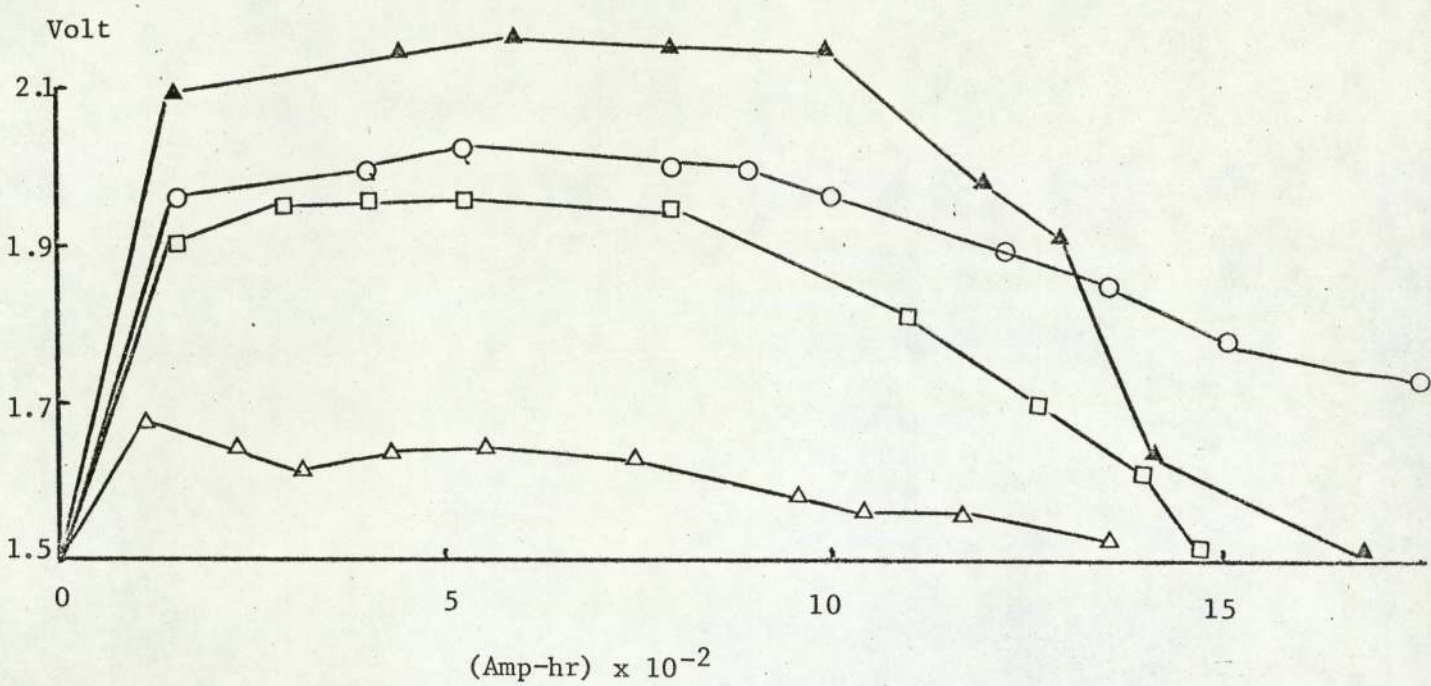

Figure 14

Performance of a single cell, discharge before storage.

Load resistance : 5 ohm.

—▲— mixed type.

—○— sandwich type with no additive at the T.C.A./acetylene black interface.

—□— sandwich type with boric acid at the T.C.A./acetylene black interface.

—△— sandwich type with fine filter paper at the T.C.A./ acetylene black interface.

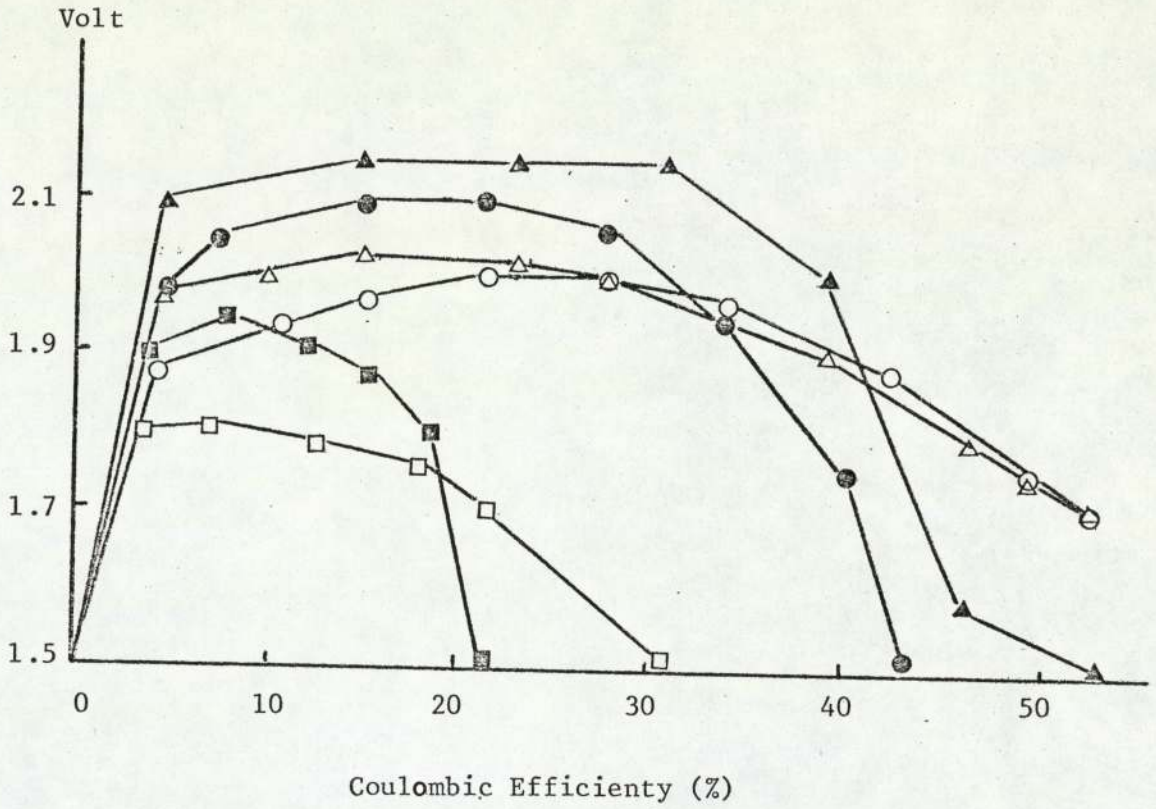

Figure 15

Voltage vs Coulombic Efficiency diagram of mixed and sandwich type single cell discharge at R = 5 ohm after storage for 0, 24 and 120 hours.

—△— —○— —□— sandwich type

—▲— —●— —■— mixed type

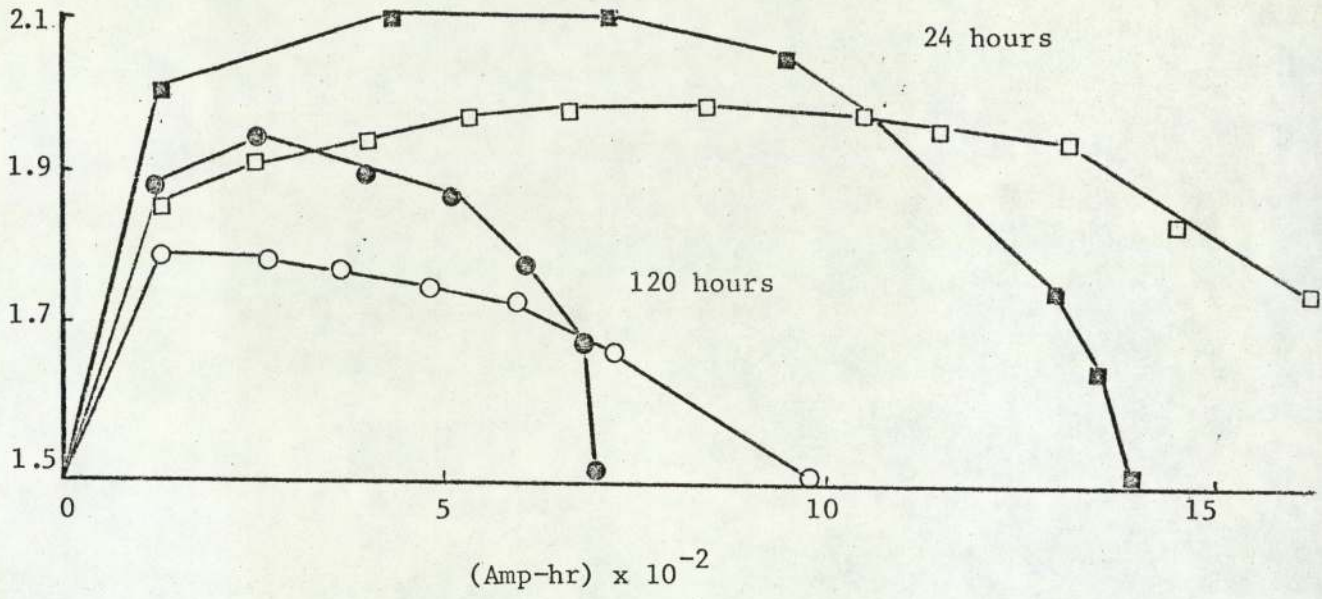

Figure 16

Performance of a single cell after storage at 40°C, 75% humidity for 24 hours and 120 hours respectively.
Load resistance : 5 ohm.

—■— —●— mixed type cathode
—□— —○— sandwich type cathode

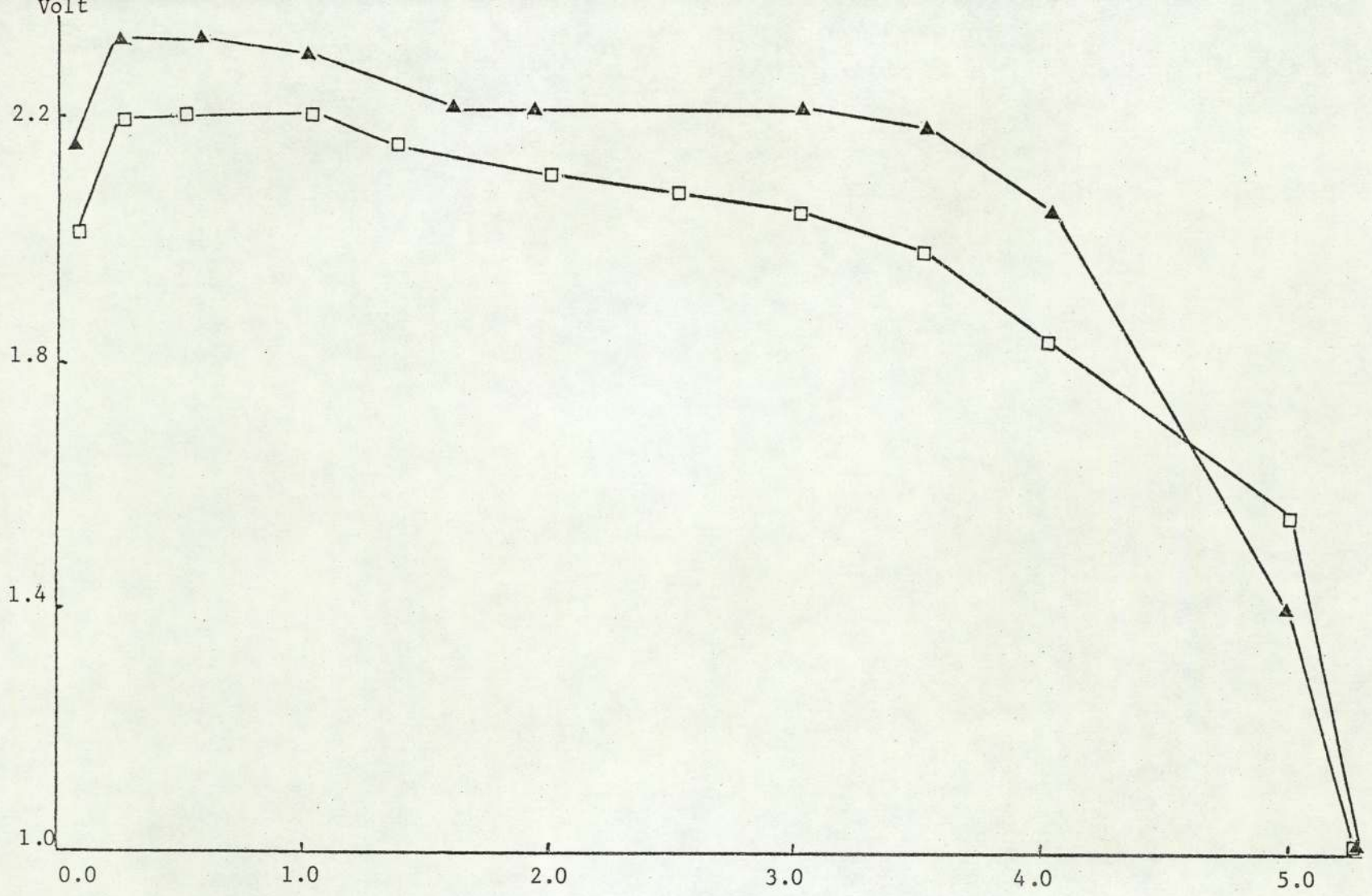

Figure 17 Cell voltage - time profile of a single cell discharged at 5 mA/cm^2 before storage.
—▲— mixed type cathode, —□— sandwich type cathode with boric oxide at interface.
T = 25°C.

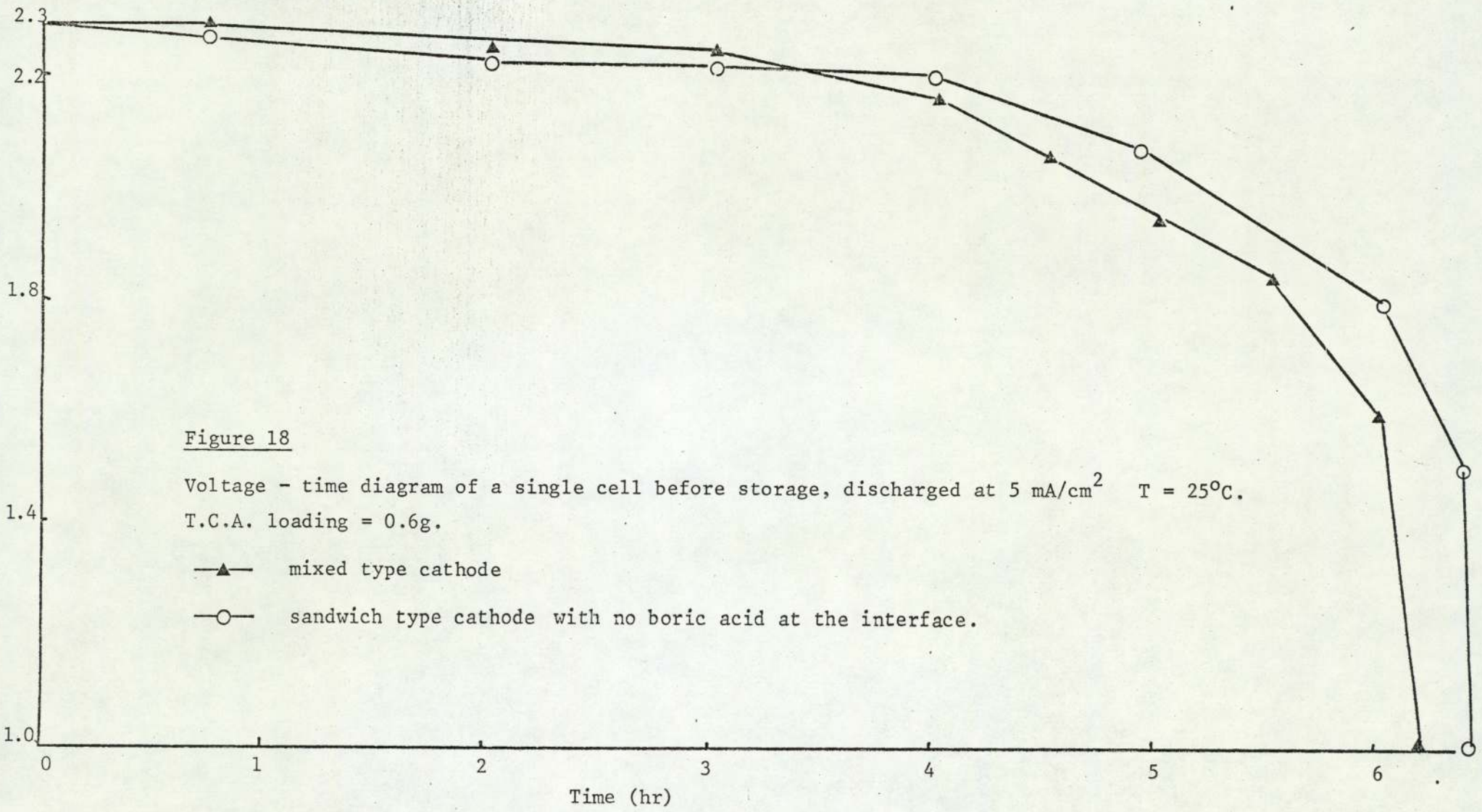

Figure 18

Voltage - time diagram of a single cell before storage, discharged at 5 mA/cm^2 T = 25°C.
T.C.A. loading = 0.6g.

—▲— mixed type cathode

—○— sandwich type cathode with no boric acid at the interface.

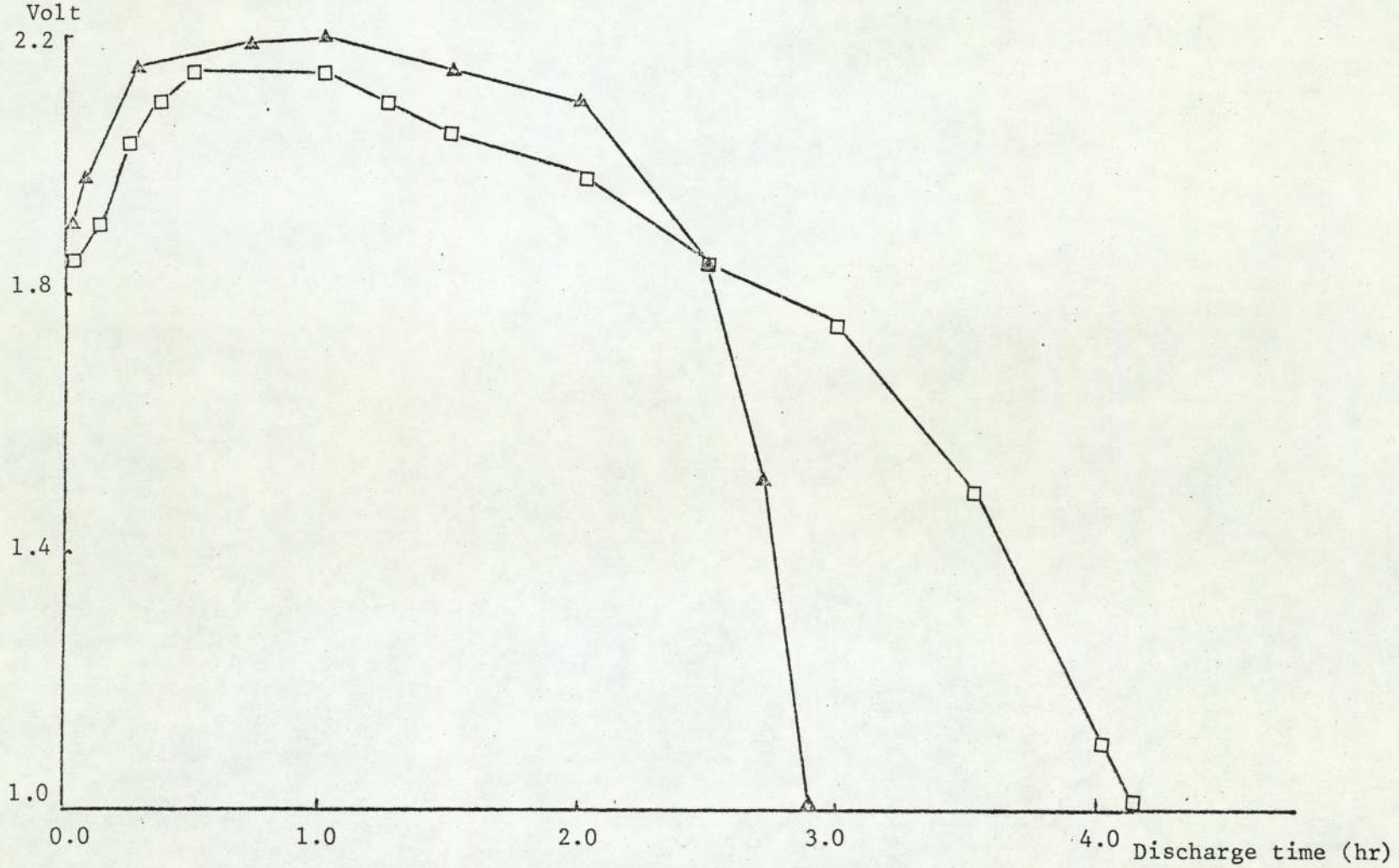

Figure 19 Cell voltage - time profile of a single cell, discharged at 5 mA/cm^2, after storage at 40^{o}C, 75% humidity for 24 hours.

—▲— mixed type cathode. —□— sandwich type cathode.

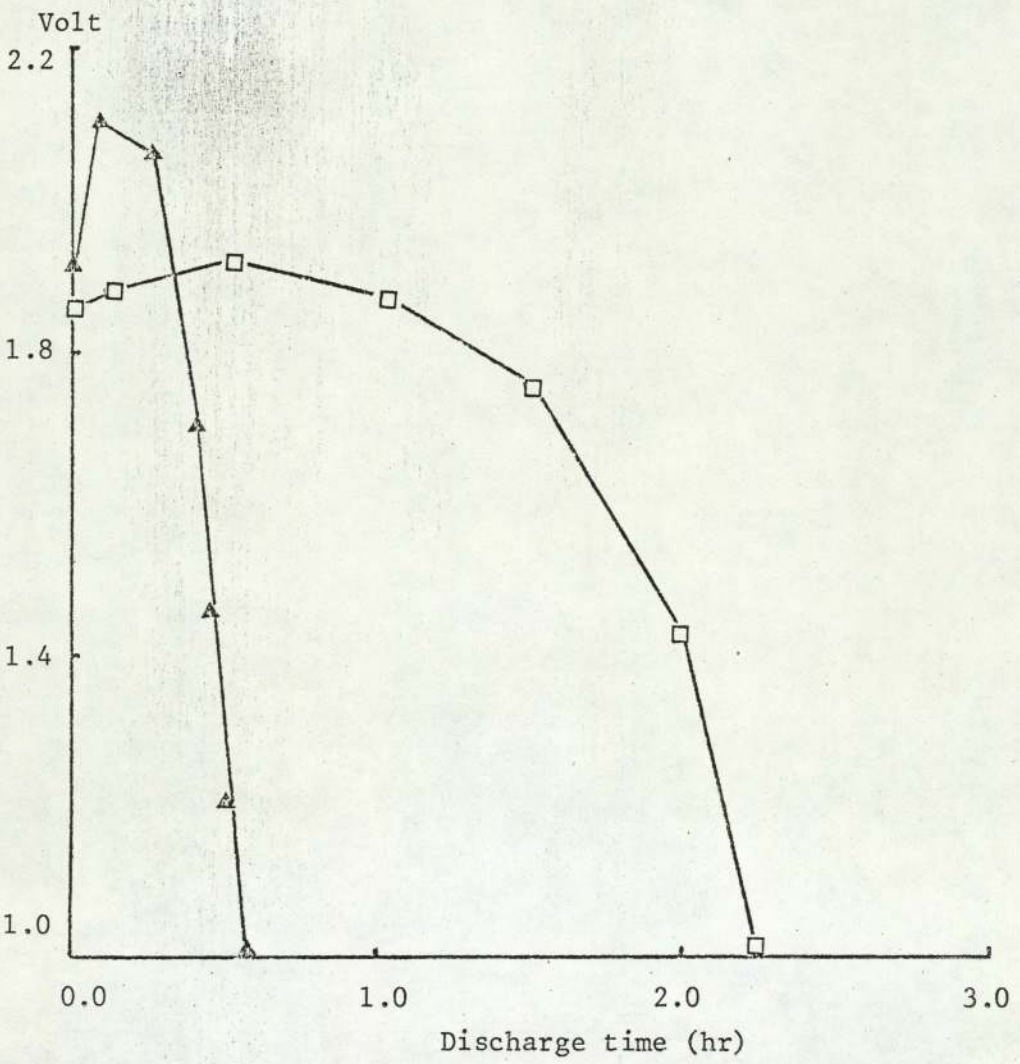

Figure 20 Cell voltage - time profile of a single cell discharged at 5 mA/cm^2, after 48 hours storage at 40^{o}C and 75% humidity.

—▲— mixed type cathode —□— sandwich type cathode

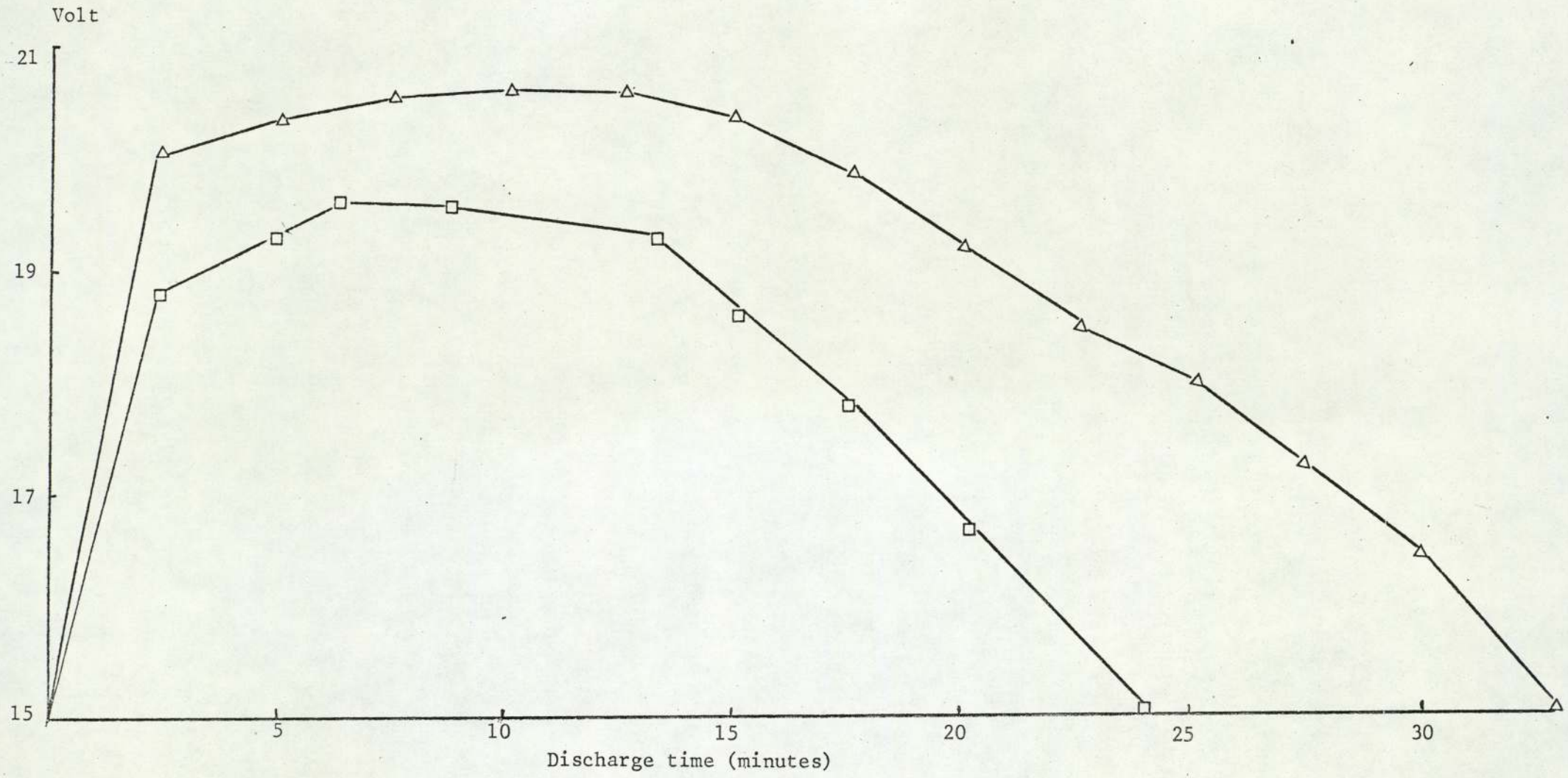

Figure 21 Voltage-time profile of sandwich type single cell before storage. Load resistance : 5 ohm.

—△— No additive at T.C.A./acetylene black interface.

—□— Cyanuric acid at T.C.A./acetylene black interface.

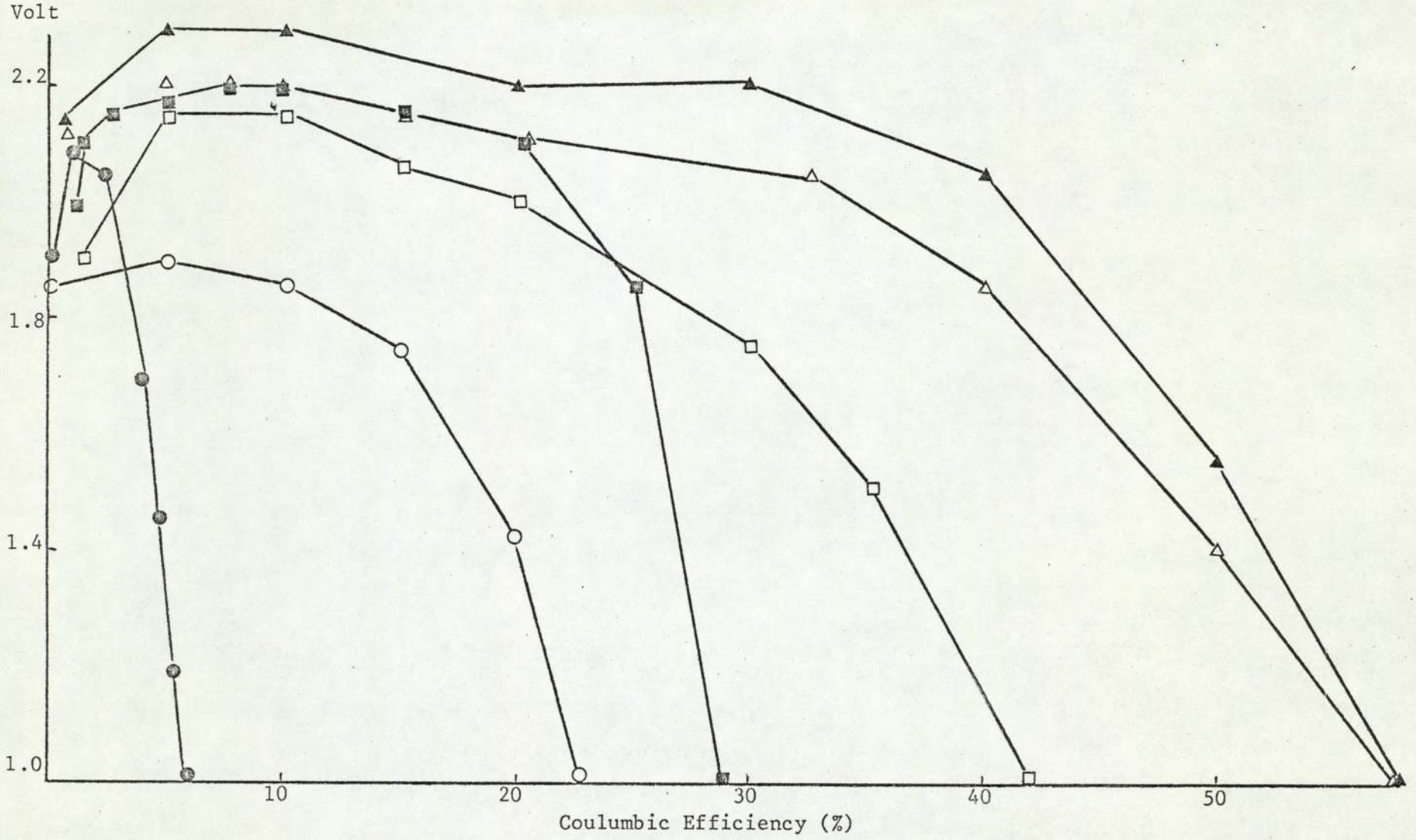

Figure 22 Voltage vs coulumbic efficiency diagram of mixed and sandwich type single cell discharged at 5 mA/cm^2, T = 25°C, after storage for 0, 24 and 48 hours at 40°C and 75% humidity.

—▲— —■— —●— mixed type

—○— —□— —△— sandwich type

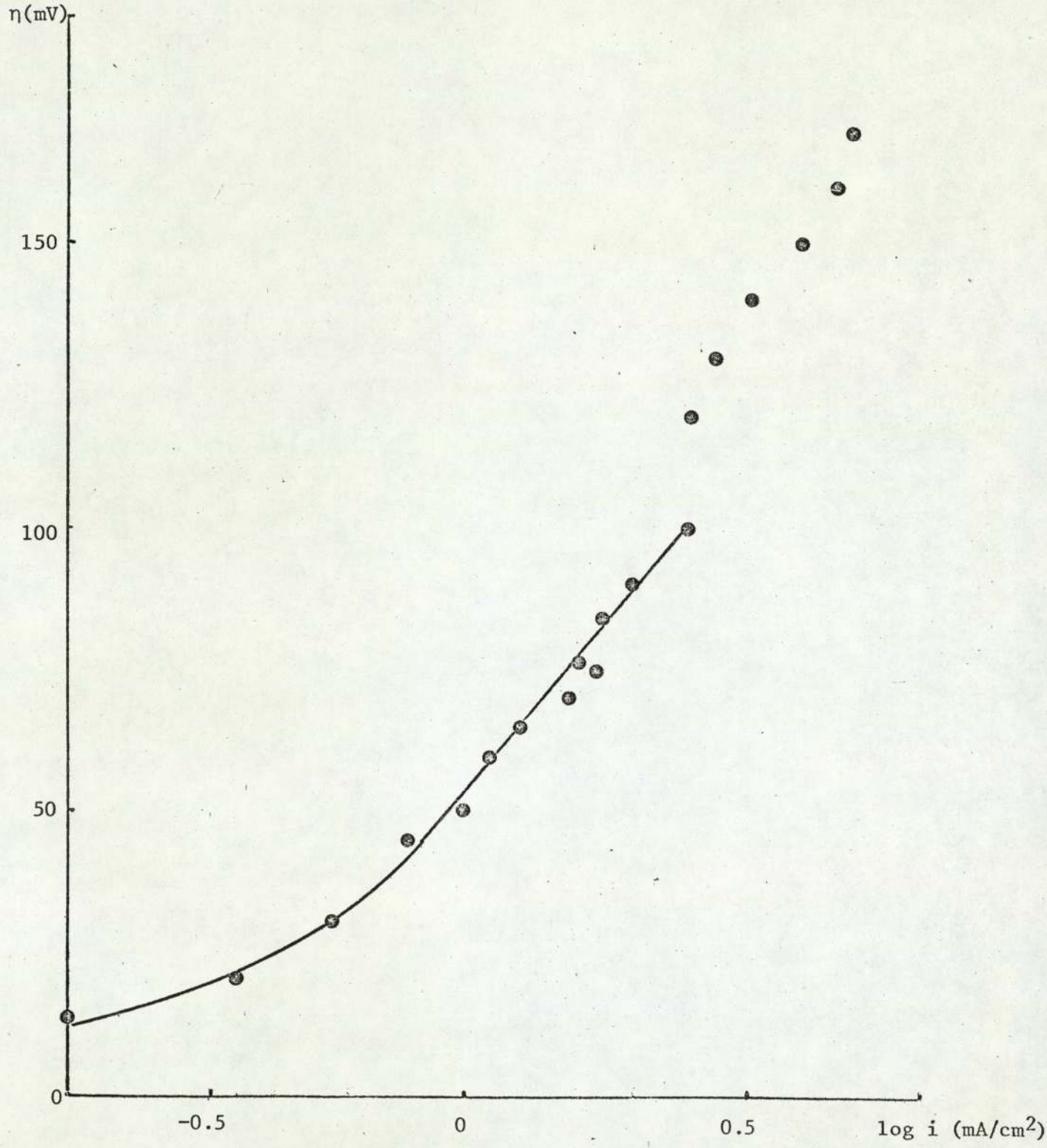

Figure 23 Tafel plot of chlorine reduction on porous carbon in saturated NaCl and 1M HCl at 20°C, using potential transient technique.

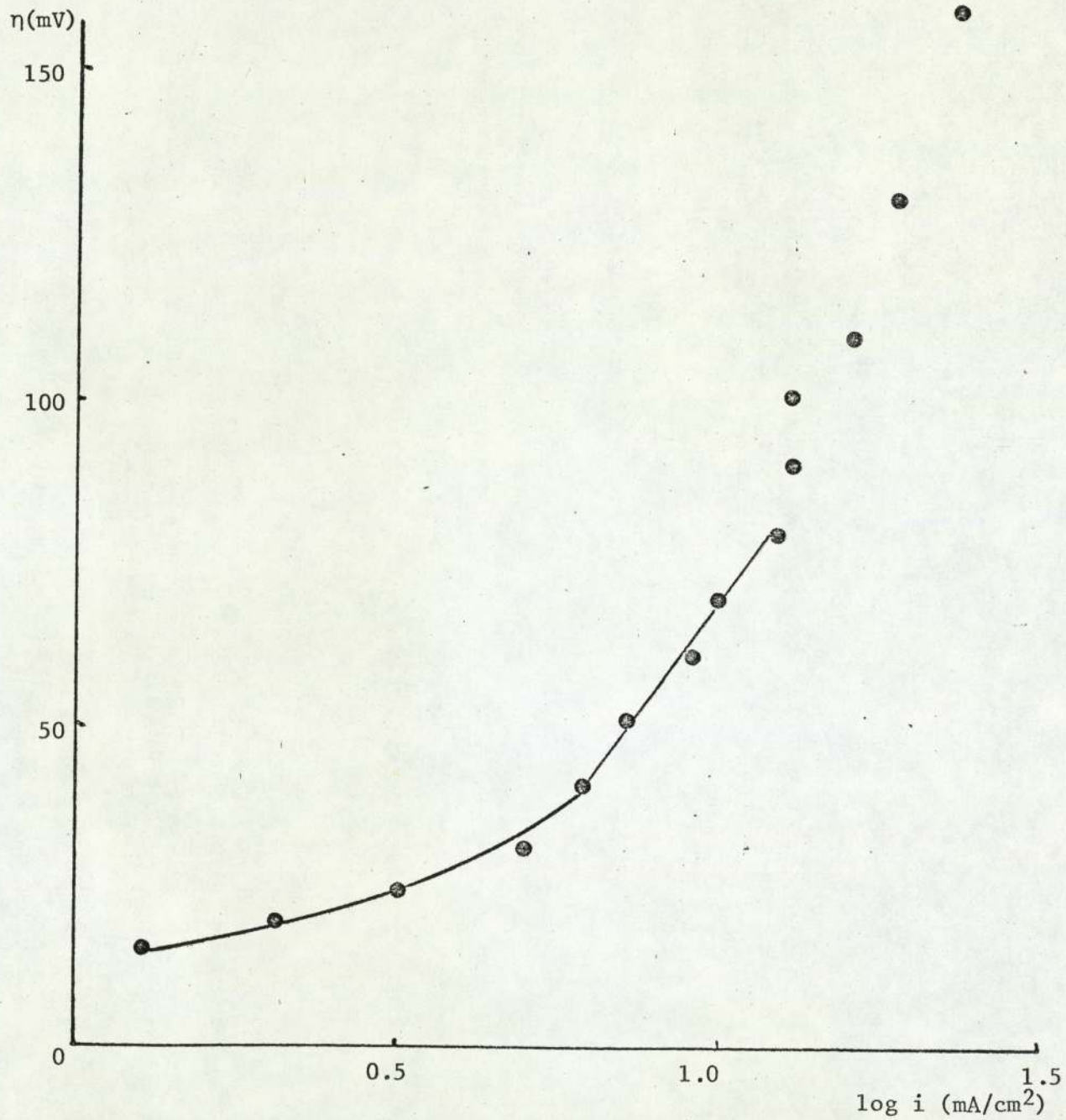

Figure 24 Tafel plot of chlorine reduction on pyrolytic graphite in saturated NaCl and 1M HCl at 20°C, using potential transient technique.

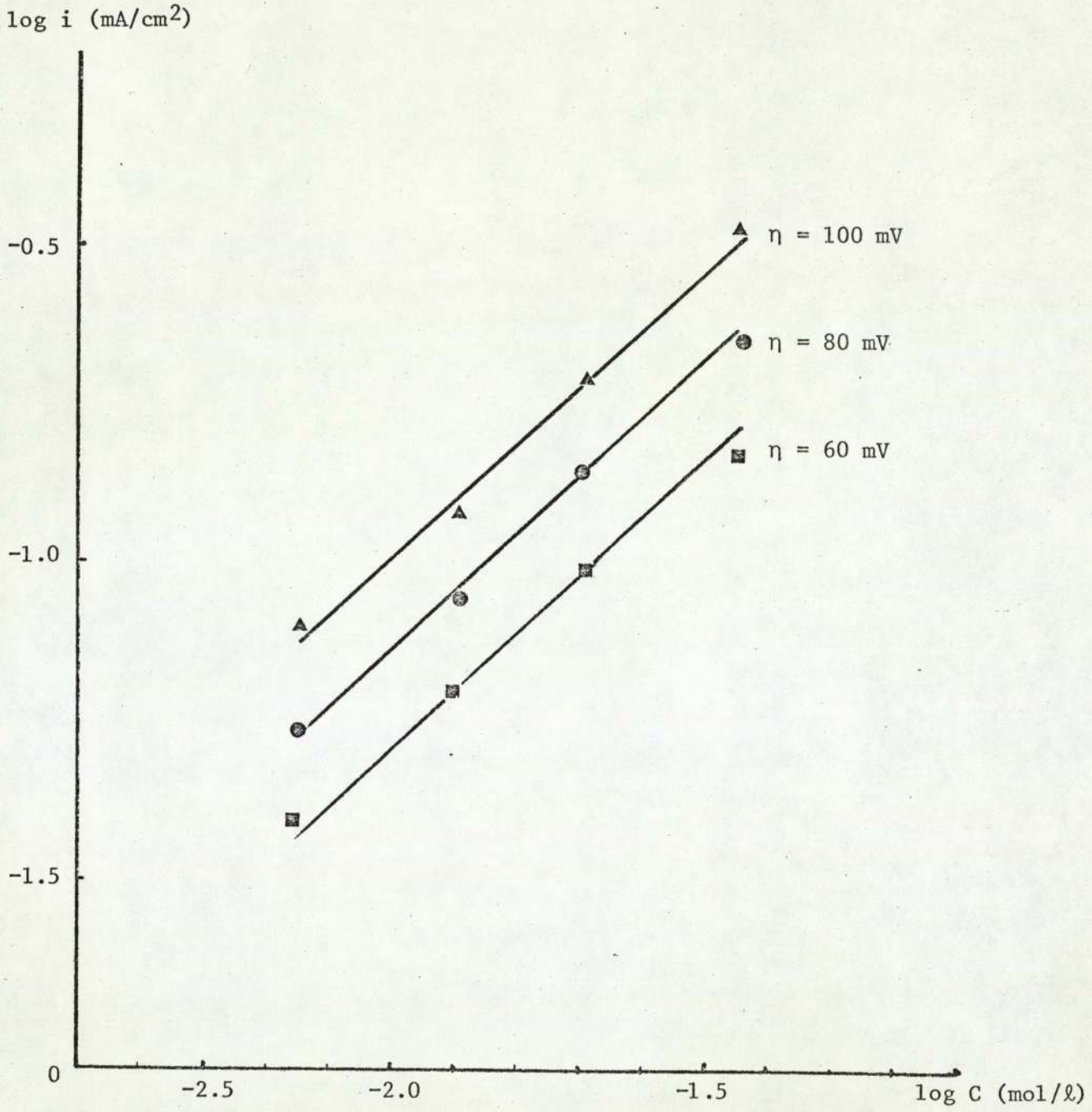

Figure 25 Log i (mA/cm^2) vs log C (mol/ℓ) plot of chlorine reduction on porous carbon rotating disc electrode at $20^{o}C$, in saturated NaCl and 1M HCl, using steady state potentiostatic technique.

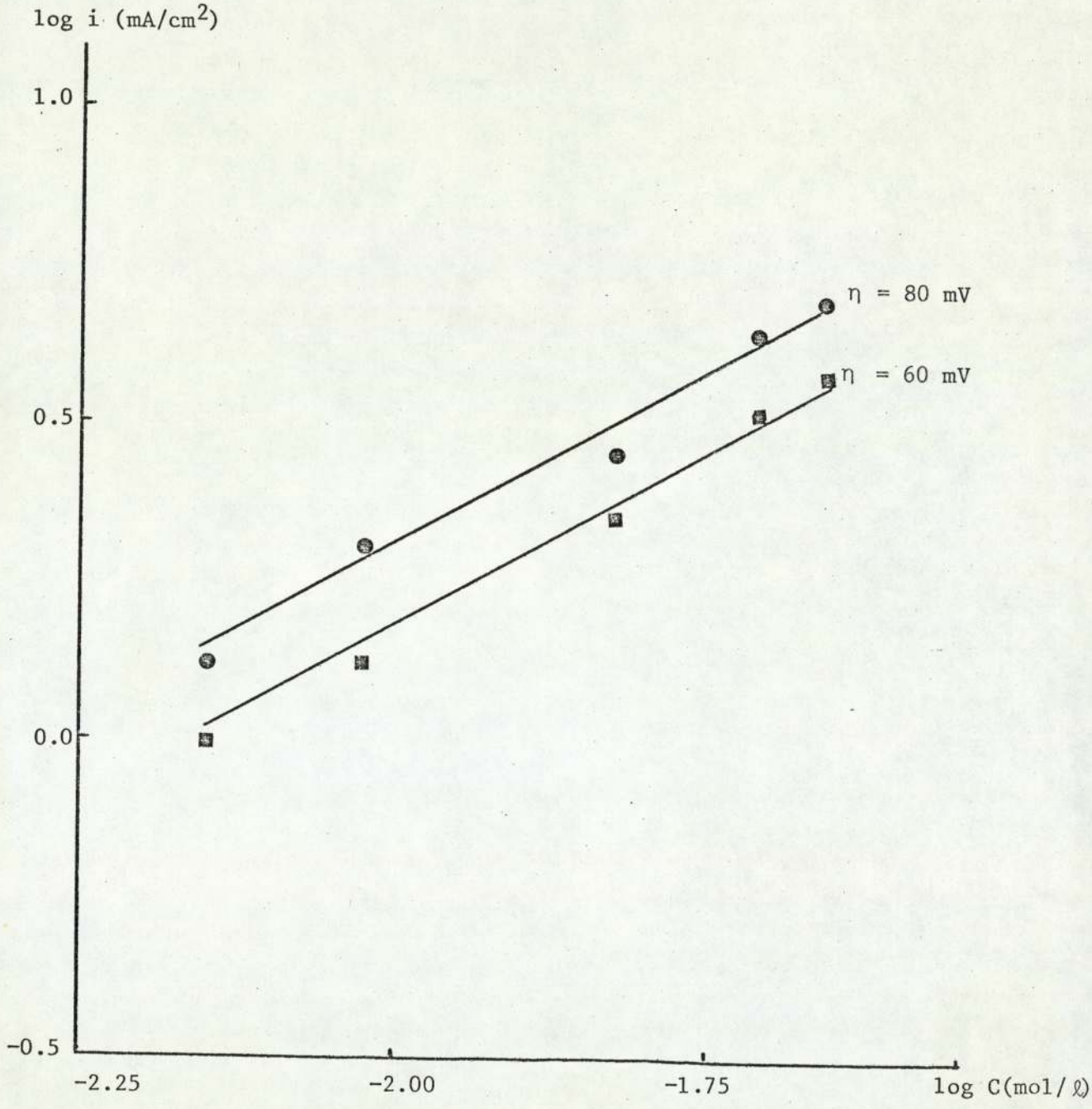

Figure 26 Log i (mA/cm^2) vs log C (mol/ℓ) plot of chlorine reduction on pyrolytic graphite in saturated NaCl and 1M HCl at 20^{o}C, using potential transient technique.

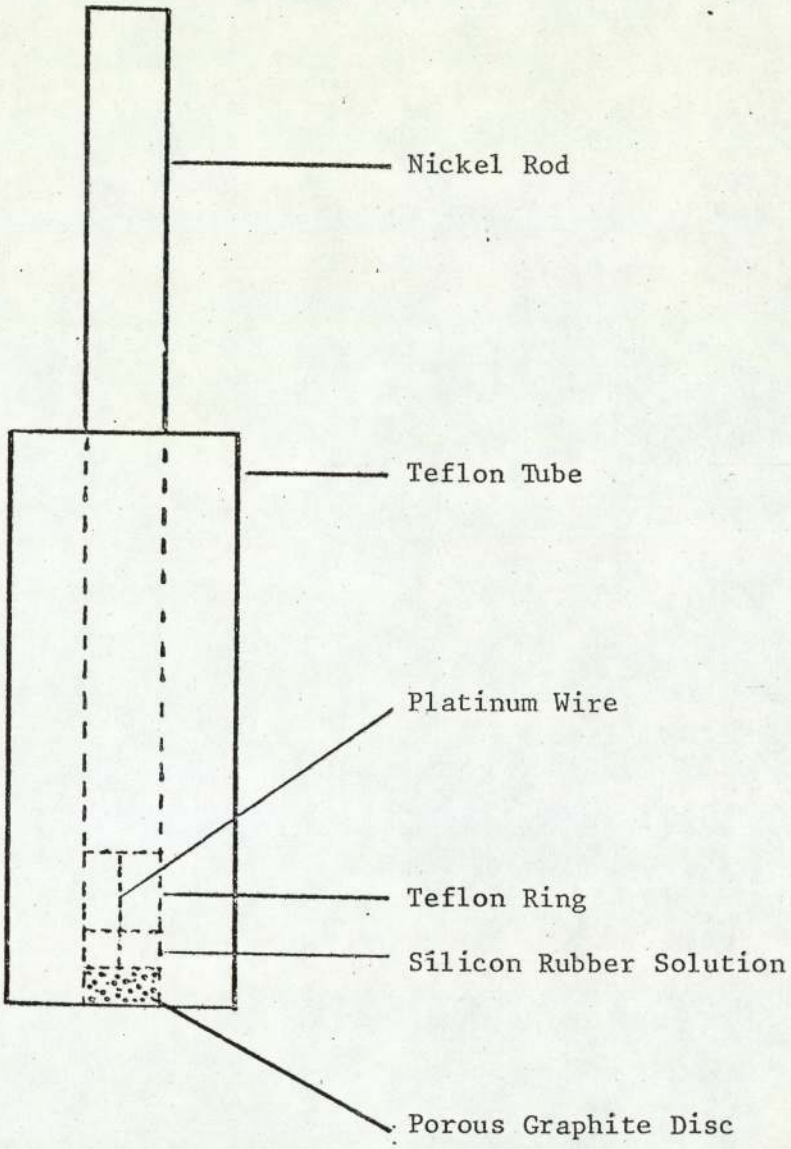

Figure 27

Schematic diagram of the rotating disc electrode.

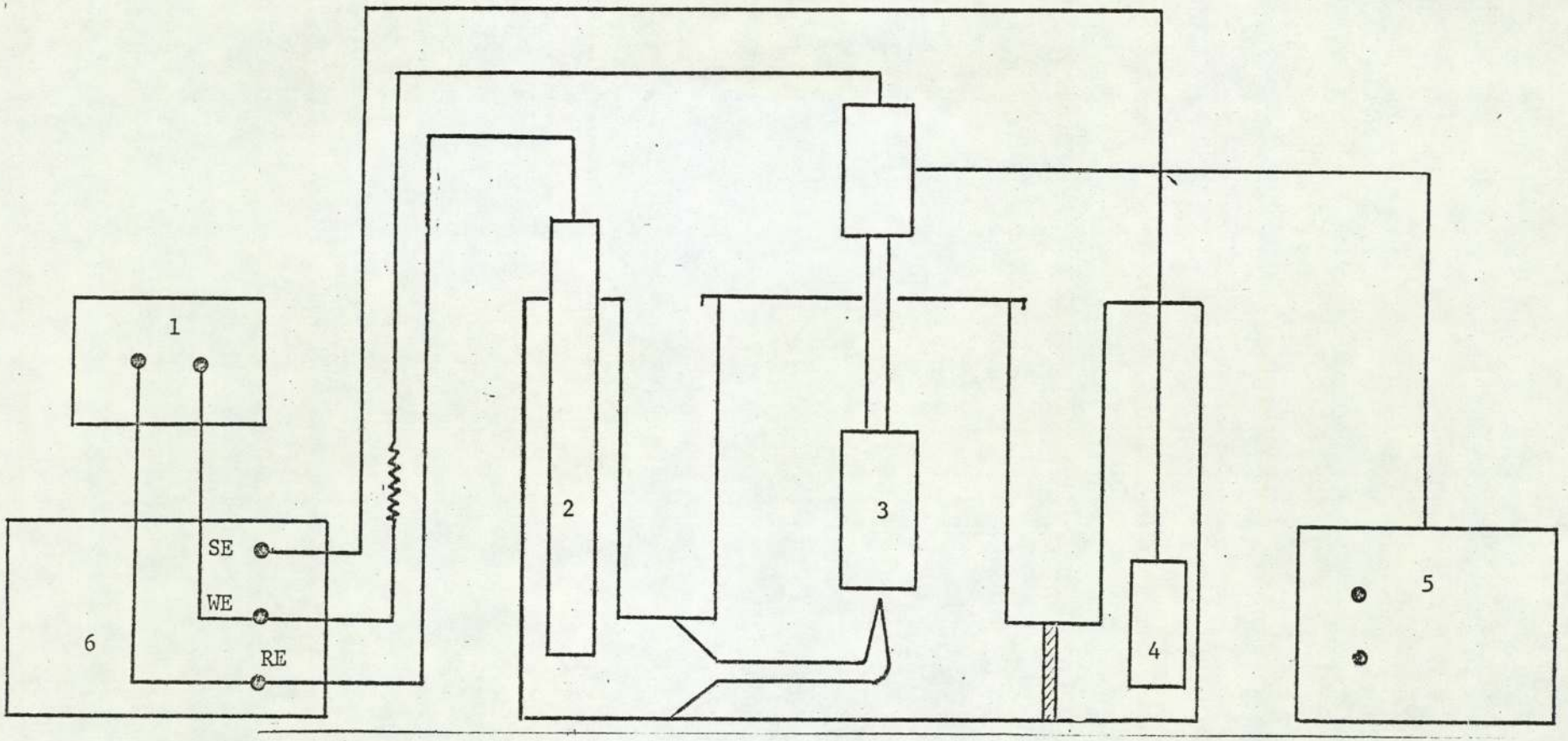

Figure 28

Electric-circuit diagram of the steady potentiostatic polarization

1. Digital volt meter,
2. Standard colomel Electrode,
3. Rotary Disc Electrode,
4. Secondary Electrode,
5. Rotating speed controller,
6. Potentiostate.

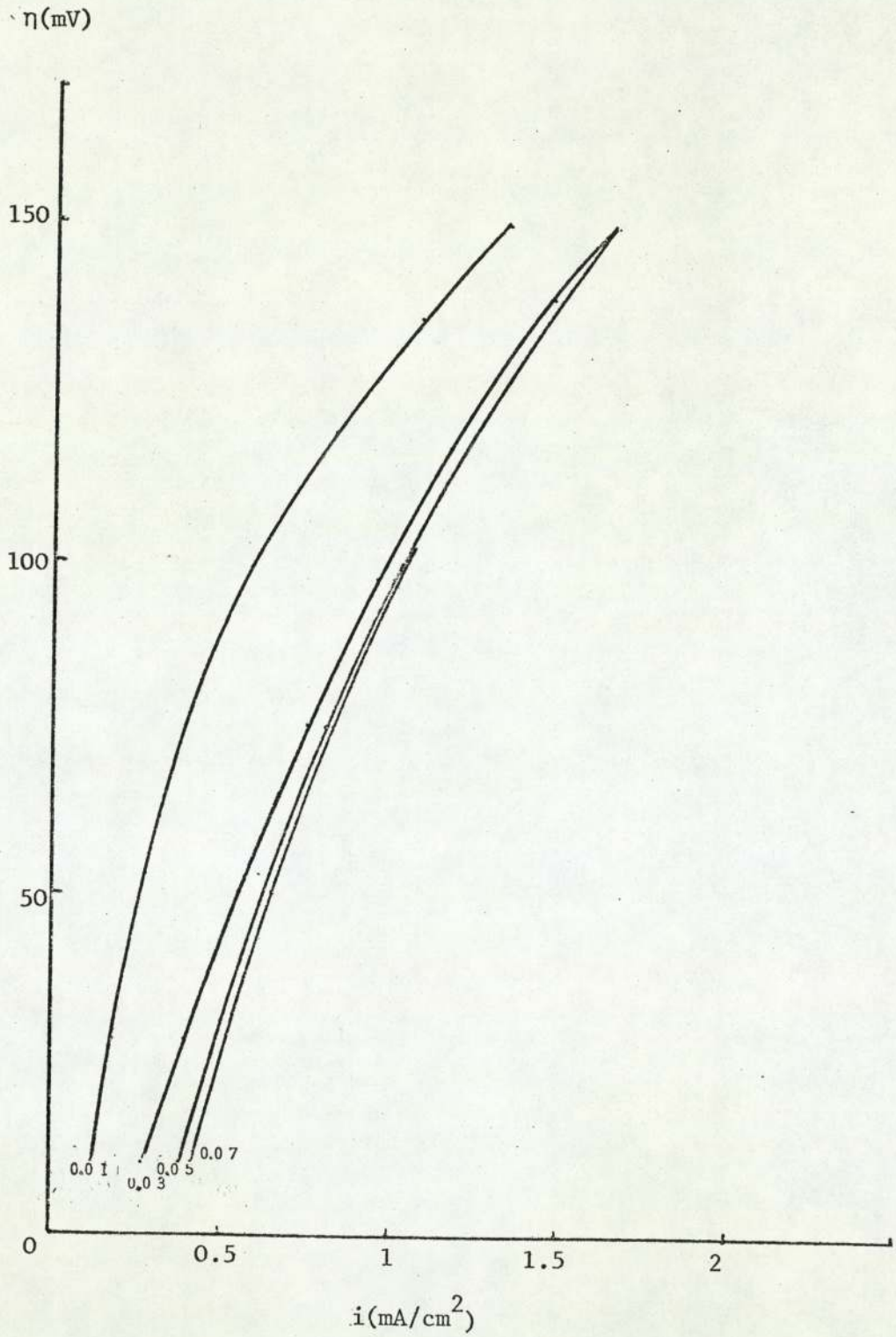

Figure 29

Theoretical current density - overpotential relationship at different electrode thicknesses. (cm)
$D = 3.7 \times 10^{-6}$ cm^2/sec.

Figure 30

Theoretical current density - electrode thickness relationship at different values of overpotential.

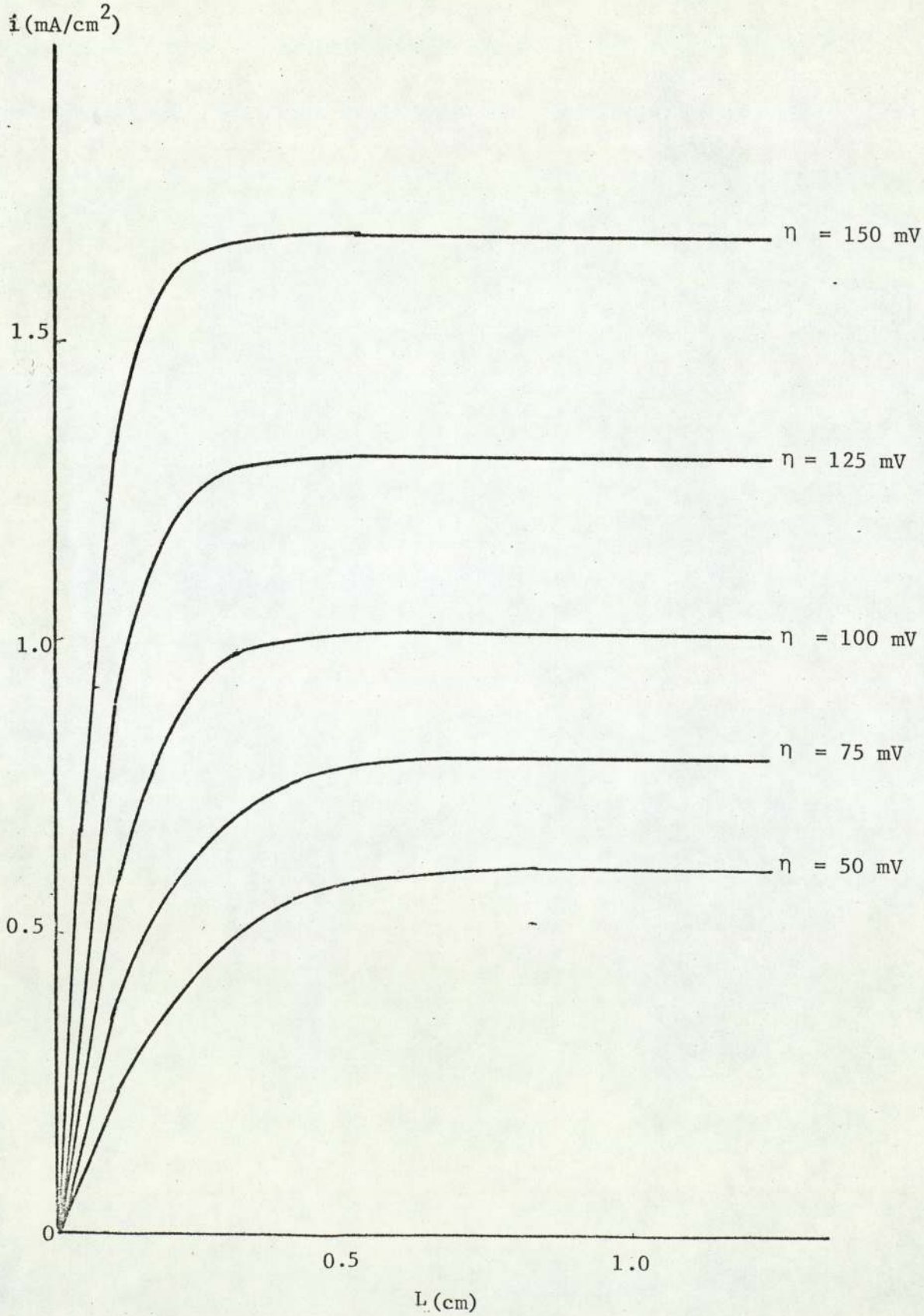

Figure 31

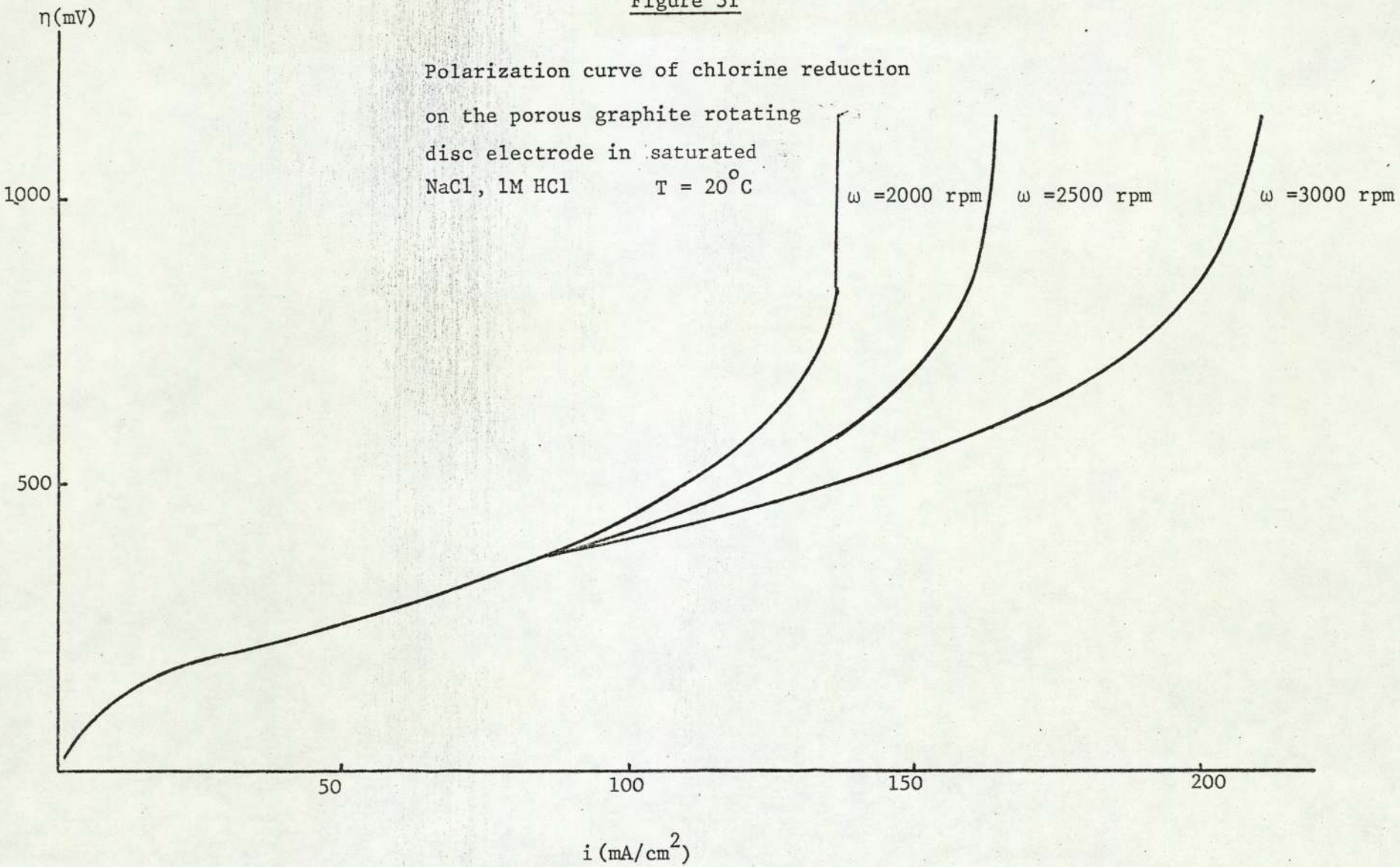
η(mV)
1000
500
Polarization curve of chlorine reduction
on the porous graphite rotating
disc electrode in saturated
NaCl, 1M HCl T = 20°C
ω =2000 rpm
ω =2500 rpm
ω =3000 rpm
50
100
150
200
i (mA/cm²)

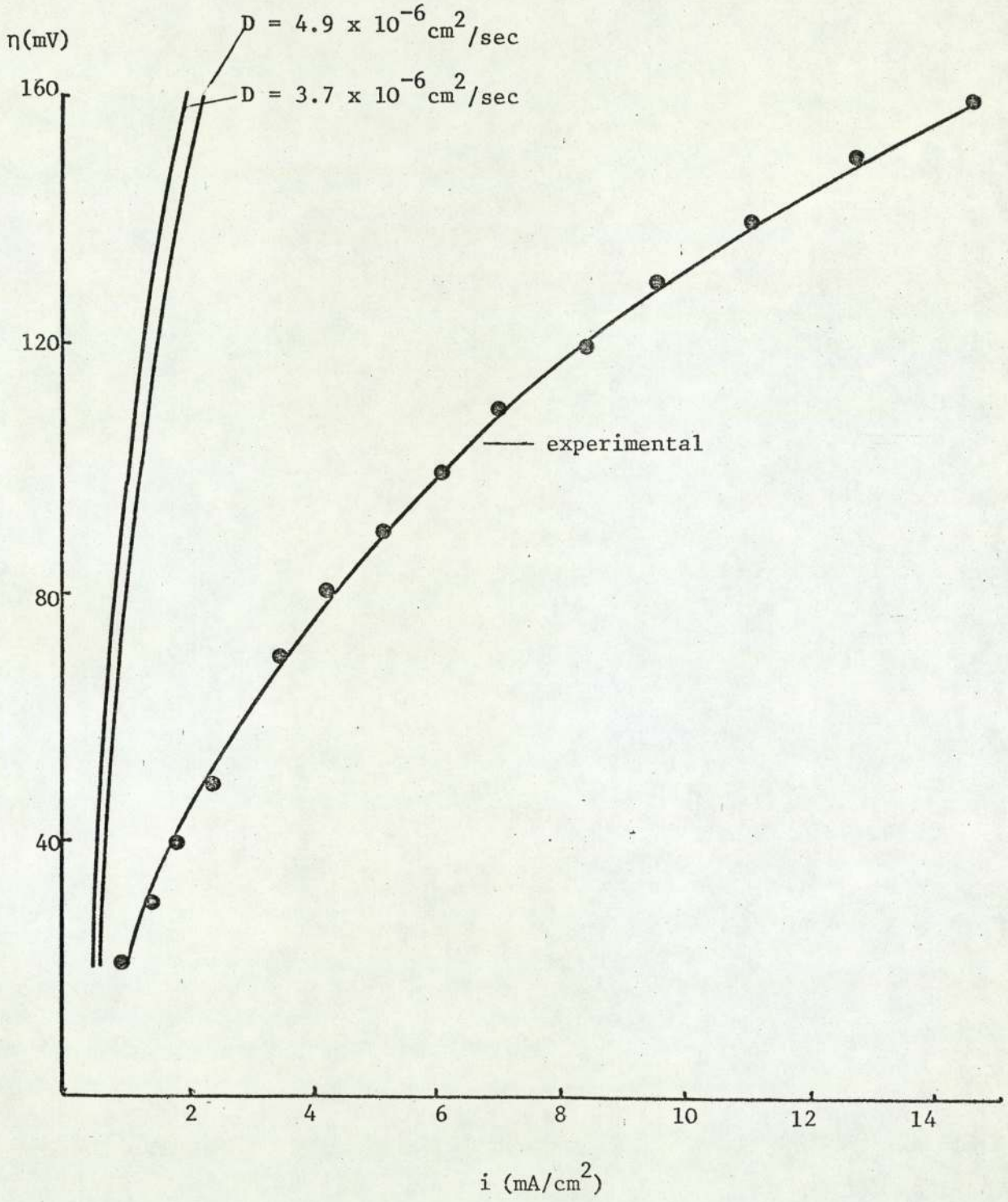

Figure 32

Comparison between theoretical polarization curve at $D = 3.7 \times 10^{-6}$ cm^2/sec, $D = 4.9 \times 10^{-6}$ cm^2/sec with the experimental curve.

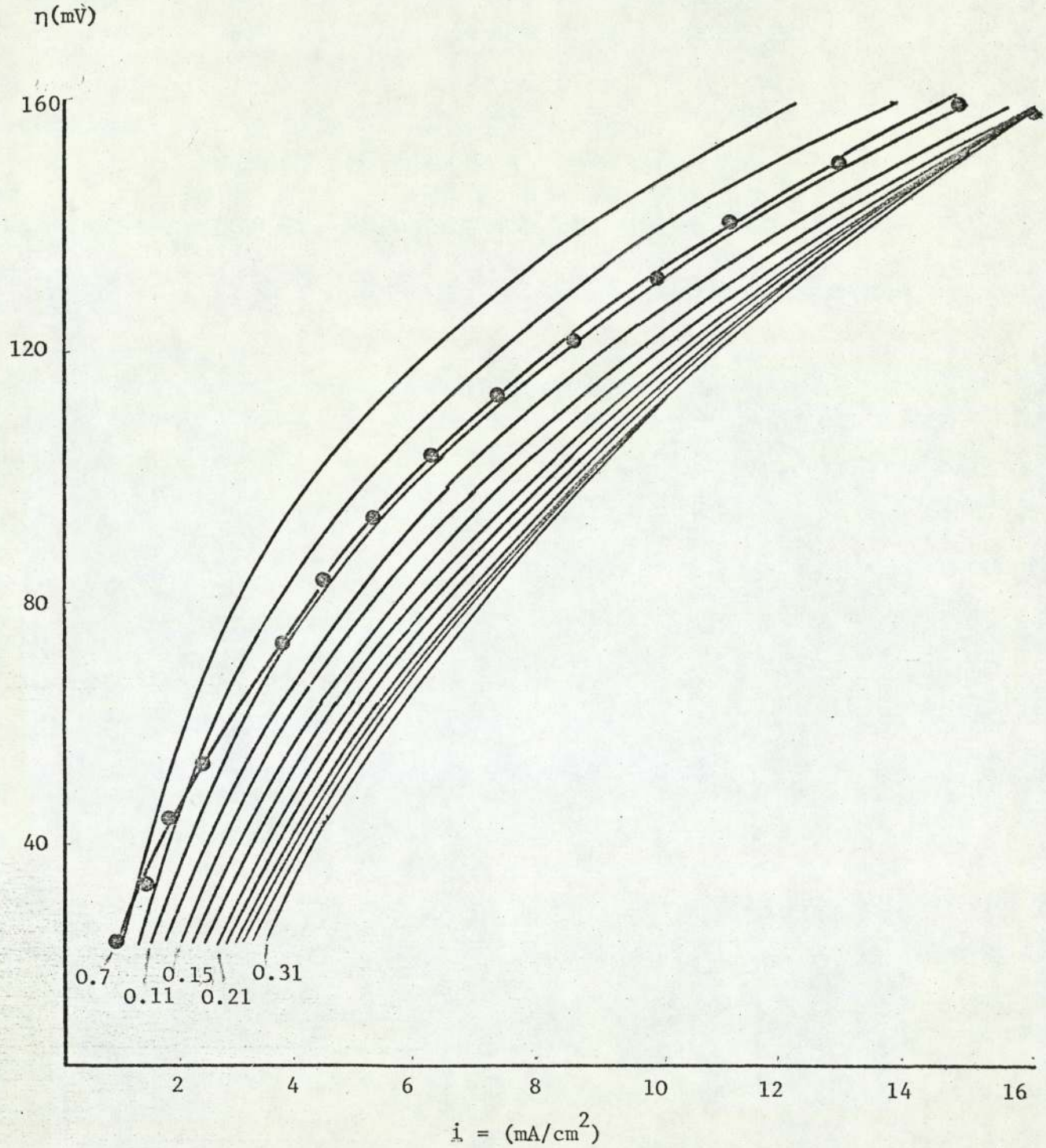

Figure 33

Comparison of the theoretical (-) and experimental (-●-) polarization curve at D = 3.0×10^{-4} cm^2/sec.

Table 1

Mixed type cathode specification.

	High rate cathode	Low rate cathode
T.C.A.	0.52 g	0.40 g
Acetylene black	0.30 g	0.30 g
Viscous fibre	0.02 g	0.02 g
Cathode diameter	2.5 cm	2.5 cm
Cathode surface area	5 cm^2	5 cm^2
Cathode thickness	0.2 cm	0.2 cm
Cathode bulk density	0.84 g/cm^3	0.72 g/cm^2

Table 2

Sandwich type cathode specification.

	High rate cathode	Low rate discharge
T.C.A.	0.52 g	0.4 g
Acetylene black	0.35 g	0.30 g
Viscous fibre	0.02 g	0.02 g
Cathode diameter	2.5 cm	2.5 cm
Cathode surface area	5 cm^2	5 cm^2
Cathode thickness	0.2 cm	0.3 cm
Cathode bulk density	0.89 g/cm^3	0.5 g/cm^3
Number of layer	6	4

Table 3

Percentage available chlorine in mixtures containing boric acid, boric oxide or zeolites, after seven days storage in ambient conditions.

Additives	% Available chlorine
Zeolite A	68.77
Zeolite X	65.58
Modernite	67.36
Cliptonilolite	67.61
Boric acid	78.10
Boric oxide	79.763
No additive (T.C.A./acetylene black)	69.80
Pure T.C.A.	88.60

Mixture composition

T.C.A. : 0.1 g

Acetylene black 0.2 g

Boric acid, boric oxide, zeolites : 0.1 g.

Table 4

Percentage available chlorine in mixtures after 60 hours storage at $40^{o}C$, 75% humidity.

Type of cathode design	% Available chlorine
Pure T.C.A.	88.60
T.C.A. mixed with acetylene black (pure)	37.20
T.C.A. sandwiched between acetylene black (pure) layers	52.10
T.C.A. mixed with acetylene black (impregnated with 4% boric acid)	52.10
T.C.A. sandwiched between acetylene black layers (impregnated with 4% boric acid)	60.27
T.C.A. sandwiched between acetylene black layers (the interface was covered with boric acid powder)	62.75

Table 5

Kinetic derivatives for rate determining step of chlorine reduction under Langmuir's adsorption condition.

Cathodic Reactions	$\theta \to 0$	$\theta \to 1$	$\theta \to 0$	$\theta \to 1$
	$n^1_{Cl_2}$	$n^1_{Cl_2}$	b(mV/ decade)	b(mV/ decade)
5.1.a (Slow),5.1.b (Fast)	$\frac{1}{2}$	-	120	-
5.1.b (Slow),5.1.a (Fast)	1	1	-	30
5.2.a (Slow),5.2.b (Fast)	1	0	40	120
5.2.b (Slow),5.2.a (Fast)	1	1	120	40

Table 6

ε	0.3 (Morganite Ltd.)
q	$\sqrt{2}$
D_b	1.74×10^{-5} cm^2/sec [16]
D_s	1.20×10^{-6} cm^2/sec [155]
i_o (apparent)	0.316 mA/cm^2
i_o (real)	0.132 mA/cm^2
ρ (graphite)	1.7 g/cm^3
$\frac{RT}{\alpha F}$	120 mV/decade

REFERENCES

1. J.B. Mullen and P.L. Howard. Trans. Electrochem. Soc., 1964, 90, 529.

2. G.W. Vinal. Primary Battery. John Willey, N.Y. 1950, 274-79.

3. I.C. Blake. J. Electrochem. Soc., 1952, 99, 202C.

4. J. Permik. Rev. Gen. Elec. 1953, 62, 294.

5. L.E. Pucher. J. Electrochem. Soc., 1952, 99, 203C.

6. M.J.H. Lemman and W.E. Carson. First Int. Symp. on Battery paper (5), 1958, p. 1-12.

7. C.K.Moorehouse and R. Glickman. J. Electrochem. Soc., 1957, 104, 467.

8. W.C. Arsem. U.S.Pat. 2, 306, 927. Dec. 29, 1942.

9. B.A. Gruber, J.J. Byrne. New Scientist 13 July 1967.

10. D.L. William, J.J. Byrne, J.S. Driscoll. J. Electrochem.Soc., 1969, 116, 2.

11. L.J. Pearce and R. Holland. Power Source 4 edited by D.H. Collins, 1973, p. 63-77.

12. L.J. Pearce, A. Gibson and D.C.P. Birt. Power Source 5 edited D.H. Collins, 1974, p. 447-462.

13. L.J. Pearce and G. Hazzard. Private communication.

14. Chlor-Chemical Limited. Product Catalog C/A/4.

15. A.P. Brady, K.M. Sancier and G. Sirine. J. Am. Chem. Soc., 1963, 85, 3101.

16. J. Phillips. PhD Thesis, University of New Castle upon Tyne, 1974.

17. Z. Khan. PhD Thesis, University of New Castle upn Tyne 1970.

18. P. de Saussure. Annals of Philosophy 1815, 6241.

19. R.A. Smith. Proc. Roy. Soc., 1863, A12, 424.

20. N. Schillow, G.D. Schatunovskaya and K. Tschumtow. Z. Physik Chem. 1930, 149, 211.

21. A. Tomita, Y. Taneoi. J. Phys. Chem. 1971, 75, 649.

22. A. Tomita. J. Colloid Interfac. Sci., 1971, 36, 153.

23. J.S. Mattson, H.B. Mark, M.D. Malbin, W.J. Weber and J.C. Crittender. J. Coll. Interfac. Sci. 1969, 31, 116.

24. D. Rivin. Rubber Chem. Tech. 1963, 36, 729.

25. V.A. Garten, D.E. Weiss, J.B. Willis. Aust. J. Chem. 1957, 10, 295.

26. B.R. Puri, R.C. Bansal. Rev. Gen. Caout. 1964, 41, 444.

27. H.P. Boehm, E. Diehl, W. Heck and R. Sappok. Angew Chem., 1964, 76, 742.

28. H.P. Boehm, E. Diehl and W. Heck. Rev. Gen. Caout, 1964, 41, 461.

29. M.C. Studebaker. Rubber Age. 1955, 77, 69.

30. R.N. Smith, A.J. Miles, S.F. Watkins. Trans. Faraday Soc., 1966, 62, 2553.

31. J.V. Hallum, H.V. Drushell. J. Phys. Chem. 1958, 62, 110.

32. J.K. Brown. J. Chem. Soc., 1955, 744.

33. R.A. Fiedel, M.G. Pelipetz. J. Opt. Soc. Amer., 1953, 43, 1051.

34. R.A. Fiedel, J.A. Queiser. J. Anal. Chem., 1956, 28, 22.

35. R.N. Smith, D.A. Young, R.A. Smith. Trans. Faraday Soc., 1966, 62, 2280.

36. R.N. Smith, P. Lesnini, F.H. Mooi. J. Phys. Chem., 1956, 60, 1063.

37. R.N. Smith, H. Swinekart, P. Lesnini. Ibid, 1959, 63, 544.

38. R.A. Fiedel, L.J.E. Hofel. Ibid, 1970, 74, 2921.

39. R. Burstein, A. Frummin. Z. Physik Chem. 1929, A141, 219.

40. B.R. Puri. Chem Phys. Carbon 1970, 6, 191.

41. B.R. Puri, Y.P. Mayer, L.R. Sharma. J. Indian Chem. Soc., 1956, 33, 781.

42. B.R. Puri, Y.P. Mayer, L.R. Sharma. Chem & Ind. B.I.F. Review 1956, R30.

43. B.R. Puri, D.D. Singh, J. Nath, L.R. Sharma. Ind. Eng. Chem. 1958, 50, 1071.

44. M.C. Studebaker. Proc. 5th Conf. Carbon, 1963, 2, 189.

45. H.P. Boehm. Adv. in Catalysis, 1966, 16, 179.

46. J. Dollimore, C.M. Freedman, B.H. Harrison, D. Quinn. Carbon 8, 1970, 587.

47. H. Harkner, J.J. Gallaher, A. Parkin. Carbon 4, 1966, 401.

48. N. Shilov, K. Chmutor. Physik Chem. 1930, A148, 233.

49. O. Bretschneider. Ibid, 1932, A159, 436.

50. B. Sternberg. Adsorption & Exchange of Ionic on Active Charcol Pub. Almquist & Wikse 1944.

51. R. Burskin, A. Frumkin. Dokl Akad Nauk SSSR, 1941, 32, 327.

52. J.B. Firth, G. Watson. J. Chem. Soc., 1923, 123, 750.

53. J.B. Firth, G. Watson. Trans. Faraday Soc., 1924, 20, 370.

54. V.A. Garten, D.E. Weiss. Aust. J. Chem. 1957, 10, 309.

55. H.P. Boehm. Angew Chem. Inst. ed. 1966, 5, 533.

56. E.J. Miller. J. Phys. Chem., 1932, 36, 2967.

57. D. Rivin. Proc. 5th Conf. Carbon Pergamon Press, 1963, 2, 199.

58. J.B. Donnett, G. Henrich. Bull. Soc. Chim. Fr. 1960, 1609.

59. V.A. Garten, D.E. Weiss. Aust. J. of Chem., 1955, 8, 68.

60. B.R. Puri, K.M. Bedi. Indian J. Chem. 1964, 2, 215.

61. B.R. Puri, R.C. Bansal. Carbon 1, 1964, 451.

62. B.R. Puri, N.K. Sandle.and O.P. Mahajan. J. Chem. Soc., 1963, 4880.

63. B.R. Puri, R.C. Bansal. Carbon 3, 1966, 533.

64. B.R. Puri, G.K. Sharma, S.K. Sharma. J. Indian Chem. Soc., 1967, 44, 64.

65. B.R. Puri. Proc. 5th Conf. Carbon Pergamon Press, 1962, 1,65.

66. R.S. Stearn, B.L. Johnson. Ind. Eng. Chem., 1951, 43, 156.

67. Mark Collin. Chlor-Chemical Ltd., Private communication.

68. Merkeley and Appleby. J. of Chem. Soc., 5,85A,489.

69. E.L. Littauer, L.L. Shreir. Electrochim. Acta, 1966, 11, 527.

70. A.N. Frumkin and G.A. Tadoradse. Z. Electrochim. 1958, 62, 251.

71. F.T. Chang and H. Wick. J. Phys. Chem. 1935, 172, 448.

72. G.R. Hennig. J. Chem. Phys. 1952, 20, 1443.

73. P. Drossboch, H. Hoff, P. Schmittinger and J. Schulz. Chem. Ing. Tech. 1965, 37, 639.

74. P. Drossboch, H. Hoff. Electrochim. Acta., 1966, 11, 679.

75. M.P.J. Brennan, O.R. Brown. J. Appl. Electrochem., 1972, 2, 43 - 49.

76. L.J.J. Janssen, J.G. Hoogland. Electrochim. Acta, 1970, 15, 941.

77. G. Mamantov, D.B. Freeman, F.J. Miller, H.E. Zittel. J. Electroanal. Chem., 1965, 9, 305.

78. F. Hine, M. Yusuda, M. Iwata. J. Electrochem. Soc. 1974,121, 749.

79. H. Bindar, A. Kohling, K. Ritchter, G. Sanstede. Electrochim. Acta, 1964, 9, 250.

80. L.J. Kristhalik and Z.A. Rotenberg. Zh. Fiz. Khim 1965, 39, 168.

81. D. Laser and M. Ariel. J. Electroanal Chem., 1974, 52, 291.

82. L.J.J. Janssen, J.G. Hoogland. Electrochim Acta, 1974, 19, 257.

83. I. Marcos, E. Yeager. Electrochim. Acta, 1970, 15, 953.

84. M. Pourbaix. Atlas d'Equilibres Electrochemiques ā 25°C. Gauthier-Villars, Paris, 1962, p. 312.

85. M. Pourbaix. Thermodynamic of aqueous solution (trans. J.N. Agar) Arnold, London, 1949.

86. E.M. Kosower. Prog. Phys. Org. Chem., 1965, 3, 81.

87. E.W.R. Steacie. Atomic and free radical reaction, 2nd ed. Chap. X, Reinhold, New York, 1954.

88. M.S. Kharasch, H.C. Brown. J. Am. Chem. Soc., 1939, 61, 2142.

89. G.A. Russell, H.C. Brown. Ibid, 1955, 77, 4031.

90. G.A. Russel. Ibid, 1958, 50, 5002.

91. C. Walling, B.B. Jacksow. Ibid, 1960, 82, 6108, 6113.

92. N.P. Buu-Hoi, P. Demerseman. J. Org. Chem. 1953, 18, 649.

93. M.F. Habbelynck, R.H. Martin. Bull. Soc. Chim. Belges, 1950, 59, 193.

94. J. Adan, P.A. Gosselain, P. Goldfinger. Nature, 1953, 704, 171. Bull Soc. Chim.Belges, 1956, 65, 523.

95. E.C. Juenge, D.A. Beal and W.P. Duncan. J. Org. Chem., 1970, 35, 719.

96. B.P. McGrath, J.M. Tedder. Proc. Chem. Soc., 1961, 80.

97. K. Ziegles et al. Justus Liebige Am Chem., 1942, 551, 80.

98. P.J. Flory. Principles of Polymer Chemistry, Cornell Univ. Ithaca, N.Y. 1953, p. 162.

99. P.D. Bartlett, H. Kwart. J. Am. Chem. Soc., 1950, 72, 1051.

100. P.J. Proll, L.H. Surcliffe. Trans. Faraday Soc., 1963, 59, 2090.

101. D.H. Solomon, Jean D. Swift. J. of Polymer Science, Part A, Vol. 3, 1965, p. 3107-3116.

102. P.C. Carman. Flow of Gases through Porous Media, Academic Press N.Y. 1956.

103. I.J. Klenkenburg. Geol Soc. Am., 1951, 62, 559.

104. D.S. Scott, F.A.C. Dullien. J. Am. Inst. Chem. Eng., 1962, 8, 113.

105. L.G. Austin, M. Ariet, R.D. Walker, G.B. Wood and R.H. Comyn. In. Chem. Eng. Fundamentals, 1965, 4, 321.

106. J.O'M. Bockris, B.D. Cahan. J. Chem. Phys., 1969, 50, 1307.

107. A.M. Adam, F.T. Bacon and R.G.H. Watson. Chap. 4, W.M. Mitchell (ed) "Fuel Cell" Academic Press Inc., N.Y. 1963.

108. E. Justi, A.W. Winsel. "Kalte-Verbrennung" Franz. Steiner Verlag, Wiesbaden, Germany, 1962.

109. R. Kh. Burstein, V.S. Markin, A.G. Pshenichnikov, Yu.A. Chrismadzhev, Yu.G. Chirkov. Electrochim. Acta, 1964, 9, 773.

110. J.O'M. Bockris and S. Srinivasan. "Fuel Cell: Their Electrochemistry" McGraw Hill, 1969.

111. D.N. Bennion, J. Newman. J. Appl. Electrochem., 1972, 2, 113.

112. A.K.P. Chu, M. Fleishman, G.J. Hill. Ibid, 1974, 4, 323.

113. R.S. Wenger, D.N. Bennion. Ibid, 1976, 6, 385.

114. A.T. Kuhn, R.W. Houghton. Ibid, 1974, 4, 69.

115. G.B. Adams, R.P. Hollandworth, D.N. Bennion. J. Electrochem. Soc., 1975, 122, 1043.

116. Wroblawa, A, Saunders. J. Electroanal.Chem. Interfacial Electro. Chem., 1973, 42, 329.

117. J. Newman, W. Tiedeman. AICHE Vol. 21, 1975, p. 25.

118. Kalnoki-Kis and R.J. Brodd. Characterisation of Flow through Porous Electrodes. J. Electrochem. Soc., 1971, 118, 510.

119. Euler and Nonenmacher. Electrochim Acta., 1960, 2, 268.

120. J. Newman, C.W. Tobias. J. Electrochem. Soc., 1962, 109, 1183.

121. L.G. Austin and H. Lerner. Electrochim. Acta, 1964, 9, 1469.

122. L.G. Austin. Trans Faraday Soc. (London), 1964, 60, 1319.

123. R.C. Alkire, E.A. Gren II, C.W. Tobias. J. Electrochem. Soc., 1969, 116, 1328.

124. J.S. Duning, D.N. Bennion. Proc. Advances in Battery, Technology Symp. Southern Calif, Nevada, Section of the Electro-Chem. Soc., vol. 5, 1969, 135.

125. J.S. Duning, D.N. Bennion, J. Newman. J. Electrochem. Soc., 1973, 120, 906.

126. D. Gidaspow, B.S. Baker. J. Electrochem. Soc., 1973, 120, 1005.

127. D. Simmonson. Ibid, 1973, 120, 151.

128. D. Simmonson. J. Appl. Electrochem., 1973, 3, 261.

129. K. Micka, I. Rousar. Electrochim. Acta. 1973, 18, 629, 633. 1974, 19, 499.

130. H. Gu, D.N. Bennion, J. Newman. J. Electrochem. Soc., 1976, 123, 1364.

131. H. Gu, J. Katan, D.N. Bennion. Ibid, 1976, 123, 1370.

132. P. Bro, H.Y. Kang. Ibid, 1971, 118, 519.

133. J. Brodd. Electrochim. Acta, 1966, 11, 1907.

134. T. Dickinson, R. Greef, Lord Wayne Jones. Electrochim. Acta, 1969, 114, 467.

135. T. Yokoyama and M. Enyo. Electrochim. Acta, 1970, 15, 1921.

136. G.A. Tadoradse, J. Russ. Phys. Chem., 1959, 33, 129.

137. G. Fiata, G. Fiori, J.W. Augnetyuski. J. Electrochem. Soc., 1969, 116, 928.

138. A.T. Kuhn, P.M. Wright. J. Electroanalytical Chem, 1972, 38, 291.

139. G. Bianchi. J. Apply Electrochem., 1971, 1, 231.

140. R.G. Erenburg, L.I. Khrishtalik, V.J. Bystrov. Sov. J. Electrochem., 1972, 8, 1690.

141. R.U. Bondar, A.A. Borisova, E.A. Kalinovski. Ibid, 1974, 10, 37.

142. R.G. Erenburg, L.I. Khrishtalik, I,P. Yaroshevskaya. Ibid, 1975, 11, 989.

143. R.G. Erenburg, L.I. Khrishtalik, I.P. Yaroshevskaya. Ibid, 1975, 11, 993.

144. R.G. Erenburg, L.I. Khristhalik, I.P. Yaroshevskaya. Ibid, 1975, 11, 1150.

145. L.I. Khrishtalik, Z.A. Rotenburg, Zh. Fit Khim 1965, 39, 328. 1965, 39, 907.

146. O.S. Ksenzhek, V.V. Stender, Dokl Akad Nauk S.S.S.R. 1956, 107, 280.

147. I.U.K. Delimarsky, G.V. Shilina. Electrochim. Acta, 1965, 10, 973.

148. A.M. Sham El Din. Ibid, 1961, 4, 242.

149. I.G. Murgulescu, S. Sternburg, L. Medinter, G. Mustetea. Ibid, 1963, 8, 65.

150. R. Tunold, H.M. Bo, K.A. Paulsen, J.O. Yhredal. Ibid, 1971, 16, 2101.

151. W.E. Triaca, C. Solomons, J.O'M Bockris. Electrochim. Acta, 1968, 13, 1949.

152. M.S. Jasem. PhD Thesis (1978), The City University.

153. K.G. Erenburg, L.I. Krishtalik. Electrokhimiya, 1968, 4, 932.

154. L.J.J. Janssen, L.M.C. Starmans, J.G. Visser, E. Barendrecht. Electrochim. Acta 1977, 22, 1093.

155. L.J.J. Janssen, J.G. Hoogland. Electrochim. Acta, 1970, 15, 339.

```
LIST

1 REM   CURRENT DENSITY-POTENTIAL RELATIONSHIP AT DIFFERENT VALUES OF ELECTRO
DE THICKNESS *****
10 DIM I(20,30)
100 D = .000132
110 S = 48
120 RS = 2.15E - 5
130 A = .5
140 B = .025
150 PS = PB * SC - 3
160 D = .0000597
170 RB = 2.15E - 5
175 PB = SC - 3
180 F = 96500
190 R = 8.02
200 K = 2
210  FOR L = .01 TO .2 STEP .02
220  FOR W = .02 TO .2 STEP .02
233 U = INT (W * 100)
235 K = INT (L * 100)
240 RT = (10 * S / (K) * F * D)) + (( EXP (A * W / D) / RB) + ( EXP ( - (1 - A
* W) / D) / RB))
255 X = L * 41 - 5
260  SET  FW B(U) =  ( EXP ( - X) / ( EXP (X) + EXP ( - X)) * 2 + 1
270 I(L,U) = (10 * S * L) + (( RS / RB) + PB * EXP (A * W / D) - (PS / PB) + EXP (
- (1 - A) * W / D) / RB) / X
280  NEXT : NEXT
285  PRINT "L= .01";"L= .03";"L= .05"
290  PRINT "W= .02"
295  PRINT I(1,2),I(3,2),I(5,2)
300  NEXT
315  PRINT
317  PRINT "L= .07";"L= .09";"L= .11"
320  FOR U = 2 TO 19 STEP 2
330  PRINT I(7,U),I(9,U),I(11,U)
340  NEXT
345  PRINT
347  PRINT "L= .13";"L= .15";"L= .17"
350  FOR U = 2 TO 19 STEP 2
360  PRINT I(13,U),I(15,U),I(17,U)
370  NEXT

380

RUN

L= .01          L= .03          L= .05
1.91373362E-04  2.21025487E-04  4.08107483E-04
1.91522125E-04  4.07621892E-04  5.24367461E-04
2.08113289E-04  5.04620887E-04  6.09999752E-04
4.04614024E-04  7.43178274E-04  8.10543756E-04
5.87570187E-04  9.79705217E-04  1.00424431E-03
8.20344421E-04  1.21270951E-03  1.23149761E-03
1.13399739E-03  1.49735757E-03  1.52063725E-03
1.53143937E-03  1.83595126E-03  1.83867226E-03
2.01774247E-03  2.24509997E-03  2.24579956E-03

L= .07          L= .09          L= .11
4.38743137E-04  4.48874247E-04  4.23620582E-04
5.44530465E-04  5.51591607E-04  5.33171757E-04
6.73463773E-04  6.77883215E-04  6.56233164E-04
8.35237141E-04  8.39469707E-04  8.16629944E-04
1.03544654E-03  1.03945602E-03  1.01696124E-03
1.28244456E-03  1.28645521E-03  1.26404982E-03
1.59038659E-03  1.59038981E-03  1.59038787E-03
1.83867226E-03  1.83867226E-03  1.83867226E-03
2.24579204E-03  2.24579204E-03  2.24579204E-03

L= .13          L= .15          L= .17
4.04614024E-04  4.52053464E-04  4.32941834E-04
5.53672952E-04  5.53354414E-04  5.32564954E-04
6.76274454E-04  6.76284333E-04  6.76288332E-04
8.24196827E-04  8.24196951E-04  8.24196952E-04
1.00596122E-03  1.00596123E-03  1.00596123E-03
1.23284975E-03  1.23284975E-03  1.23284975E-03
1.50538787E-03  1.50538787E-03  1.50538787E-03
1.83867545E-03  1.83867539E-03  1.83867539E-03
2.24579204E-03  2.24579204E-03  2.24579204E-03

L= .19          L= .21          L= .23
4.32941834E-04  4.52053464E-04  4.32941834E-04
5.53672952E-04  5.53354414E-04  5.32564954E-04
6.76274454E-04  6.76284333E-04  6.76288332E-04
8.24196827E-04  8.24196951E-04  8.24196952E-04
1.00596122E-03  1.00596123E-03  1.00596123E-03
1.23284975E-03  1.23284975E-03  1.23284975E-03
1.50538787E-03  1.50538787E-03  1.50538787E-03
1.83867545E-03  1.83867539E-03  1.83867539E-03
2.24579204E-03  2.24579204E-03  2.24579204E-03

L= .25          L= .27          L= .29
4.32941834E-04  4.52053464E-04  4.32941834E-04
5.53672952E-04  5.53354414E-04  5.32564954E-04
6.76274454E-04  6.76284333E-04  6.76288332E-04
8.24196827E-04  8.24196951E-04  8.24196952E-04
1.00596122E-03  1.00596123E-03  1.00596123E-03
1.23284975E-03  1.23284975E-03  1.23284975E-03
1.50538787E-03  1.50538787E-03  1.50538787E-03
1.83867545E-03  1.83867539E-03  1.83867539E-03
2.24579204E-03  2.24579204E-03  2.24579204E-03

L= .31          L= .33          L= .35
4.32941834E-04  4.52053464E-04  4.32941834E-04
5.53672952E-04  5.53354414E-04  5.32564954E-04
6.76274454E-04  6.76284333E-04  6.76288332E-04
8.24196827E-04  8.24196951E-04  8.24196952E-04
1.00596122E-03  1.00596123E-03  1.00596123E-03
1.23284975E-03  1.23284975E-03  1.23284975E-03
1.50538787E-03  1.50538787E-03  1.50538787E-03
1.83867545E-03  1.83867539E-03  1.83867539E-03
2.24579204E-03  2.24579204E-03  2.24579204E-03

L= .37          L= .39
4.32941834E-04  4.52053464E-04
5.53672952E-04  5.53354414E-04
6.76274454E-04  6.76284333E-04
8.24196827E-04  8.24196951E-04
1.00596122E-03  1.00596123E-03
1.23284975E-03  1.23284975E-03
1.50538787E-03  1.50538787E-03
1.83867545E-03  1.83867539E-03
2.24579204E-03  2.24579204E-03

LIST

1 REM   CURRENT DENSITY-POTENTIAL RELATIONSHIP AT DIFFERENT VALUES OF ELECTRO
DE THICKNESS *****
10 DIM I(20,30)
100 D = .000132
110 S = 48
120 RS = 2.15E - 5
130 A = .5
140 B = .025
150 PS = PB * SC - 3
160 D = .0000597
170 RB = 2.15E - 5
175 PB = SC - 3
180 F = 96500
190 R = 8.02
200 K = 2
210  FOR L = .01 TO .2 STEP .02
220  FOR W = .02 TO .2 STEP .02
233 U = INT (W * 100)
235 K = INT (L * 100)
240 RT = (10 * S / (K) * F * D)) + (( EXP (A * W / D) / RB) + ( EXP ( - (1 - A
* W) / D) / RB))
255 X = L * 41 - 5
260  SET  FW B(U) =  ( EXP ( - X) / ( EXP (X) + EXP ( - X)) * 2 + 1
270 I(L,U) = (10 * S * L) + (( RS / RB) + PB * EXP (A * W / D) - (PS / PB) + EXP
( - (1 - A) * W / D) / RB) / X
280  NEXT : NEXT
285  PRINT "L= .01";"L= .03";"L= .05"
290  PRINT "W= .02"
295  PRINT I(1,2),I(3,2),I(5,2)
300  NEXT
315  PRINT
317  PRINT "L= .07";"L= .09";"L= .11"
320  FOR U = 2 TO 19 STEP 2
330  PRINT I(7,U),I(9,U),I(11,U)
340  NEXT
345  PRINT
347  PRINT "L= .13";"L= .15";"L= .17"
350  FOR U = 2 TO 19 STEP 2
360  PRINT I(13,U),I(15,U),I(17,U)
370  NEXT

380

RUN

L= .01          L= .03          L= .05
1.91373362E-04  2.21025487E-04  4.08107483E-04
1.91522125E-04  4.07621892E-04  5.24367461E-04
2.08113289E-04  5.04620887E-04  6.09999752E-04
4.04614024E-04  7.43178274E-04  8.10543756E-04
5.87570187E-04  9.79705217E-04  1.00424431E-03
8.20344421E-04  1.21270951E-03  1.23149761E-03
1.13399739E-03  1.49735757E-03  1.52063725E-03
1.53143937E-03  1.83595126E-03  1.83867226E-03
2.01774247E-03  2.24509997E-03  2.24579956E-03

L= .07          L= .09          L= .11
4.38743137E-04  4.48874247E-04  4.23620582E-04
5.44530465E-04  5.51591607E-04  5.33171757E-04
6.73463773E-04  6.77883215E-04  6.56233164E-04
8.35237141E-04  8.39469707E-04  8.16629944E-04
1.03544654E-03  1.03945602E-03  1.01696124E-03
1.28244456E-03  1.28645521E-03  1.26404982E-03
1.59038659E-03  1.59038981E-03  1.59038787E-03
1.83867226E-03  1.83867226E-03  1.83867226E-03
2.24579204E-03  2.24579204E-03  2.24579204E-03

L= .13          L= .15          L= .17
4.04614024E-04  4.52053464E-04  4.32941834E-04
5.53672952E-04  5.53354414E-04  5.32564954E-04
6.76274454E-04  6.76284333E-04  6.76288332E-04
8.24196827E-04  8.24196951E-04  8.24196952E-04
1.00596122E-03  1.00596123E-03  1.00596123E-03
1.23284975E-03  1.23284975E-03  1.23284975E-03
1.50538787E-03  1.50538787E-03  1.50538787E-03
1.83867545E-03  1.83867539E-03  1.83867539E-03
2.24579204E-03  2.24579204E-03  2.24579204E-03

L= .19          L= .21          L= .23
4.32941834E-04  4.52053464E-04  4.32941834E-04
5.53672952E-04  5.53354414E-04  5.32564954E-04
6.76274454E-04  6.76284333E-04  6.76288332E-04
8.24196827E-04  8.24196951E-04  8.24196952E-04
1.00596122E-03  1.00596123E-03  1.00596123E-03
1.23284975E-03  1.23284975E-03  1.23284975E-03
1.50538787E-03  1.50538787E-03  1.50538787E-03
1.83867545E-03  1.83867539E-03  1.83867539E-03
2.24579204E-03  2.24579204E-03  2.24579204E-03

L= .25          L= .27          L= .29
4.32941834E-04  4.52053464E-04  4.32941834E-04
5.53672952E-04  5.53354414E-04  5.32564954E-04
6.76274454E-04  6.76284333E-04  6.76288332E-04
8.24196827E-04  8.24196951E-04  8.24196952E-04
1.00596122E-03  1.00596123E-03  1.00596123E-03
1.23284975E-03  1.23284975E-03  1.23284975E-03
1.50538787E-03  1.50538787E-03  1.50538787E-03
1.83867545E-03  1.83867539E-03  1.83867539E-03
2.24579204E-03  2.24579204E-03  2.24579204E-03

L= .31          L= .33          L= .35
4.32941834E-04  4.52053464E-04  4.32941834E-04
5.53672952E-04  5.53354414E-04  5.32564954E-04
6.76274454E-04  6.76284333E-04  6.76288332E-04
8.24196827E-04  8.24196951E-04  8.24196952E-04
1.00596122E-03  1.00596123E-03  1.00596123E-03
1.23284975E-03  1.23284975E-03  1.23284975E-03
1.50538787E-03  1.50538787E-03  1.50538787E-03
1.83867545E-03  1.83867539E-03  1.83867539E-03
2.24579204E-03  2.24579204E-03  2.24579204E-03

L= .37          L= .39
4.32941834E-04  4.52053464E-04
5.53672952E-04  5.53354414E-04
6.76274454E-04  6.76284333E-04
8.24196827E-04  8.24196951E-04
1.00596122E-03  1.00596123E-03
1.23284975E-03  1.23284975E-03
1.50538787E-03  1.50538787E-03
1.83867545E-03  1.83867539E-03
2.24579204E-03  2.24579204E-03

LIST

1 REM   CURRENT DENSITY-POTENTIAL RELATIONSHIP AT DIFFERENT VALUES OF ELECTRO
DE THICKNESS *****
10  DIM I(20,30)
100 D = .000132
110 S = 48
120 RS = 2.15E - 5
130 A = .5
140 B = .025
150 PS = PB * SC - 3
160 D = .0002
170 RB = 2.15E - 5
175 PB = SC - 3
180 F = 96500
190 R = 8.02
200 K = 2
210  FOR L = .01 TO .2 SET .02
220  FOR W = .02 TO .2 SET .02
233 U = INT (W * 100)
235 K = INT (L * 100)
240 RT = (10 * S / (K) * F * D)) + (( EXP (A * W / D) / RB) + ( EXP ( - (1 - A
* W) / D) / RB))
255 X = L * 41 - 5
260  SET  FW B(U) =  ( EXP ( - X) / ( EXP (X) + EXP ( - X)) * 2 + 1
270 I(L,U) = (10 * S * L) + (( RS / RB) + PB * EXP (A * W / D) - (PS / PB) + EXP
( - (1 - A) * W / D) / RB) / X
280  NEXT : NEXT
285  PRINT "L= .01";"L= .03";"L= .05"
290  PRINT "W= .02"
295  PRINT I(1,2),I(3,2),I(5,2)
300  NEXT
315  PRINT
317  PRINT "L= .07";"L= .09";"L= .11"
320  FOR U = 2 TO 19 STEP 2
330  PRINT I(7,U),I(9,U),I(11,U)
340  NEXT
345  PRINT
347  PRINT "L= .13";"L= .15";"L= .17"
350  FOR U = 2 TO 19 STEP 2
360  PRINT I(13,U),I(15,U),I(17,U)
370  NEXT

380

RUN

L= .01          L= .03          L= .05
1.33858614E-04  4.40443967E-04  4.42358175E-04
1.49685674E-04  5.76422464E-04  5.85645644E-04
2.97774817E-04  8.45758295E-04  8.64615357E-04
4.44055955E-04  1.31964145E-03  1.35903208E-03
6.62366194E-04  1.99429452E-03  2.17644679E-03
9.86829883E-04  2.89955878E-03  4.44534174E-03
1.41924681E-03  4.23728895E-03  6.72805707E-03
2.10716427E-03  6.27351998E-03  9.63565533E-03
3.56444757E-03  9.19387574E-03  1.01585202E-02

L= .07          L= .09          L= .11
9.21818122E-04  1.17124964E-03  1.42121E-03
1.36378243E-03  1.73374765E-03  2.06533015E-03
2.26957114E-03  2.55314887E-03  2.79435055E-03
2.94231195E-03  3.03533368E-03  3.20952345E-03
3.31772139E-03  3.42139888E-03  3.61615966E-03
3.74677784E-03  3.86411642E-03  4.56599101E-03
8.78791120E-03  .010208225      .012913959
.013583888      .013787026      .014071491
.014497108      .01816505E2     .019118873

L= .13          L= .15          L= .17
1.64226325E-03  1.86057331E-03  2.06623994E-03
2.38449502E-03  2.68153368E-03  2.95248839E-03
3.43431044E-03  3.80935902E-03  4.15019956E-03
4.64423917E-03  5.13631031E-03  5.71473895E-03
6.71732785E-03  7.25279141E-03  7.68427009E-03
8.01842217E-03  9.46667729E-03  .010702603
.011842797      .013555593      .017910489
.019545988      .021988557      .024603757
.019634847      .019953807      .020641391

L= .19          L= .21          L= .23
2.00113205E-04
5.86203807E-04
6.59990792E-04
6.27462977E-04
6.75032216E-04
6.74275547E-04
6.74274456E-04
6.74288332E-04
6.74288845E-04
6.74288845E-04

L= .25          L= .27          L= .29
6.68412264E-04
7.45738274E-04
8.24196827E-04
8.28527141E-04
8.24069278E-04
8.24069277E-04
8.24196952E-04
8.24196952E-04
8.24196952E-04
8.24196952E-04

L= .31          L= .33          L= .35
1.12399939E-03
1.48705213E-03
1.50532238E-03
1.50538699E-03
1.50538787E-03
1.50538787E-03
1.50538787E-03
1.50538787E-03
1.50538787E-03
1.50538787E-03

L= .37          L= .39
1.53149379E-03
1.83951124E-03
1.83867225E-03
1.83867225E-03
1.83867539E-03
1.83867539E-03
1.83867539E-03
1.83867539E-03
1.83867539E-03
1.83867539E-03

L= .41          L= .43
2.03714347E-03
2.24509797E-03
2.24579204E-03
2.24579204E-03
2.24579204E-03
2.24579204E-03
2.24579204E-03
2.24579204E-03
2.24579204E-03
2.24579204E-03

L= .45          L= .47
2.24579204E-03
2.24579204E-03
2.24579204E-03
2.24579204E-03
2.24579204E-03
2.24579204E-03
2.24579204E-03
2.24579204E-03
2.24579204E-03
2.24579204E-03

L= .49
2.24579204E-03
2.24579204E-03
2.24579204E-03
2.24579204E-03
2.24579204E-03
2.24579204E-03
2.24579204E-03
2.24579204E-03
2.24579204E-03
2.24579204E-03

LIST

1 REM   CURRENT DENSITY-ELECTRODE THICKNESS RELATIONSHIP AT DIFFERENT
VALUES OF ELECTRO POTENTIAL *****
10 DIM I(20,30)
100 D = .000132
110 S = 48
120 RS = 2.15E - 5
130 A = .5
140 B = .025
150 PS = PB * SC - 3
160 D = .0000597
170 RB = 2.15E - 5
175 PB = SC - 3
180 F = 96500
190 R = 8.02
200 K = 2
205  FOR W = .02 TO .2 SET .02
210  FOR L = .01 TO .2 SET .02
233 U = INT (W * 100)
235 K = INT (L * 100)
240 RT = (10 * L / (W * F * D)) + (( EXP (A * W / D) / RB) + ( EXP ( - (1 - A
* W) / D) / RB))
250 X = L * 41 - 5
260  SET  FW B(U) =  ( EXP ( - X) / ( EXP (X) + EXP ( - X)) * 2 + 1
270 I(W,U) = (10 * S * L) + (RS / RB) + PB * EXP (A * W / D) - (PS / PB) + EXP (
- (1 - A) * W / D) / RB
275  PRINT I(8,U)
280  NEXT : PRINT : NEXT

RUN

W= .02
1.33173362E-04
9.21337403E-04
4.08103483E-04
4.38743137E-04
4.48874247E-04
4.51620582E-04
4.52053464E-04
4.52053464E-04
4.52941834E-04
4.52941834E-04

W= .04
2.91152125E-04
1.86203807E-03
9.24221615E-04
9.44530465E-04
9.51591607E-04
9.53672952E-04
9.53354414E-04
9.53564954E-04
9.53564932E-04

W= .06
3.00113205E-04
5.86203807E-04
6.59990792E-04
6.27462977E-04
6.75032216E-04
6.74275547E-04
6.74274456E-04
6.74288845E-04
6.74288845E-04

W= .08
4.06412264E-04
7.45738274E-04
8.24196827E-04
8.28527141E-04
8.24069278E-04
8.24069277E-04
8.24196952E-04
8.24196952E-04
8.24196952E-04

W= .1
1.12399939E-03
1.48705213E-03
1.50532238E-03
1.50538699E-03
1.50538787E-03
1.50538787E-03
1.50538787E-03
1.50538787E-03
1.50538787E-03

W= .12
1.53149379E-03
1.83951124E-03
1.83867225E-03
1.83867225E-03
1.83867539E-03
1.83867539E-03
1.83867539E-03
1.83867539E-03
1.83867539E-03

W= .14
2.03714347E-03
2.24509797E-03
2.24579204E-03
2.24579204E-03
2.24579204E-03
2.24579204E-03
2.24579204E-03
2.24579204E-03
2.24579204E-03
```